C.P. No. 962

C.P. No. 962

MINISTRY OF TECHNOLOGY

AERONAUTICAL RESEARCH COUNCIL

CURRENT PAPERS

The Effect of Base Bleed on the Base Pressure of Several Shrouded and Unshrouded Propelling Nozzles at $M_\infty = 1.96$

by

M. M. Shaw

LONDON: HER MAJESTY'S STATIONERY OFFICE

1967

PRICE 16s 6d NET

U.D.C. No. 533.6.048.2 : 533.697.5 : 533.697.4 : 533.6.011.5

C.P. No.962*
June 1966

THE EFFECT OF BASE BLEED ON THE BASE PRESSURE OF SEVERAL SHROUDED AND UNSHROUDED PROPELLING NOZZLES AT $M_\infty = 1.96$

by

M.M. Shaw

SUMMARY

Base pressure measurements have been made on a bluff area surrounding a propulsive jet with and without base bleed. The effects of altering the jet Mach number and the ratio of jet exit area to total base area have been indicated. The tests were extended to measuring base pressure inside a shroud, and a correlation between the unshrouded and shrouded results is obtained. The results from the shrouded tests are compared with those from simple one dimensional theories, with some success.

Calculations of thrust efficiency show that high values can be obtained with the right combination of nozzle design Mach number, bleed flow and jet to maximum area ratio. If air of low total head, e.g. from an intake bleed, has to be disposed of, then feeding it into a duct surrounding a shrouded jet nozzle can be an efficient means of disposal.

* Replaces R.A.E. Tech. Report No.66102 - A.R.C. 28721.

CONTENTS

1 INTRODUCTION

One of the design problems during the development of a new aircraft is how best to match the engine to the airframe. It is desirable to retain a high engine thrust and to keep the installed drag of the engine-airframe combination low. A proposed supersonic airliner has a pair of engines slung under each wing in a single nacelle. Each nacelle consists of a pair of intakes, a central portion containing the engines themselves, and a pair of nozzles. The intakes and the nozzles both have a smaller frontal area than the maximum engine cross section. This means that the underside of each nacelle has a curvature, convex downwards, over the whole of its length; which at supersonic speeds leads to a positive forebody and a positive afterbody drag. The afterbody also gives a negative lift. This deleterious lift and drag effect of the afterbody could be eliminated by keeping the nacelle depth constant from the station where it first reaches a maximum to the exit. This would then yield a base area of naoelle greater than the area occupied by a fully-expanded jet nozzle. The present tests were undertaken in order to determine whether such a bluff area round the nozzle could be made to give lower drag than the afterbody which it replaced, It is known' that the base pressure in the presence of an external stream and a jet is well below free stream static pressure, giving a high drag, but evidence [2] has been presented which shows that if a small quantity of low energy air is introduced into the base region, then base pressure rises considerably.

2 EXPERIMENTAL DETAILS

At the time of the tests it was considered essential that results should be obtained quickly, so some sophistication was sacrificed in the interest cf speed. In spite of this, apart from some early troubles with leaks and poor flow distribution near the base, the rig has proved well suited to the purpose for which it was made.

The model was mounted in the 9" x 8" supersonic tunnel in the High Speed Laboratory at R.A.E. (Bedford). Fig.1 shows the arrangement of pipes, model and reflection plate placed on the $M_\infty = 1.96$ liner.

The single jet nozzle plus reflection plate is intended to simulate the two nozzles placed side by side in the supersonic transport.

In the early stages of the experiment an approximately conical fairing was made to cover the right angle bend of the main jet pipe after it had come through

the liner into the tunnel stream. This arrangement led to non-uniformities of Mach number in the vicinity of the exit plane (measured by static pressure holes on the cowl (Fig.2)), and so it was abandoned in favour of a wedge-shaped fairing. This fairing was even less successful, the flow poured off the wedge surface at the edges, separated and rolled up into vortioes which made the base flow quite unacceptable. Oil flow photographs (Figs.3 and 4) show clearly the nature of the flow, indicating also a reversed flow in the corner of a type studied by Eminton[3].

The solution finally adopted was to replace the relatively short conical and wedge shaped fairings by a long wooden fairing extending upstream beyond the tunnel throat. It was realized that this might result in (1) deterioration of the Mach number distribution in the main flow compared with the original configuration (Figs.3 and 6) and (2) a thick boundary layer which develops on the long fairing (Pigs.6, 7, and 8). In spite cf these disadvantages oil flow photographs taken of the fairing (Figs.9 and IO) indicate that the flow in the modified tunnel was reasonably uniform, and measurements of static pressure on the cowl show the same thing. On balance it was considered that a sensible experiment could be performed with the apparatus as shown in Fig.1.

Fig.2 gives details of the instrumentation near the base. Base pressures throughout the note, except when otherwise indicated are a mean of the pressures recorded by rearward facing pitots numbers 17, 18, 19, 20, 21, 22, 23, and static holes 25 and 26. Pressures 8 and 9 are pitot tubes placed to measure the bleed total head. They were removed at one stage in order to test square nozzles. Pressures 12, 13 and 14 were used to monitor local pressure on the cowl, although in fact all measurements were referred to a tunnel static pressure measured a little way upstream of the base.

The bleed mass flow was controlled by a valve in the bleed pipe, and measured with a venturi. To make sure that no extraneous air was able tc get to the base region at zero bleed flow a plug was pushed into the end cf the pipe to seal a small leak through the valve. Dry air supplied from the tunnel pressurising compressor was used for the main jet. The mass flow in this jet was not measured directly but calculated from nozzle geometric choking area and mean upstream total pressure.

The shroud when used was attached tc the reflection plate and the joint between model and shroud was sealed with sellotape.

3 RANGE OF EXPERIMENTS

The tunnel total pressure was constant near atmospheric pressure, the free stream Mach number was also constant, and the size of the simulated nacelle remained the same throughout the tests. The variables were bleed mass flow, the external and internal shapes of the nozzles, the length of the shroud and the jet total pressure.

4 RESULTS AND DISCUSSION

4.1 Preliminaries

A number of subsidiary experiments were performed in order to check certain aspects of the rig's behaviour. These are described in the present section before the main results are discussed in section 4.2.

4.1.1 Boundary layer measurements

It was originally intended that boundary layer thickness should be increased by artificial means and hence be one of the variables of the experiment, but for the reasons given in section 2 the minimum boundary layer thickness was large and therefore this was not increased during the tests. The measurements of pitot pressure in the boundary layer, plotted in Figs.7 and 8 as velocity distributions were taken with the rake designed for a thinner layer and hence do not cover the boundary layer adequately. Reasonable agreement exists between the measured points and a 1/7 power law, assuming a boundary layer thickness which makes the theoretical curve agree with the middle measured point. This thickness is 0.8 in. ±10%, whereas a measurement from Fig.6 (allowing for the scale of the photograph) gives 0.6 in. The boundary layer on the side of the fairing is roughly 0.2 in thinner than on the top (Fig.8)).

When the shroud is present and long enough to ensure that the mixing processes take place without reference to the external stream then the thickness of boundary layer on the outside of the model is irrelevant. The boundary layer of primary interest under those conditions is that on the internal nozzle surface and no measurements were made of' this.

4.1.2 Reflection plate length and drape

Four plates were made: the standard one, used for all tests without shroud extending 4.5 in. (three base heights) beyond the base; two more extending respectively 7.5 and 8.5 in. beyond the base; and a *rectangular* one almost spanning the tunnel and extending 6 in. beyond the base. No differences in base pressure were

found among any of the reflection plates. All the tests with a shroud were done on one of the two lunger plates, as the position of the rear of the afterbody moved backwards with the addition of a shroud and a plate length of three base heights was felt to be the minimum desirable.

Oil flow photographs (Figs.11 and 12) were taken with no jet and no bleed.

4.1.3 Main jet pressure distribution

For reasons mentioned earlier the length of the model was kept as small as possible, with the result that the nozzle throat was only a short distance downstream of the last bend in the main jet pipe. This lack of settling length might have resulted in some maldistribution in the nozzles. To minimize the effect of the corner, the cross-sectional area of the pipe was reduced through the turn, and a pitot rake was placed immediately downstream of it so that the distribution could be monitored.

These pressure distributions (Fig.13) remain virtually unchanged at all pressure ratios up to about thirteen to one. Most of the tests were done at higher pressures than this, but as an increase of pressure implies an increase of Reynolds number, it is unlikely that any worsening of the distribution occurred.

As an additional check, a rake was constructed to measure pitot pressure in the exit plane of nozzle 3. The pressure varied from the mean by ±5%, and the Mach number computed from the ratio of the mean pitot pressure to the total pressure gives $M_j \simeq 1.933$. The value obtained by using the geometrical area ratio of the nozzle is 1.949. This difference corresponds to a one per cent change in area ratio and indicates for the initial series at least that the air was filling the nozzle and choking at the geometric throat.

4.1.4 Nozzle internal pressure distributions

It was considered desirable to check some nozzle internal pressure distributions against isentropic one-dimensional values. Figs.14 and 15 show these distributions for the series of nozzles with increasing throats at a jet Mach number of 1.9. Nozzle 3, the one having the smallest throat shows good agreement near the exit plane, but rather poor agreement near the throat. The reason for this discrepancy is not understood, but unpublished work at N.G.T.E. indicates that it may be due to the rapidly changing flow in the region of a non-planar sonic surfaoe. The agreement between one-dimensional flow and the measured flow at the exit plane becomes progressively less good as throat size is increased.

Bearing in mind the small size of the supply pipe it is possible the flow was choking at a section other than the geometric throat, and that less air was passing through the nozzle than was intended. This effect would become more noticeable as throat size increased. In particular square nozzles F and G had throats almost as big as the supply pipe. Thus it is possible that base pressure is too low, at zero bleed (because the static pressure at the nozzle exit is lower than intended) but that the rate of increase with bleed shown is too high because the bleed flow has been referred to too large a main flow.

4.1.5 Measurement of pressure with bleed flow present

The bleed air came into the model from atmosphere at right angles to the direction of the nozzle instead of ideally from upstream. It was thought likely that at the largerbleed flows the bleed total head near the top of the nozzle would be greater than at the bottom. Fig.16 illustrates this effect but shows that it is relatively small at bleed flows of the order of $2\frac{1}{2}\%$ of the main flow. Fig.17 shows bleed Mach number calculated from the ratio of static to pitot pressure at the base compared with a curve computed from the bleed mass flow.

The use of rearward facing pitots to measure base pressure is sensible for a solid base, where they become static holes, and similarly in an area of zero velocity they measure pressure correctly. For appreciable base flows however a rearward facing pitot is likely to measure a pressure somewhat lower than the local static. The indications from Figs.18 and 19 are that this effect is barely measurable, particularly at bleed flows less than or equal to $2\frac{1}{2}\%$ where later sections will show the main interest to lie.

441.6 Non-uniformities of base pressure due to the reflection plate

At zero bleed flow the pressure was constant over the nine pressure measuring points distributed round the base, but as bleed was introduced and increased, non-uniformities occurred. The reflection plate, placed to represent the interface between the symmetrical flows from two nozzles was the main source of asymmetry on the single nozzle. On the top and on the two sides of the model the interactions between jet, bleed and free stream occurred in free shear layers, whereas the solid boundary of the plate on the bottom edge gave different conditions. Figs.20 and 21 show how the pressure near the plate rises faster than that elsewhere, particularly for the square nozzle. The conditions on the plate near to the square nozzle approximate to those at a backward facing step, but this approximation does not hold for the round nozzle, hence the smaller difference between pressures on the plate and elsewhere.

4.1.7 Base pressure with no jet

Fig.22 compares the no-bleed, no-jet base pressure with other experimental results[4,5] and with the variation of base pressure with boundary layer momentum thickness calculated in Ref.6 for two-dimensional flow. Figs.23(a) and (b) show the variation of base pressure (still with no jet) with bleed mass flow and bleed total pressure and compares with results given in Refs.1, 7, and 8.

It can be seen that the no jet case lies between axisymmetric and two-dimensional results obtained by other investigators.

4.2 Nozzles without shroud Effect of:-

4.2.1 Nozzle design Mach number

Five conical nozzles (Nos. 1-5 in Table 1) were made each having the same throat area and external shape. The nozzle divergence angle for all except the sonic nozzle was 13°. The results are plotted in Figs.24 and 25. The graphs of base pressure against bleed flow (Fig.24) are typical of all the nozzles tested. They rise steeply as the bleed increases from zero to about 2½% of the main mass flow, and less steeply thereafter. Fig.25 shows the rise in base pressure as design Mach number is reduced while throat area is held constant, If the jet exit area rather than the throat area had been held constant the base pressure would have risen rather more steeply with decrease in nozzle design Mach number (see section 4.2.3).

For a given bleed the increment in base pressure remains roughly constant as jet Mach number changes.

4.2.2 Nozzle divergence angle

Nozzles IO, 8, 11, 12 were designed to explore the effect of nozzle divergence angle at constant jet Mach number. The results are plotted in Fig.26 which shows that base pressure rises as the nozzle divergence angle increases. It is clear from all the theoretical analyses in two dimensions that the angles turned through by the internal and external flows play an important part in determining the pressure in the dead air region between them. More particularly, the stronger and nearer the recompression is to the base as the expanding jet turns streamwise, the higher the base pressure will be.

It is also interesting to note that changing the nozzle divergence angle from 10° to 20° at a design M_j of 1.9 gives very similar increases in base pressure to changing the design M_j from 1.0 to 2.45.

4.2.3 Ratio of jet exit area to total base area

The above description has been chosen to introduce the idea of 'step height' - the separation distance at the base between the external and primary jet flows. As the ratio of jet exit area to total base area goes up, the step height goes down.

To keep the jet exit Mach number the same, yet decrease the step height it was necessary to increase the throat area and the jet exit area. Nozzles 3, 15 and 14 form a series with decreasing step heights at a design Mach number of about 1.9, and nozzles 2 and 13 a pair at $M_j \simeq 2.2$. Fig.27 shows that the base pressure rises rapidly as the ratio of jet exit area to total base area increases. The parameter giving scale to the base flow is the ratio of the boundary layer momentum thickness to the step height, but when two flows are present as in the unshrouded nozzles it is difficult without more theoretical work to predict whether the outer and the inner layers are equally important.

It is interesting to compare these results at zero bleed with those obtained in Ref.9 for $M_j = 1.0$ and for different free stream Mach numbers (Fig.28). The influence of free stream Mach number appears to be large.

4.2.4 Ratio of bleed exit area to total base area

Nozzles 3 and 8 had nominally identical interior surfaces. They were designed to produce a jet Mach number of about 1.9. The external surface of nozzle 3 was cylindrical but that of nozzle 8 was tapered to form an expanding passage for the bleed air. The effect of this change of area was to inject the bleed air into the separated region with lower velocity. According to Ref.10 this should raise the base pressure. Fig.29 shows that appreciable increases do occur for bleed flows greater than two and a half' per cent of the main flow. The variation of maximum base pressure with bleed velocity appears to follow the same trend as was given in Ref.1 (Fig.30).

42.5 Jet total pressure ratio

A number of experiments on base pressure in the presence of an issuing jet have shown the effect of jet pressure ratio without a base bleed. Some results are extracted (Fig.31) from Ref.1 which show the effect of A_j/A_m and some from Ref.9 which show the effect of nozzle divergence angle and jet Mach number. There are indicaticms that the difference between the results of Ref.1 and those of the present investigation is probably due to the difference in θ_j and the difference with respect to the results of Ref.9 is probably attributable to differences in M_j and possibly also to boundary layer thickness at the base.

The effect of base bleed and jet pressure ratio combined is shown in Fig.32. As can be seen the general variation of base pressure with bleed flow already noted at a pressure ratio of 16 appears to be repeated at all other pressure ratios down to six or less.

4.3 Nozzles with shroud

4.3.1 General

A study of the distribution of base pressure round the nine measuring points shows (Figs.20 and 21) that the pressure on the side of the square base nearest to the plate gives a higher increment in base pressure due to bleed than any pressure on the other three sides. As one of the objects of the experiment was to find ways of increasing base pressure it seemed reasonable to reproduce the pressure conditions at the reflection plate on all sides by enclosing the jet in a shroud.

As has been seen, both designing the nozzle for a lower pressure ratio than the one available (i.e. running the nozzle under expanded) and increasing the nozzle divergence angle have increased the base pressure. These two changes however, adversely affeot primary jet thrust, whereas adding a parallel shroud should only give perhaps small weight and skin friction penalties. Thus, as this addition of a shroud was found to substantially increase base pressure it was considered important to test the full range of nozzles again with a shroud present.

The work on nozzles without shroud showed that if 'step height' could be reduced, then the base pressure would rise and therefore a series of square ended nozzles was tested which yielded high values of jet exit area relative to total base area,

The comparison of Fig.33 typically indicates the large increase in base pressure on the addition of a parallel shroud. Fig.34 is equivalent to Fig.24 (the vertical scale is halved) and shows the effect of nozzle design Mach number. Fig.35 indicates a linear relation between base pressure with shroud end that without shroud.

4.3.2 Shroud length

The length of shroud originally chosen was based on the Schlieren photograph of Fig.36 which shows the sonic jet spreading and turning to the free stream direction at about 0.86 of the base height behind the jet exit plane.

Fig.37(a) shows that for $M_j = 1.57$ this value of $\ell/h = 0.86$ was a good choice in that this is approximately the minimum length to achieve all the available pressure rise. As might be expected, for $M_j = 2.45$ (Fig.37(b)) where 'step height' is *very* much less the majority of the pressure rise is achieved for $\ell/h = 0.6 - 0.7$. These results are for a divergence angle of 13° and it is obvious that the length needed to obtain the full pressure rise will increase with decrease in nozzle divergence angle.

4.3.3 Comparison of experimental and calculated variation of base pressure with bleed flow

Several methods are available for calculating the characteristics of supersonic ejector nozzles, which consist of a convergent choked primary nozzle operating within a cylindrical shroud. The majority of them are one-dimensional treatments which depend on applying continuity and momentum considerations (together with assumptions such as isentropic flow in one or both streams) between the exit plane of the primary nozzle and a plane within the parallel shroud where it is considered that the static pressure over the whole cross-sectional areaisuniform. The methods are readily adapted to accommodate a supersonic rather than a sonic primary nozzle. A far more sophisticated treatment which matches primary and secondary flows as they proceed downstream from the nozzle exit in a laborious step-by-step procedure and which also considers viscous interaction effects between the primary stream and the shroud boundary layer is available in Ref.11. This is probably the method which should be used for studying specific cases, but for wider studies of trends the results from one-dimensional treatments are still useful. Their relative ability to predict base pressure is assessed in this Report by comparing results with experimental measurements. It should be emphasized however that the absolute worth of the comparisons is somewhat limited in that the methods do not take account of nozzle divergence angle (as does Ref.11) and as has been seen this is a fairly important parameter in deciding base pressure. Their use may be justified however if' they give fairly good agreement with experiment for practical values of nozzle divergence angle (i.e. $8^\circ - 12^\circ$).

All the one-dimensional theories assume no mixing between primary and secondary flows and ignore skin friction on the inside of the parallel shroud. It should be noted that the combination of shroud length and primary pressure ratio in this present comparison is such that we are only interested in the so-called supersonic régime of Fabri and Paulon[13].

The theories used here can be summarized as follows:-

Kochendorfer and Rousso[12] (Fabri and Paulon[43] make identical assumptions)

Application of continuity and momentum equations to the two streams assuming:-

(i) The primary stream is isentropic.

(ii) The secondary stream Mach number is unity at the plane where static pressure is considered to be uniform across the total cross-section.

Pearson, Holliday and Smith[14]

Application of continuity and momentum equations to the two streams assuming:-

(i) The secondary stream is isentropio.

(ii) The solution is obtained at a minimum possible value of the secondary total pressure. This condition holds when curves obtained from continuity and momentum considerations just touch.

Filleul[15]

Application of the continuity equation to the two streams assuming:-

(i) The primary flow is isentropic.

(ii) The secondary flow is isentropic.

(iii) A minimum secondary flow total pressure criterion.

It is interesting to note that this method cannot distinguish between the nozzles of the first series i.e. nozzles d-5 in that it would give identical answers for base pressure variation with bleed flow. The method has therefore only been used to compare with the experimental results given for sonic primary nozzles.

Fig.38(a) ccanpares experimental measurements for *sonic* nozzles with a cylindrical shroud from Ref.12 and the present tests with results calculated by the methods of Ref.12, 14 and 15. As can be seen Ref.12 gives very reasonable agreement until the area ratio A_j/A_m becomes too small, Ref. 15 gives poor agreement throughout the range and Ref.14 gives fairly good agreement at the smallest area ratio.

On increasing the nozzle design Mach number and the area ratio this general pattern is repeated (Figs.38(b)-(f)) reasonable agreement being given by Ref.12 for all nozzles except for numbers 4 and 5.

Ref.14 successfully gives the trend of changes of base pressure with nozzle design Mach number for round nozzles (Fig.39), but not so successfully for square nozzles (Fig.40).

4.3.4 Ratio of jet exit area to ejector area, A_j/A_m

The variation of base pressure with A_j/A_m for the round nozzles appears to be nearly linear (Fig.41) as it was without shroud (Fig.27) but the rate of increase as step height goes down has roughly doubled. This rate of increase is well calculated by Ref.12.

Unfortunately the same linear increase in base pressure is not followed by the square nozzles (Fig.42). It should however be remembered for large A_j/A_m there is considerable doubt as to the uniformity of the jet exit Mach number distribution and the accuracy of the main jet mass flow.

43.5 Ratio of bleed exit area to ejector area A_b/A_m

The increase of base pressure due to reduced bleed velocity is not so large with shroud (Fig.43) as without shroud (Fig.29), however the general trend between the two appears to be well predicted by Ref.12.

43.6 Nozzle divergence angle

Fig.&(a) shows the effect of nozzle divergence angle for round nozzles, the changes being very similar to those for unshrouded nozzles (Fig.26). As has been noted the one dimensional theories do not predict the effect of nozzle divergence angle, and the agreement between the 10° nozzle and the theory of Ref.12 (Fig.&(b)) is not so good as for the equivalent 13° nozzles (Fig.38(b) and (d)).

4.3.7 Jet total pressure

Fig.45 illustrates the effect of jet total pressure on a typical shrouded nozzle. The curves are somewhat similar to those of Fig.32, having a minimum near a pressure ratio of five. A description of the flow changes leading to these shapes is given in Ref.1 and the similarity of the curves indicates that the discussion there applies also to shrouded nozzles. When the pressure ratio is great enough the pressure increase due to bleed is proportionalto jet total pressure as predicted by one-dimensional theories.

4.3.8 Schlieren photographs

Many Schlieren photographs were taken of the flow immediately downstream of the shroud. A seleotion is shown in Figs.46, 47, and 48. Sometimes it

was possible to identify the shock wave which turned the flow streamwise inside the shroud, and by measuring angles and distances one could (by extrapolation) find the longitudinal position of this turn, The results of some of the measurements are shown in Fig.49. They show that m, the distance from the nozzle of the point of flow turning of the jet along the shroud just increases (except for $M_j = 2.45$) and then decreases as bleed is increased. This indicates that base bleed just fills out and elongates the triangle of dead air thereby reducing the expansion at the jet exit and hence *raising* the base pressure. As bleed increases further the decrease in m is explained by assuming that more and more of the secondary air goes straight downstream along the shroud walls and thus forces the origin of the turning shock away from the shroud walls.

4.3.9 Comparison of N.G.T.E. and R.A.E. measurements

Somewhat similar experiments on base bleed[16] were made at the National Gas Turbine Establishment concurrently with the R.A.E. tests.

These tests were made with circular nozzles in circular shrouds and covered a range of free stream Mach numbers from 0.7 to 2.2, but with only two nozzle geometries. A comparison of both shrouded and unshrouded nozzle results can be made (Fig.50) if the N.G.T.E. results are corrected to $p_{Jt}/p_\infty = 16$ (a linear variation with p_{Jt}/p_∞ has been assumed) and if the R.A.E. results are corrected to $\theta_j = 10^\circ$ (the variation with θ_j given in Fig.&(a) has been assumed to hold for $M_j = 2.2$). As A_j/A_m is greater for the N.G.T.E. nozzles it would be expected that the base pressures would be higher. This is so for the shrouded nozzles, but not for the unshrouded ones. The lack of agreement in the unshrouded case is probably due mainly to the influence of the reflection plate which, as was seen earlier substantially *increases* the mean base pressure. Other differences could be due to the difference in shroud shapes, the lack of uniformity of base pressure, and difficulties in measuring secondary mass flow in Ref. 16.

4.3.10 Bleed drag and gross nozzle thrust minus bleed drag (shrouded axisymmetric nozzles)

Knowing the static pressure at the bleed exit and the bleed mass flow, *net* bleed drag i.e. the change of momentum from free stream conditions to the bleed exit, can readily be calculated.

As can be seen fromFig.51, minimum bleed drag is obtained at $2\frac{1}{2}\%$ bleed flow for the two highest nozzle design Mach numbers; the minimum then shifts progressively to about 5% bleed flow as M_j decreases to 1.0. This minimum value also decreases considerably with decrease of M_j.

These bleed drags can be combined with a calculated nozzle gross thrust T_{G_θ}, using nozzle efficiencies (which take account of nozzle skin friction and divergence angle losses) supplied by NGTE and quoted in Table 1 to give an overall thrust efficiency $\frac{T_{G_\theta} - D_{B_L}}{T_{G_{ideal}}}$. As can be seen in Fig.52 the large decreases in bleed drag obtained by decreasing M_j are substantially outweighed by decreases in nozzle gross thrust so that as regards design point performance there appears to be no advantage in deliberately underexpanding the primary nozzle.

Fig.53 shows the effect of both nozzle design Mach number and the jet-exit-to-shroud area ratio on bleed drag. As has been seen (apart from the results of Fig.42) base pressure rises as 'step height' decreases, but the bleed drag does not drop as rapidly as the base pressure rises because of the smaller area over which the higher pressure acts. Thus the tendency towards optimum step heights indicated in Fig.53 is obtained. The optimum step height may not of course coincide with the difference between the fully expanded nozzle exit area and the maximum cross-section of the nacelle. In this case the optimum arrangement is probably a combination of the near optimum step height and a small amount of externalboattailing.

The tests do not establish an optimum configuration as regards nozzle design Mach number and step height, nevertheless the indications from Figs.54 and 55 are that:-

(a) If low total head air flow, say, an intake boundary layer bleed has to be disposed of, then ducting it through a vented base surrounding the nozzle can lead to high propulsive efficiencies.

(b) If it is desired to deliberately sacrifice some cruise nozzle efficiency by choosing an under-expanded nozzle so as to ease transonic thrust penalties or geometry changes then a base bleed can enhance the propulsive efficiency by 1-2%.

Fig.56 introduces calculations making certain assumptions about the rear end geometry. The base bleed curves from Fig.54 are repeated for ease of comparison. If an aircraft engine size is fixed it may be assumed that the ratio of the nacelle maximum cross-section to nozzle throat area is also fixed, and allowance must be made for this in comparing the two nozzles 2 and 13 which have different values cf A_m/A^*_j. This has been done by assuming that the

nozzle with the larger throat relative to the maximum cross-sectional area has been installed in a boattailed body so that the results obtained at small step heights can be used. A $2\frac{1}{2}^{o}$ boattail yielded the equivalent D/TG_{ideal} of 0.005.

With no boundary layer bleed air to dispose of high propulsive efficiencies can be achieved by allowing the nozzles to expand to the full area of the nacelle base, although no allowance has been made for the change of shape from circular to square,

Assuming the total head of the boundary layer air is 0.3 of the free stream total head, we see that for nozzle 13 and $2\frac{1}{2}\%$ bleed the base bleed solution is marginally better than disposal through a convergent-divergent nozzle, indicating as before that base bleed is well to the fore among the solutions that must be considered.

5 CONCLUSIONS

The experiment has demonstrated for a number of different configurations the increase of base pressure which can be produced by bleeding low energy air into the *base* area surrounding the primary jet. *In many cases* the pressure can be raised above ambient level ($p_b / p_\infty > 1$), thereby providing a thrust which tends to offset the bleed internal drag.

The more important detail results are as follows:-

(i) The addition of a shroud of sufficient length raises the base pressure by an amount strongly dependent on the base pressure without shroud.

(ii) When used with care, the one-dimensional theory of Ref.12 is capable of predicting trends of shrouded base pressure movement.

(iii) The addition of bleed flow to a shrouded base raises base pressure considerably. For bleed flows less than $2\frac{1}{2}\%$ of the primary jet flow, and for ratios of jet exit area to maximum area less than 0.7, this increase is more than enough tc compensate for the drag cf the bleed air.

(iv) If boundary layer air must be disposed of, a combination of base bleed and boattailing may be better than any arrangements in which the low total head air is disposed of separately from the primary nozzle.

6 FURTHER WORK

The conclusions of this paper have indicated that the trends follow simple one-dimensional theories, but that absolute values differ. This suggests that the situation is complex and leaves room for further experimental work to explore means of achieving the highest possible base pressures,

Acknowledgment

The author is indebted to Mr. E.L. Goldsmith for many helpful. suggestions through all stages of the work.

Table 7

Round nozzle dimensions

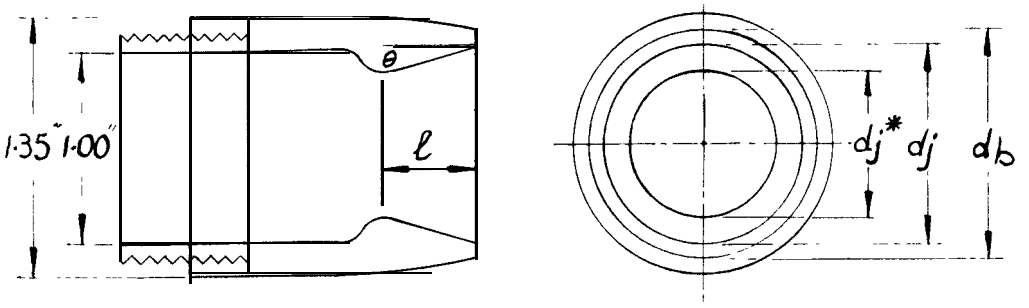

Nozzle	M_j	d_j^*	A_j^*	A_j	A_j/A_m	d_b	θ	$\eta_{F_{max}}$
1	2.453	0.846	0.562	1.419	0.654	1.350	13°	0.983
2	2.223	0.847	0.563	1 150	0.530	1.350	13°	0.980
3	1.949	0.846	0.562	0.909	0.419	1.350	13°	0.976
4	1.567	0.846	0.562	0.688	0.317	1.350	13°	0.980
5	1.000	0.845	0.561	0.562	0.259	1.350	13°	0.999
8	1.951	0.845	0.561	0.909	0.419	1.144	13°	0.976
10	1.884	0.846	0.562	0.863	0.398	1.144	10°	0.986
11	1.884	0.846	0.562	0.863	0.398	1.144	16°	0.967
12	1.884	0.846	0.562	0.863	0.398	7.144	20°	0.959
13	2.192	0.956	0.717	1.427	0.658	1.350	13°	0.980
14	1.867	0.956	0.717	1.086	0.507	1.350	13°	0.975
15	7.861	0.905	0.644	0.971	0.458	1.350	13°	0.975

Table 2

Square nozzle dimensions

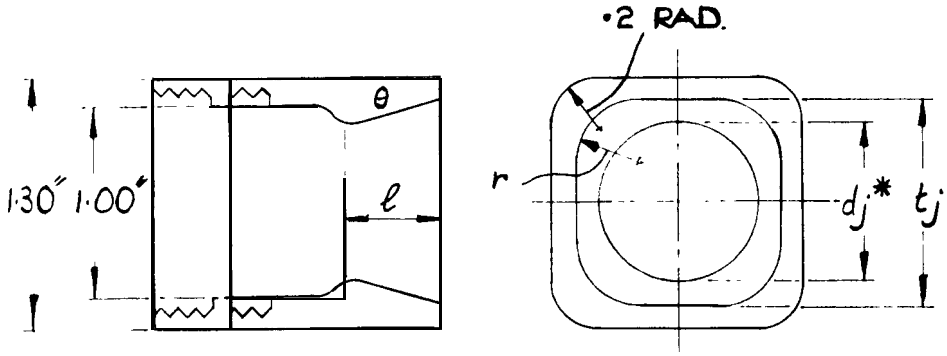

Nozzle	M_j	d_j^*	A_j^*	t_j	r	A_j	A_j/A_m	θ	$\bar{\theta}$
A	2.444	0.929	0.679	7.315	0.198	1.697	0.782	13°	17° 39'
B'	1.925	0.926	0.674	7.077	0.326	1.069	0.493	13°	18° 28'
C	2.102	0.930	0.679	7.162	0.336	1.248	0.575	13°	18° 53'
D	2.266	0.952	0.712	7.252	0.250	1.574	0.698	13°	17° 45'
E	2.002	0.946	0.703	7.125	0.300	1.188	0.547	13°	17° 38'
F	2.208	0.970	0.739	1.248	0.275	1.493	0.688	13°	18° 10'
G	2.009	0.984	0.761	7.752	0.200	1.293	0.596	13°	18° 03'
H	2.424	0.926	0.674	7.298	0.200	1.655	0.763	10°	13° 27'
J	2.242	0.918	0.662	7.203	0.275	1.382	0.637	10°	13° 46'
K	1.962	0.921	0.666	7.100	0.375	1.089	0.502	10°	13° 56'

Symbols

A_{B_P} Base area over which base pressure acts. Includes bluff nozzle base and vented area. Excludes base of shroud

A_{B_M} Base area used for determining Mach number of bleed flow. Vented area only

A_M Internal shroud area

A_j Plane nozzle exit area

A_j^* Plane nozzle throat area

M_B Mach *number at* bleed exit

M_j Mach number at nozzle exit

M_∞ Mach number in free stream

p_B base pressure, static pressure at bleed exit

p_{B_T} bleed total pressure

p_j static pressure at jet exit

p_{j_t} jet total pressure

p_∞ free stream static pressure

p_{∞_T} free stream total pressure

μ ratio of bleed flow to nozzle flow

$F_{G_{ideal}}$ fully expanded isentropic gross thrust corresponding to pressure ratio p_{j_t}/p_∞

T_{G_θ} calculated gross thrust of nozzle at given exhaust pressure ratio

D_B net bleed drag $= \gamma M_\infty^2 \frac{p_\infty}{p_{\infty_t}} \frac{A_\infty}{A_\infty^*} p_{j_t} A_j^* \cdot \mu$

$$- A_{B_M} \{(p_B - p_\infty) + \gamma M_B^2 p_B\}$$

γ ratio of specific heats

$\eta_{F_{max}}$, gross thrust efficiency of primary nozzle $= \dfrac{\text{measured gauge thrust at design pressure ratio}}{\text{gauge thrust of an isentropic nozzle passing the same flow at the same pressure ratio fully expanded}}$

$$\frac{T_{G_\theta} - D_B}{T_{G_{ideal}}} = \frac{1}{\gamma M^2_{jfe.} \frac{A_{jfe.}}{A^*_j} \frac{}{p_{j_t}}} \left\{ \frac{p_j A_j}{A^*_j p_{j_t}} + \frac{\eta_{F_{max}} \gamma M_j A_j p_j}{A^*_j p_{j_t}} \right.$$

$$\left. + \frac{A_{B_p} p_B}{A^*_j p_{j_t}} \left(1 + \gamma \frac{A_{B_M}}{A_{B_p}} M^2_B\right) - \frac{p_\infty A_M}{p_{j_t} A^*_j} - \gamma \frac{p_\infty}{p_{\infty_t}} \frac{A_\infty}{A^*_\infty} M^2_\infty \cdot \mu \right\}$$

where

$$\frac{A_\infty}{A^*_\infty} = \frac{A}{A^*} \text{ corresponding to } M_{CO}$$

$$\frac{A_{jfe.}}{A^*_j} = \frac{A}{A^*} \text{ corresponding to } M_{jfe.}$$

$M_{jfe.}$ = Mach number corresponding to the pressure ratio $\frac{p_\infty}{p_{j_t}}$ (= 1/16 in all the calculations).

REFERENCES

No.	Author	Title, etc
1	J. Reid R.C. Hastings	The effect of a central jet on the base pressure of a cylindrical afterbody in a supersonic stream. A.R.C. R & M 3224, December 1959
2	I. Leynaert J.M. Brasseur	Problèmes d'aérodynamique interim posés par l'avion de transport supersonique Mach 2. 5th congrès Aéronautique Européan: Venice September 1962
3	E. Eminton	Simple theoretical and experimental studies of the flow through a three shock system in a corner. A.R.C. C.P. 727, September 1961
4	J. Reid R.C. Hastings	Experiments on the axisymmetric flow over afterbodies and bases at M = 2.0. R.A.E. Report Aero 2628, October 1959, A.R.C. 21707
5	L. Fuller J. Reid	Experiments on two-dimensional base flow at M = 2.4. A.R.C. R & M 3064, February 1956
6	J.F. Nash	An analysis of two dimensional turbulent base flow including the effect of the approaching boundary layer. A.R.C. R & M 3344, July 1962
7	E.M. Cortright A.H. Schroeder	Preliminary investigation of effectiveness of base bleed in reducing drag of blunt base bodies in supersonic stream. NACA RM E51A26, March 1951
8	D.R. Chapman	Aerodynamic characteristics of bodies at supersonic speeds - Base pressure on wings end bodies with turbulent boundary layers. NACA RM A51J25, November 1951
9	A.F. Bromm R.M. O'Donnell	Investigation at supersonic speeds of the effect of jet Mach number and divergence angle of the nozzle upon the pressure of the base annulus of a body of revolution. NACA RM L54I16, December 1954

REFERENCES (Contd)

No.	Author	Title. etc
10	P. Carrière M. Siriéix	Facteurs d'influence du recollement d'un écoulement supersonique. ONERA Publication 102 (1961)
11	W.L. Chow A.L. Addy	Interaction between primary and secondary streams of supersonic ejector systems and their performance characteristics. AIAA Journal Vol.2 No.4 pp 686-695, 1964
12	F.D. Kochendorfer M.D. Rousso	Performance characteristics of aircraft cooling ejectors having short cylindrical shrouds. NACA RM E51E01 May 1951
13	J. Fabri J. Paulon	Theory and experiment on supersonic air-to-air ejectors. NACA TM1410 September 1958
14	H. Pearson J.B. Holliday S.F. Smith	A theory of the cylindrical ejector supersonic propelling nozzle. Journal of R.Ae.Soc, Vol.62 pp 746-751, 1958
15	N.C.S. Filleul	Basic theory of the supersonic ejector nozzle. A.R.C. 25,646
16	J.B. Roberts G.T. Golesworthy	An experimental investigation of the influence of base bleed on the base drag of various propelling nozzle configurations. .A.R.C. C.P. 892, February 1964

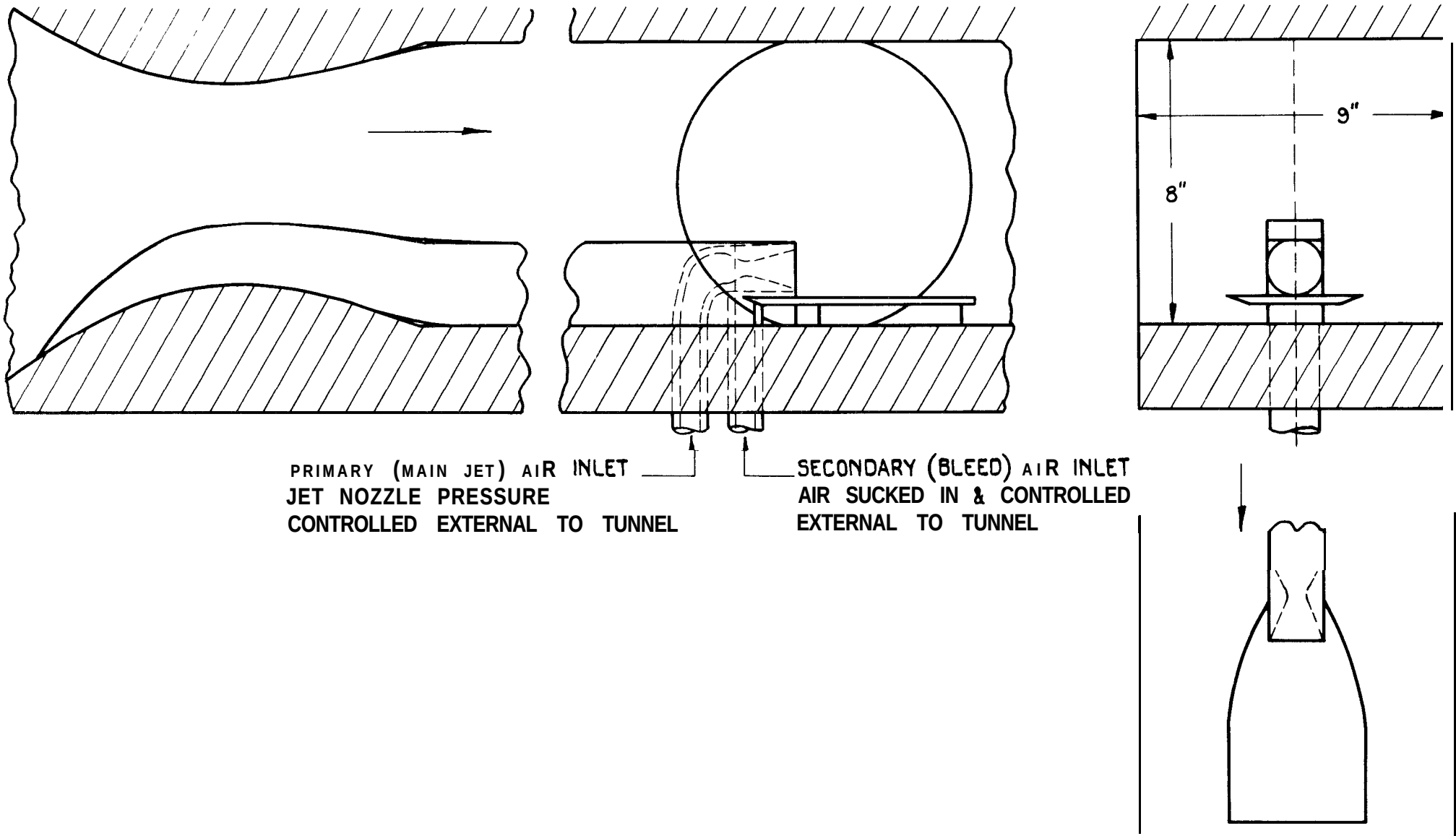

FIG. I GENERAL ARRANGEMENT OF THE RIG.

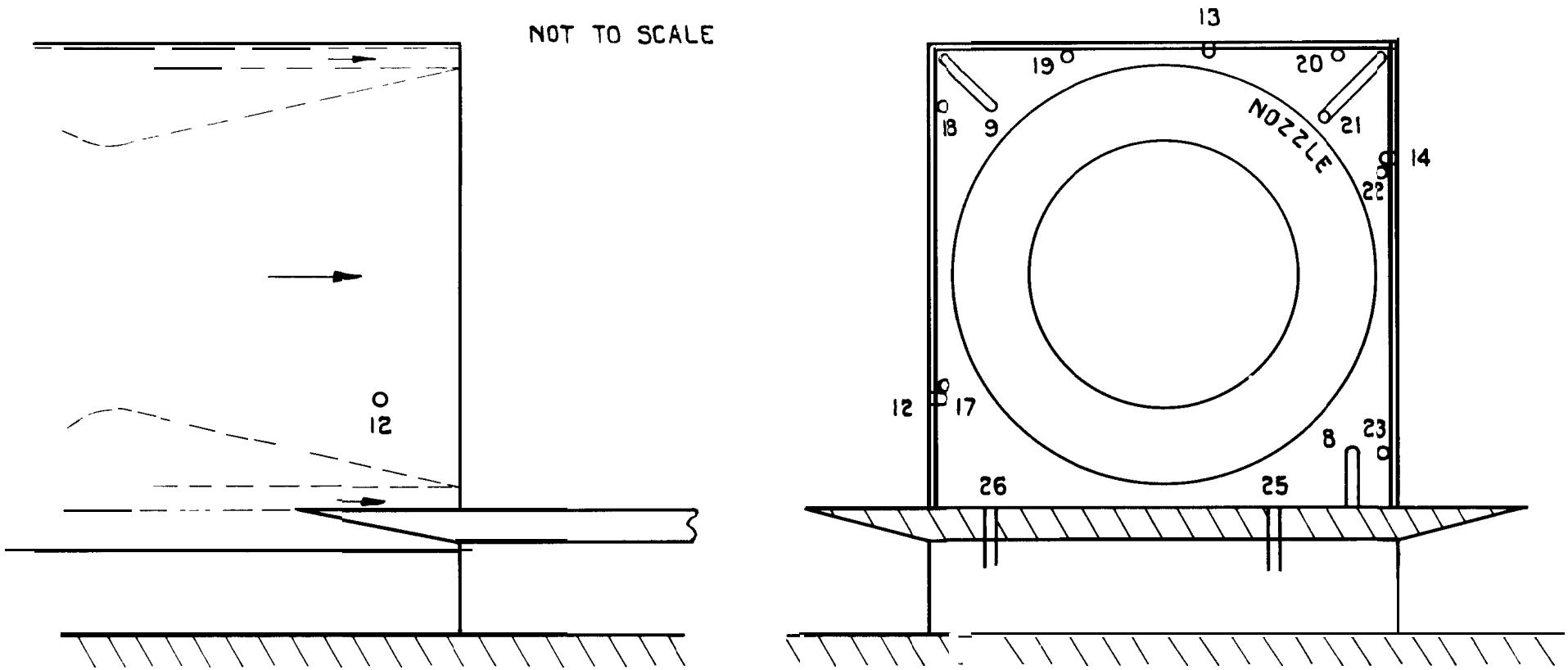

FIG 2 DETAILS OF PRESSURE TUBES NEAR THE BASE

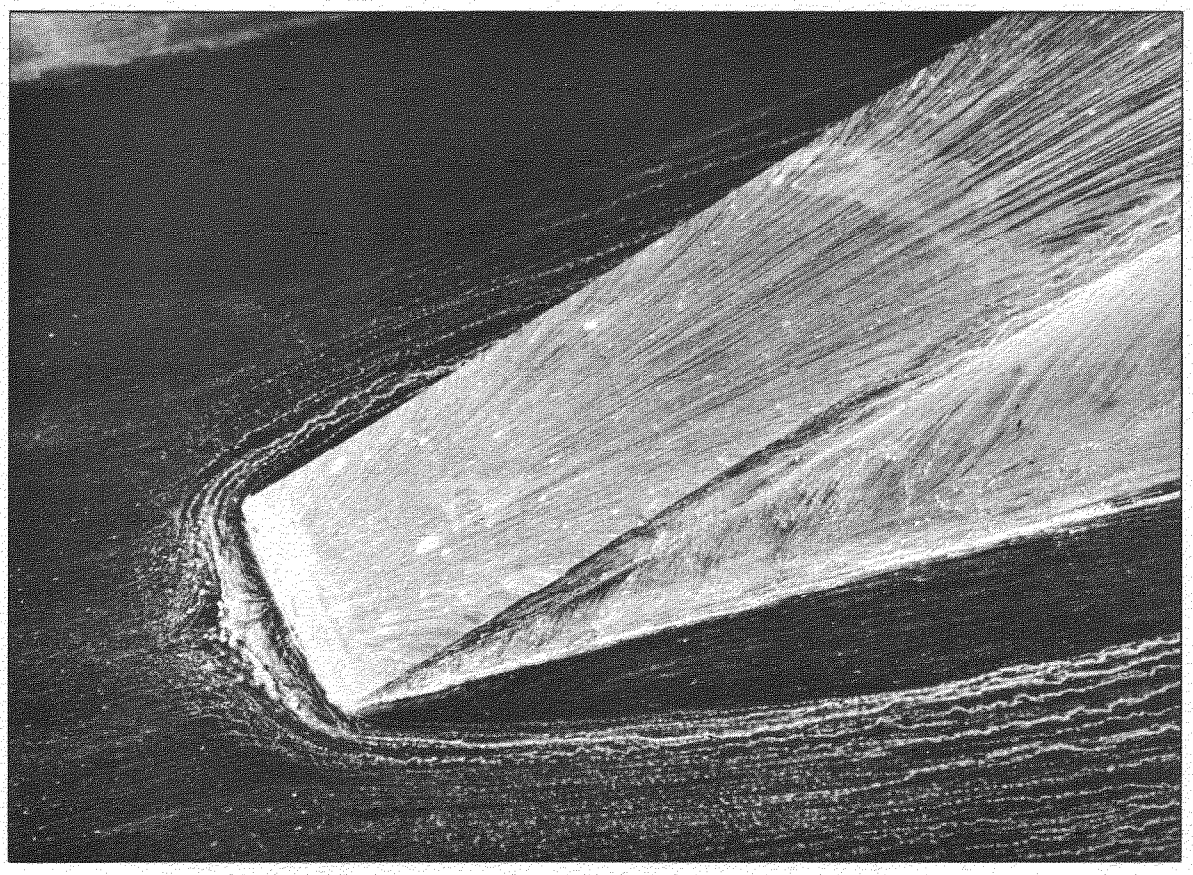

Fig.3. Flow on a wedge

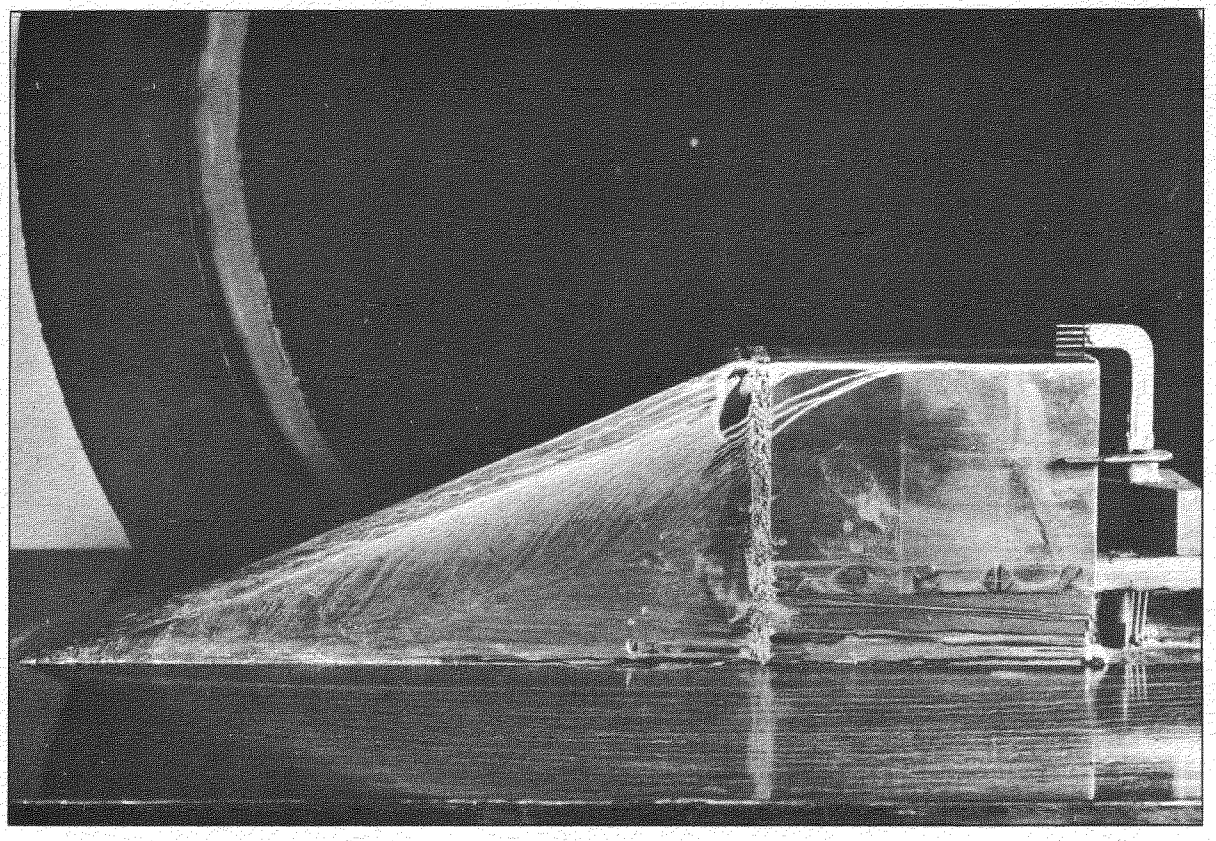

Fig.4. Vortices on the wedge side

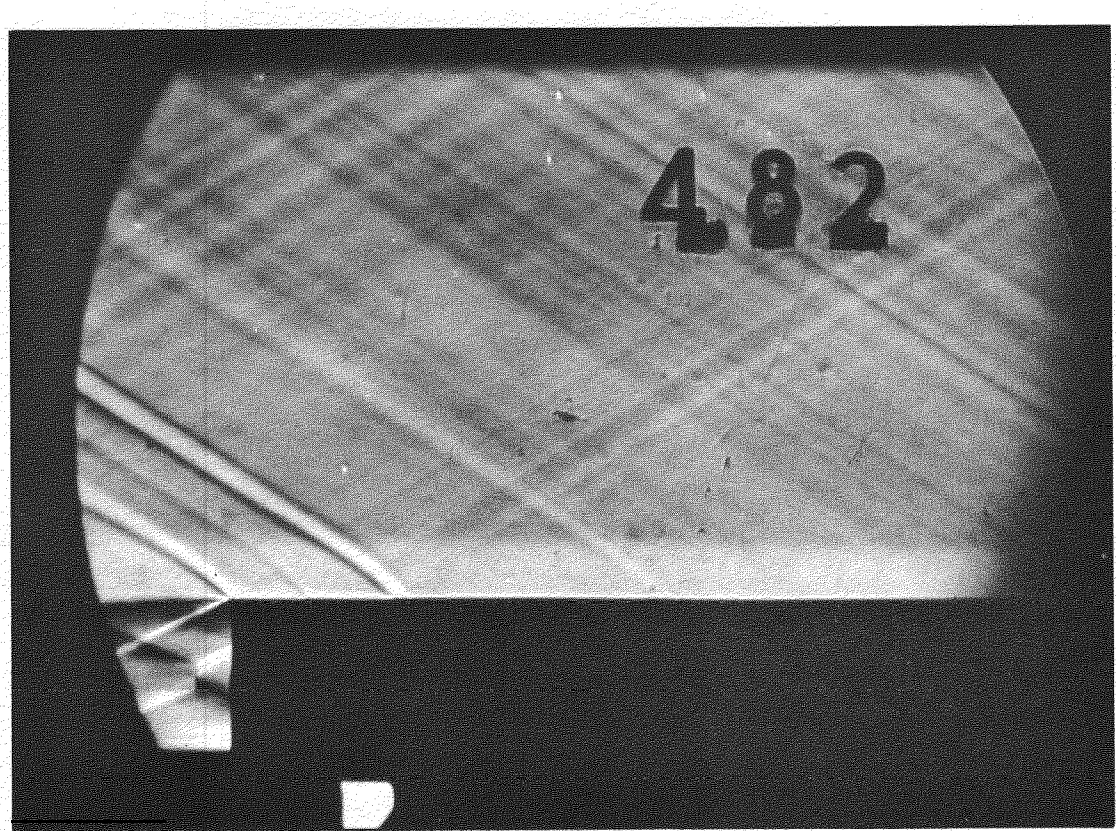

Fig.5. Tunnel and boundary layer flow, shrouded

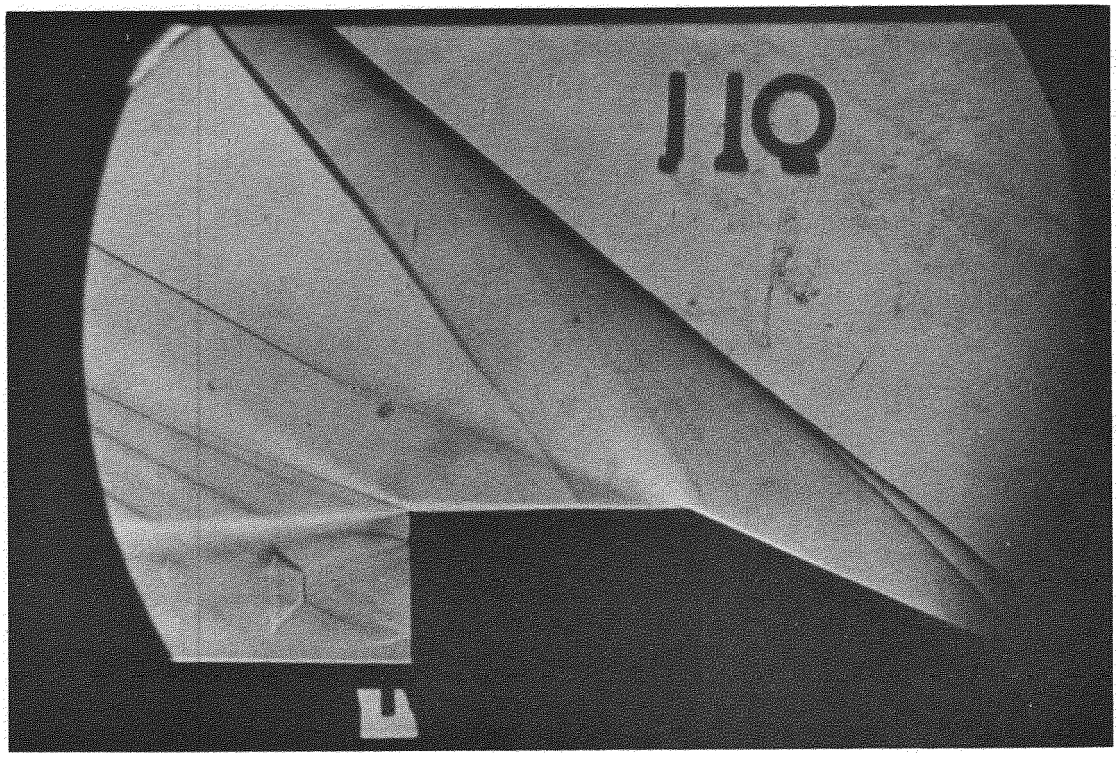

Fig.6. Tunnel and interference flow, unshrouded

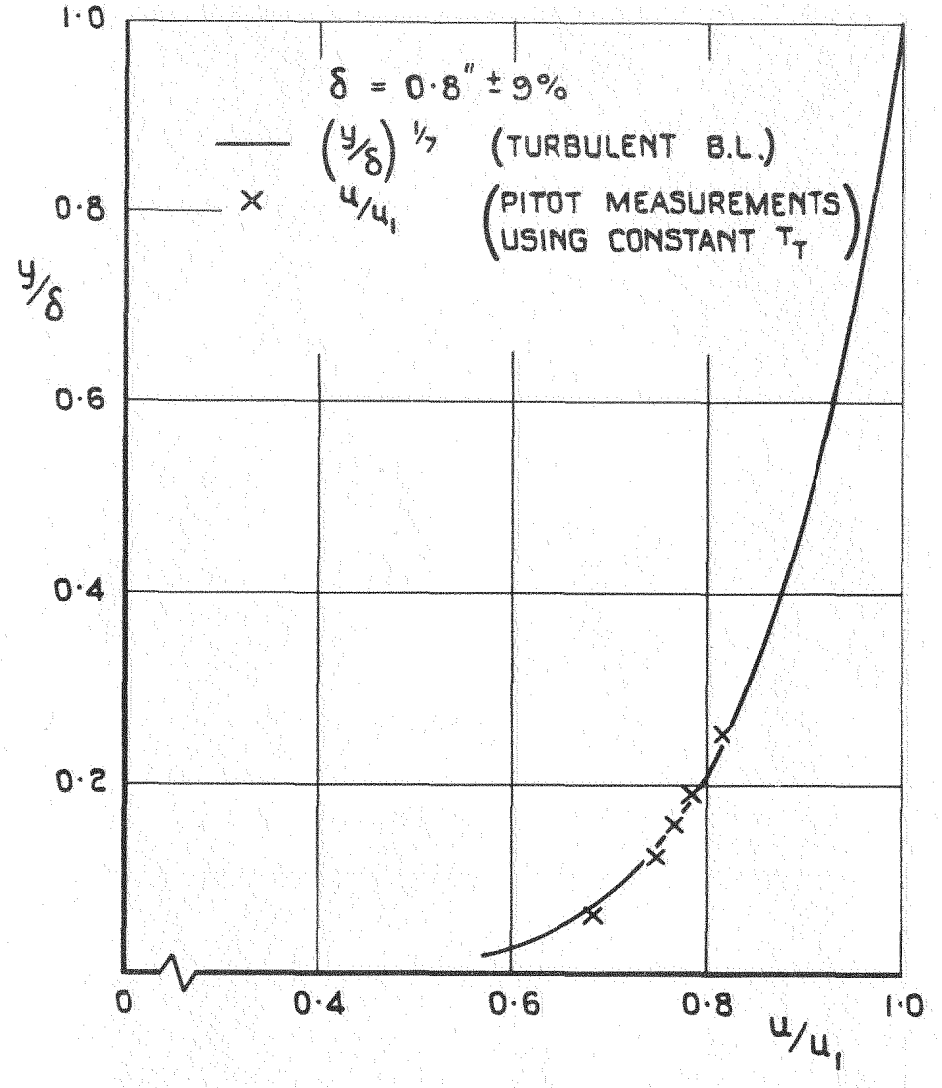

FIG. 7 FAIRING TOP BOUNDARY LAYER

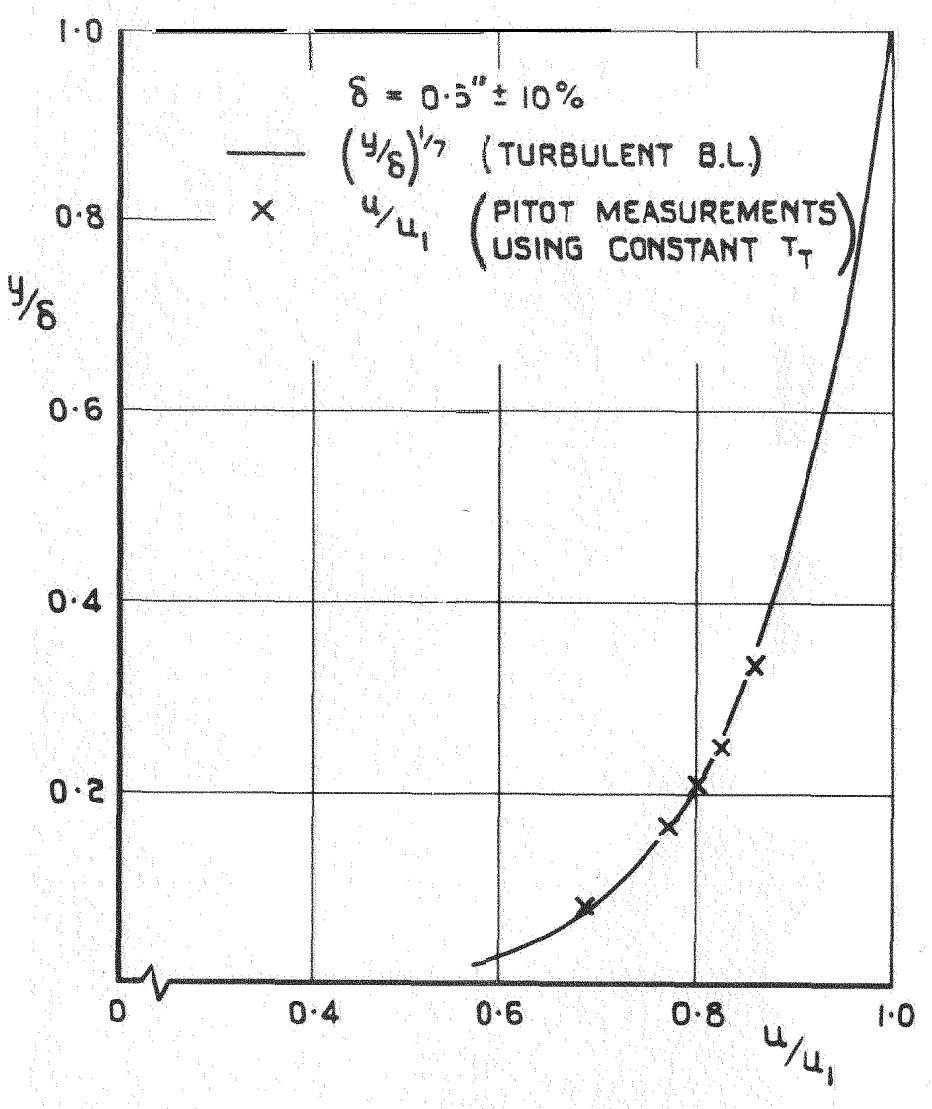

FIG. 8 FAIRING SIDE BOUNDARY LAYER

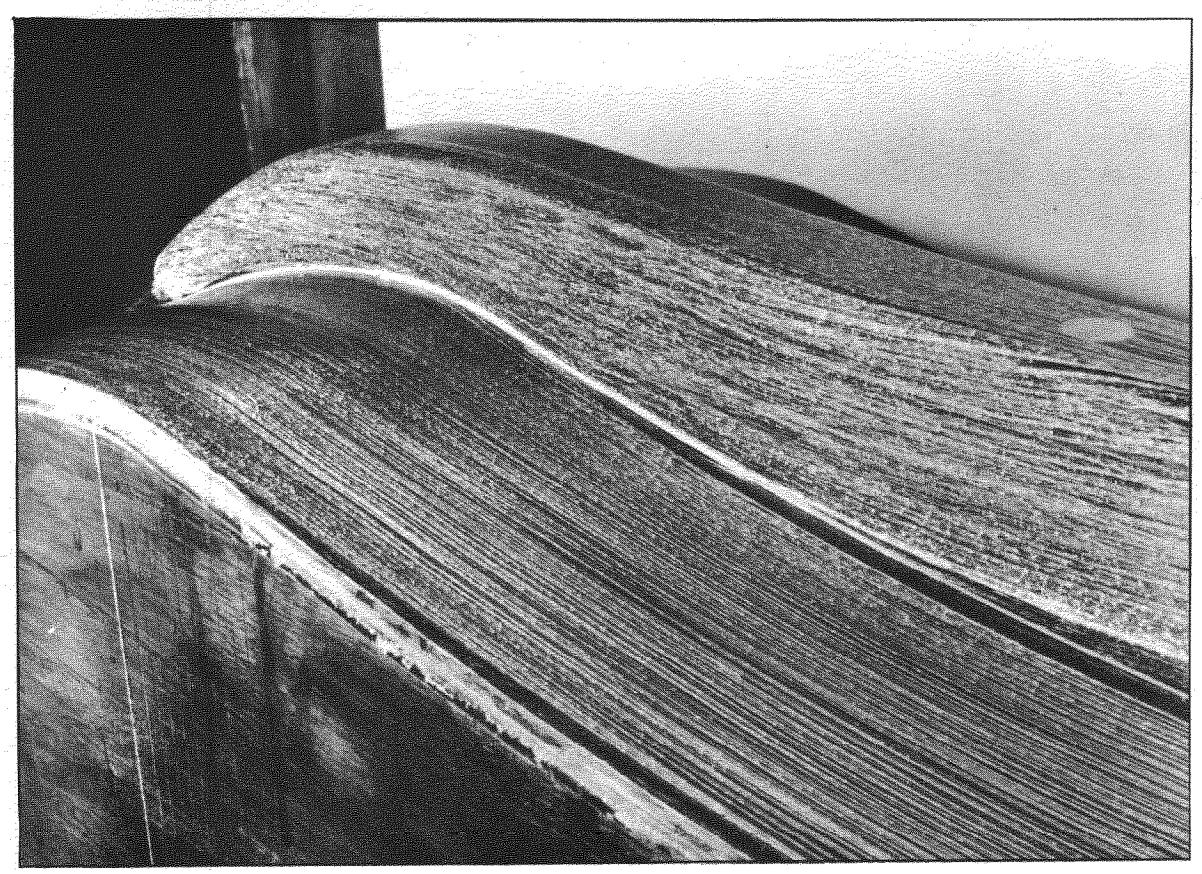

Fig.9. Throat end of long fairing

Fig.10. Model end of long fairing

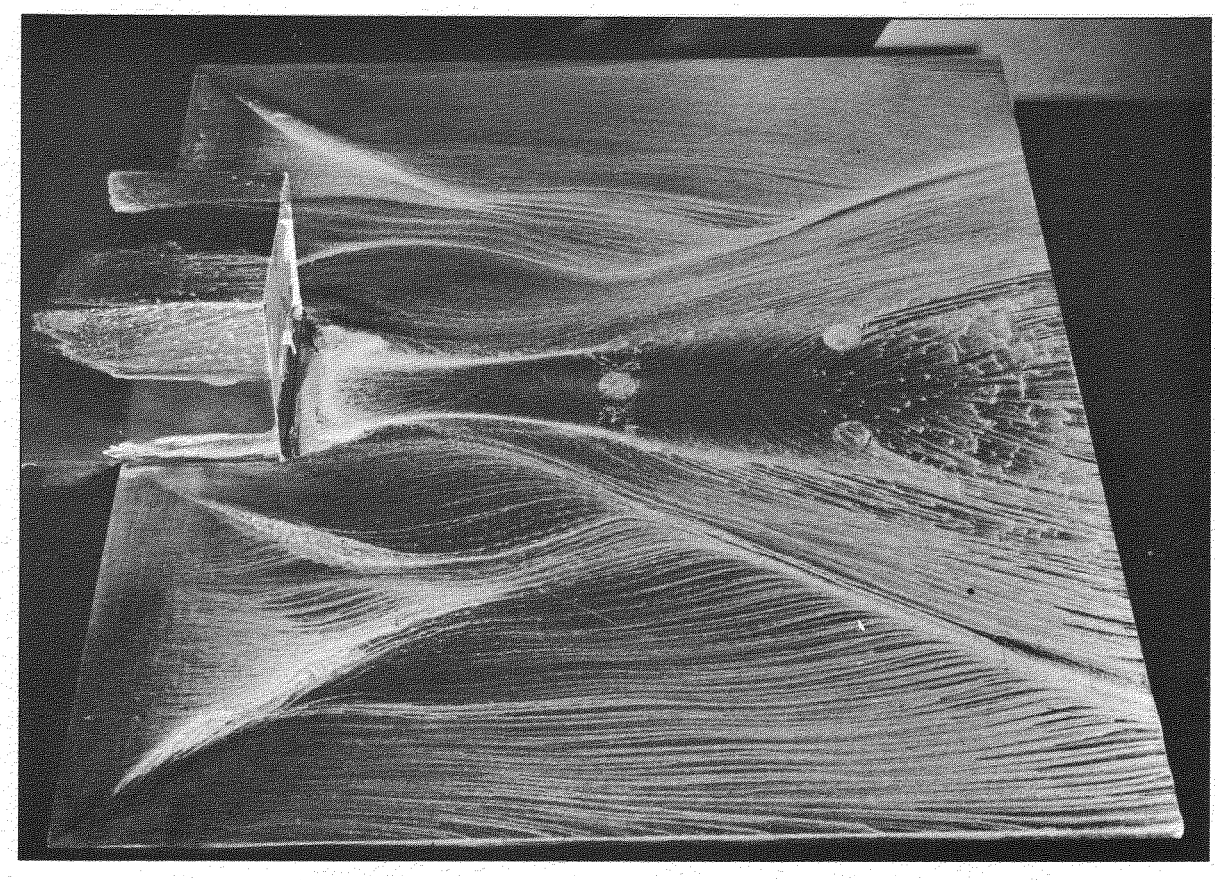

Fig.11. Oil flow, no jet or bleed

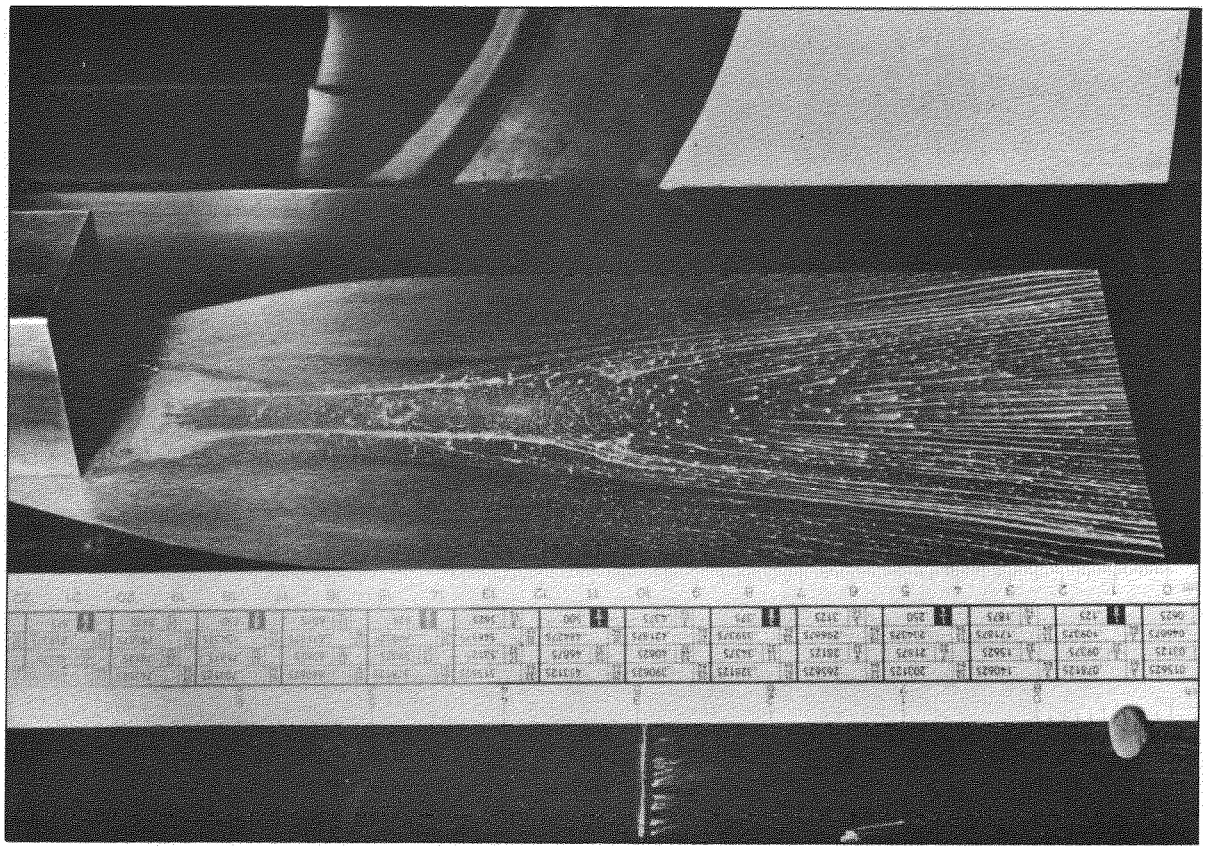

Fig.12. Oil flow, no jet or bleed

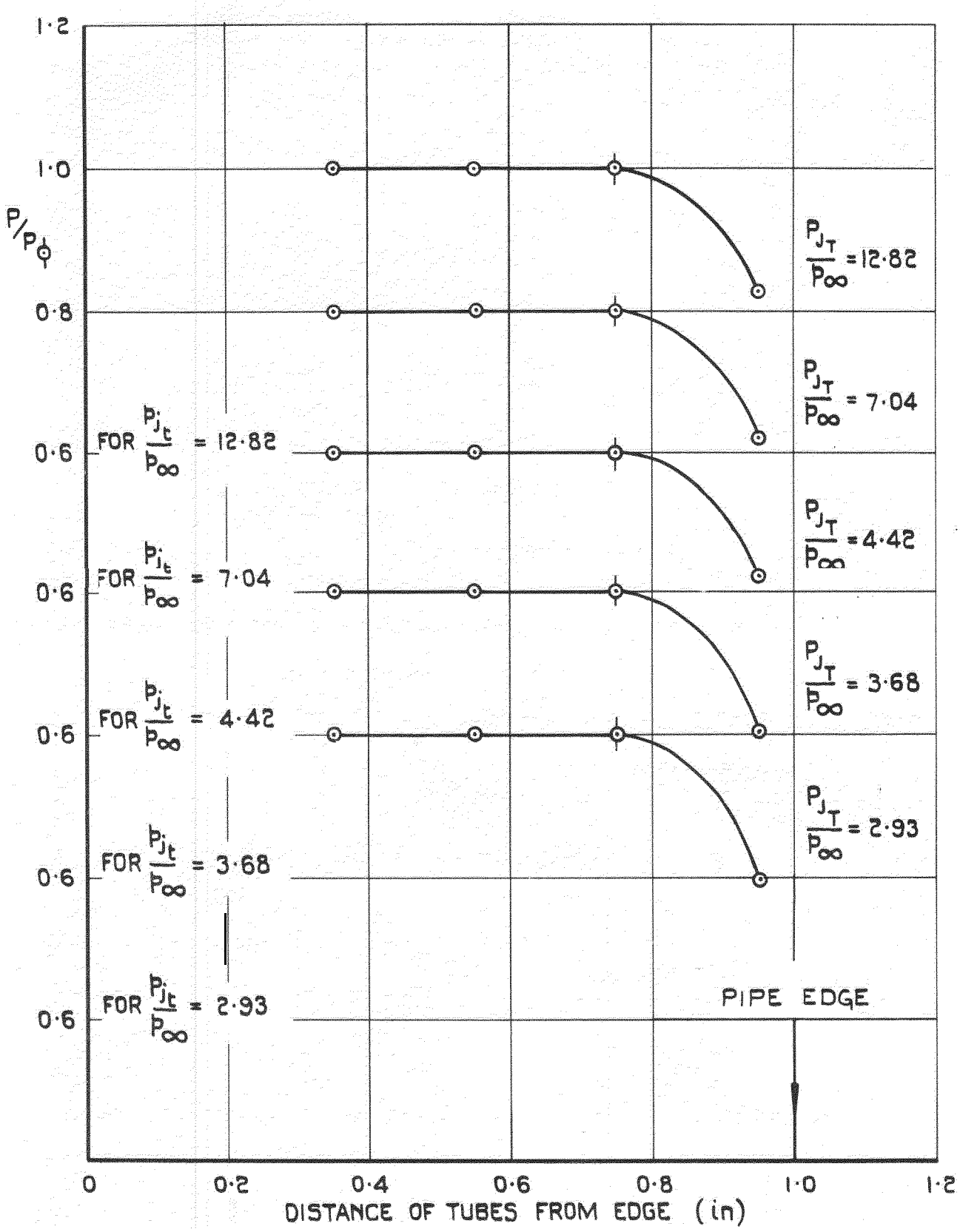

FIG. 13 TOTAL PRESSURE DISTRIBUTION IN SUPPLY PIPE

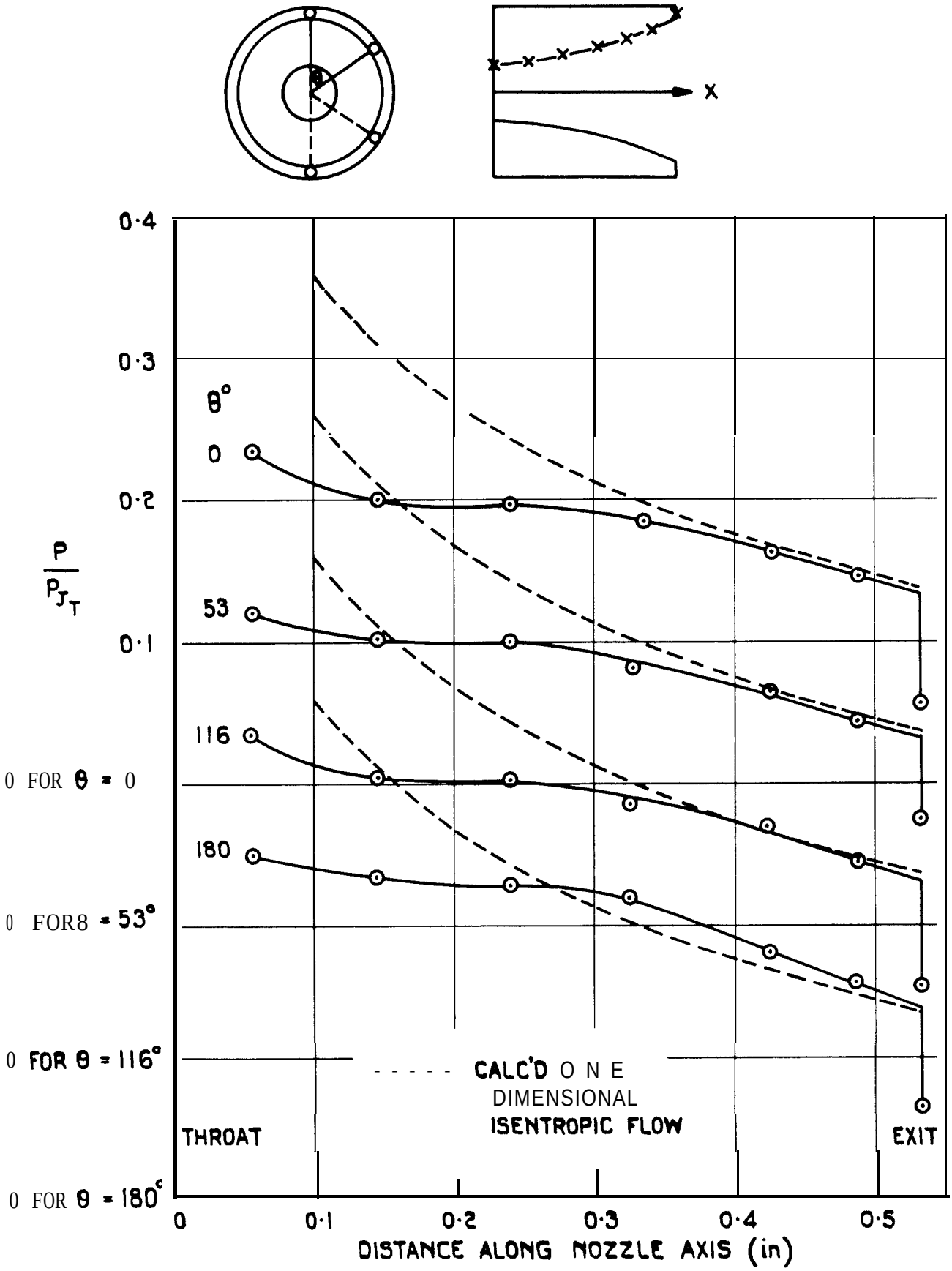

FIG 14 NOZZLE 3, INTERNAL PRESSURE DISTRIBUTION

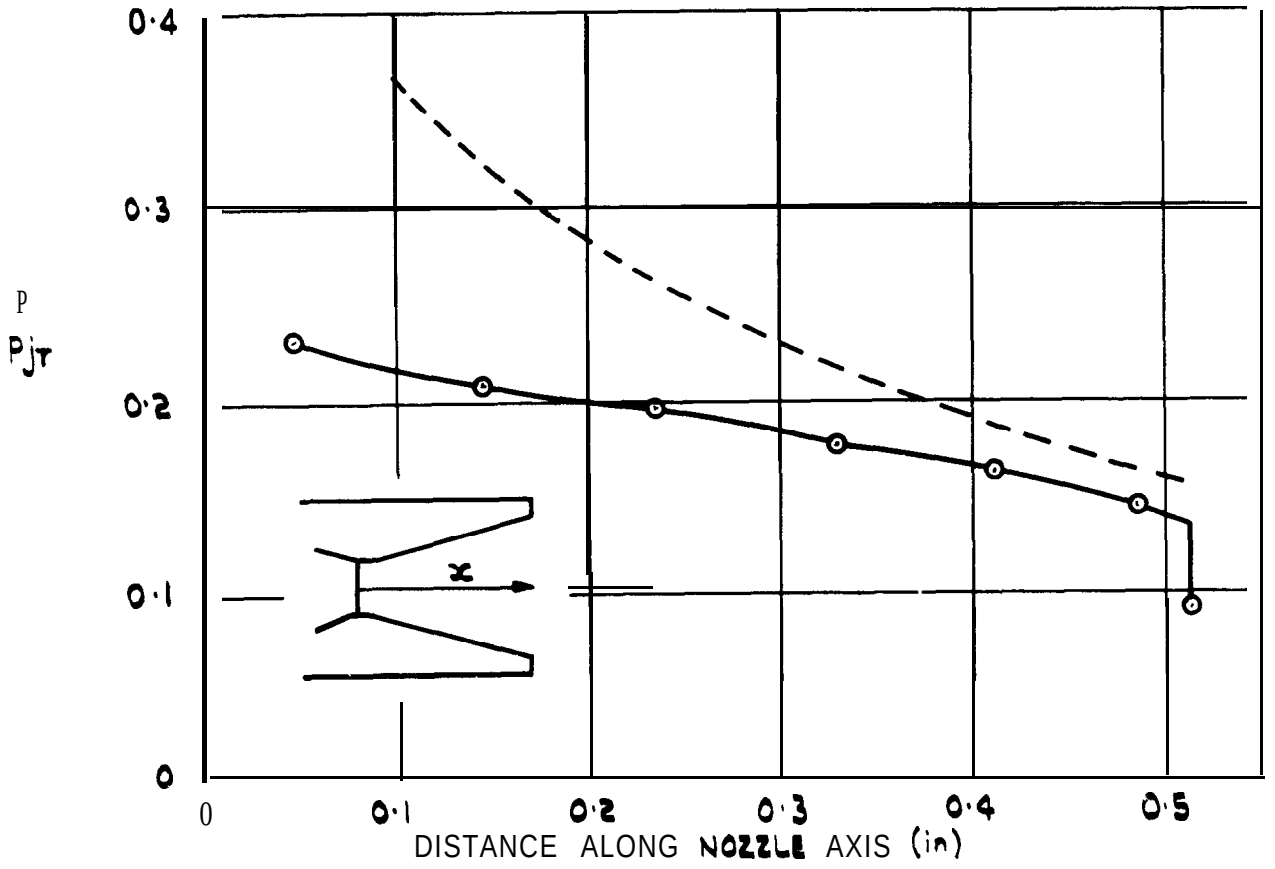

FIG.15 (a) NOZZLE 15 Mj = 1·89 A_j/A_m = ·458

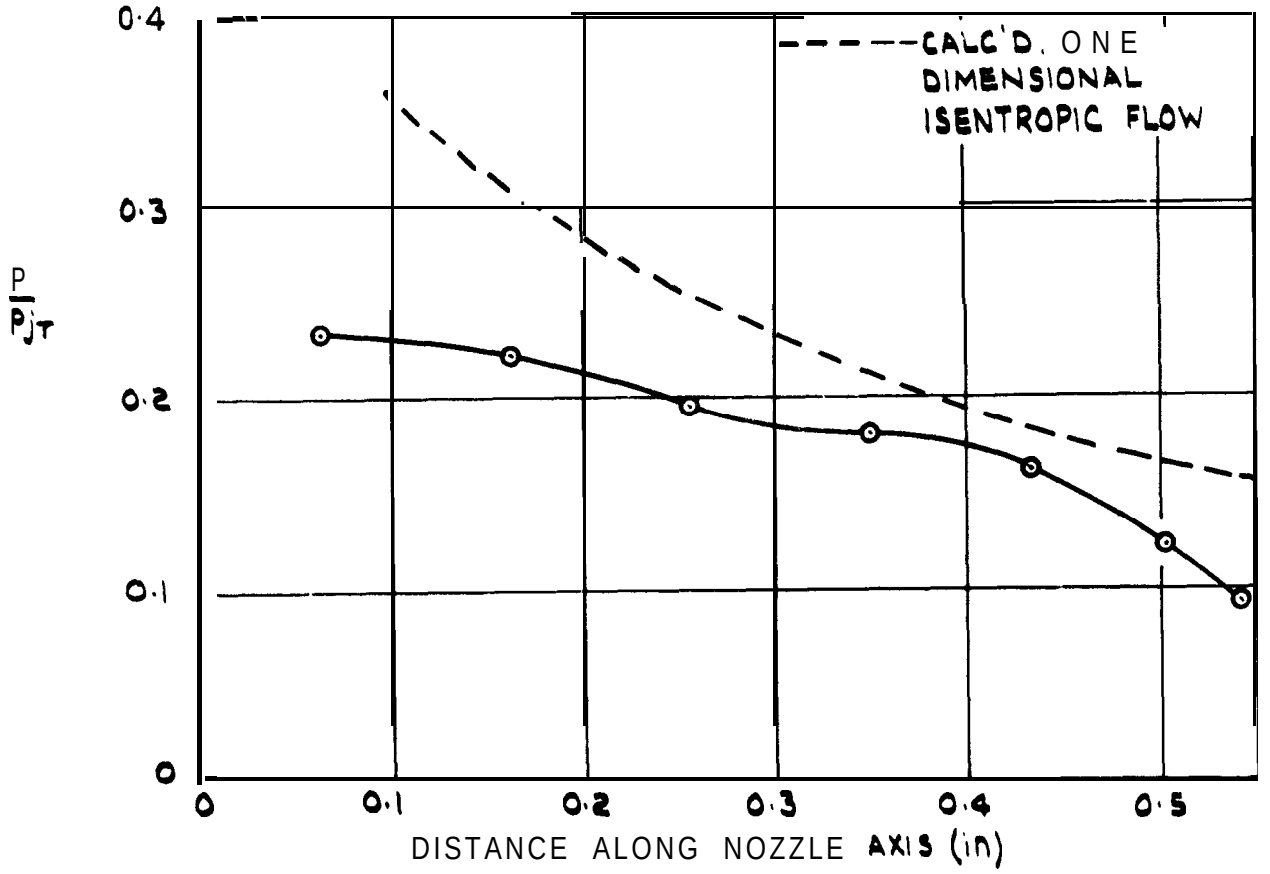

FIG. 15 (b) NOZZLE 14 Mj = 1·88 A j/A_m = ·507

FIG. 15 INTERNAL PRESSURE DISTRIBUTIONS

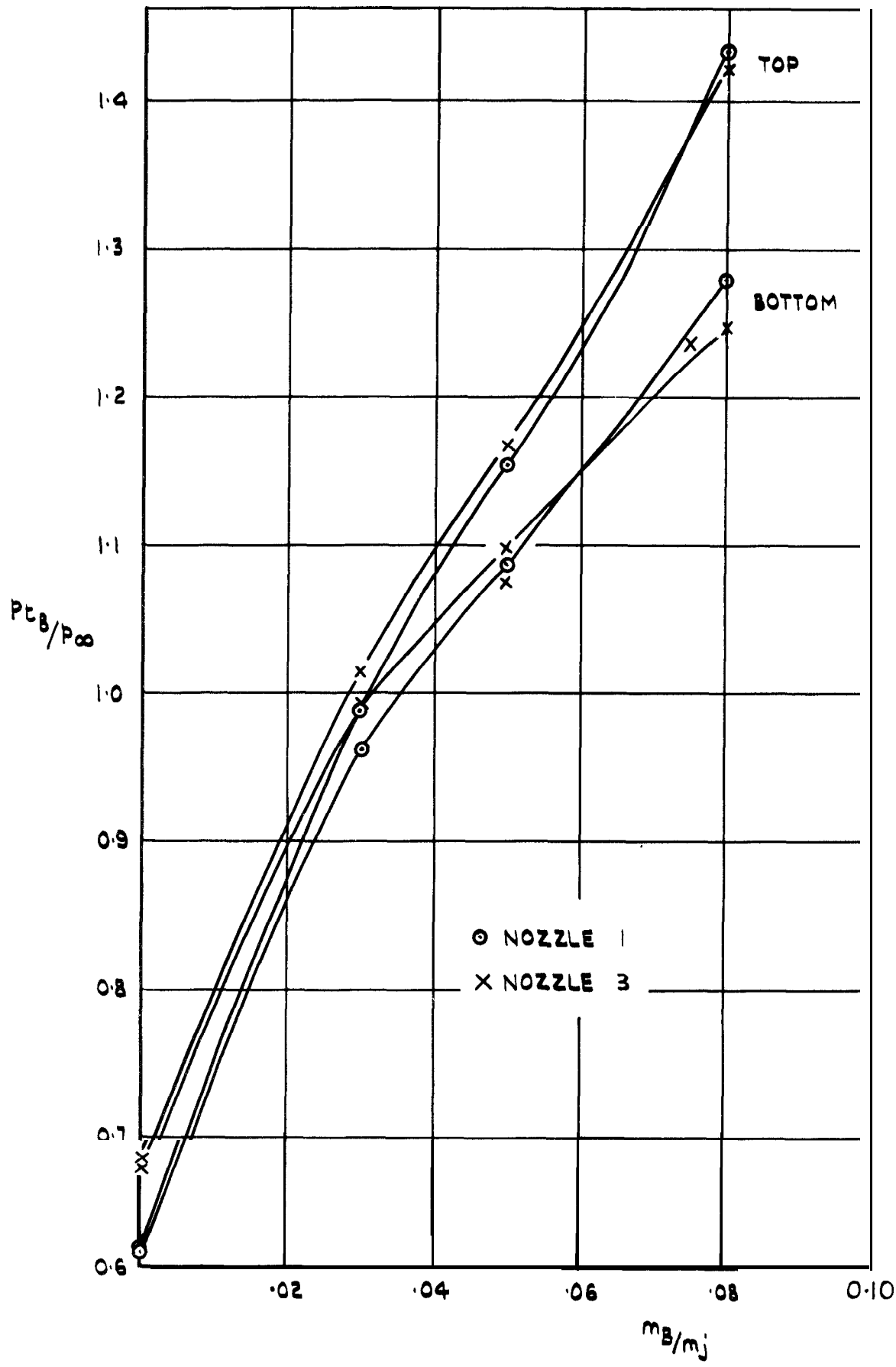

FIG. 16 BLEED TOTAL PRESSURE vs BLEED FLOW, (UNSHROUDED)

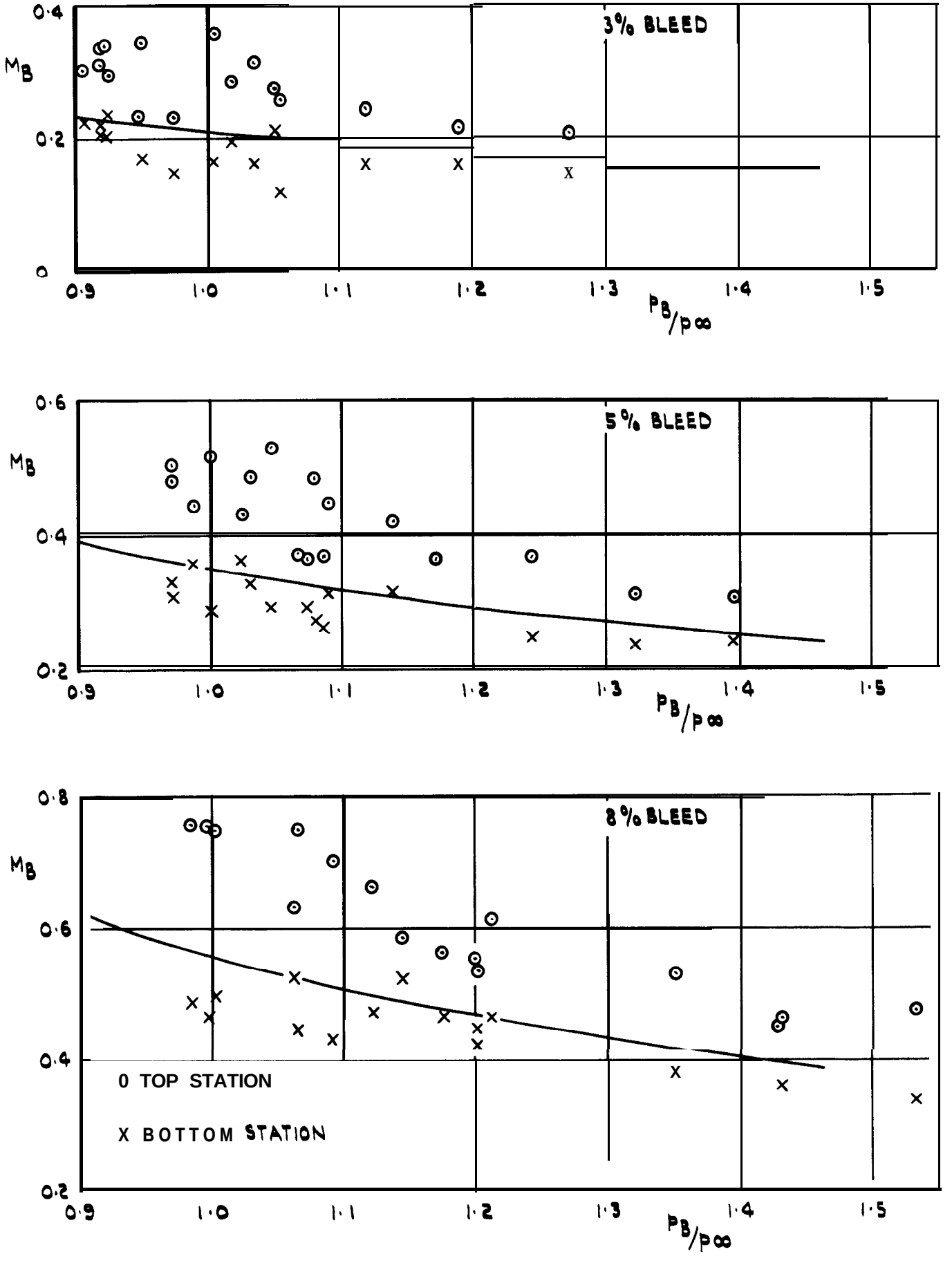

FIG.17 BLEED MACH NUMBER vs BASE PRESSURE

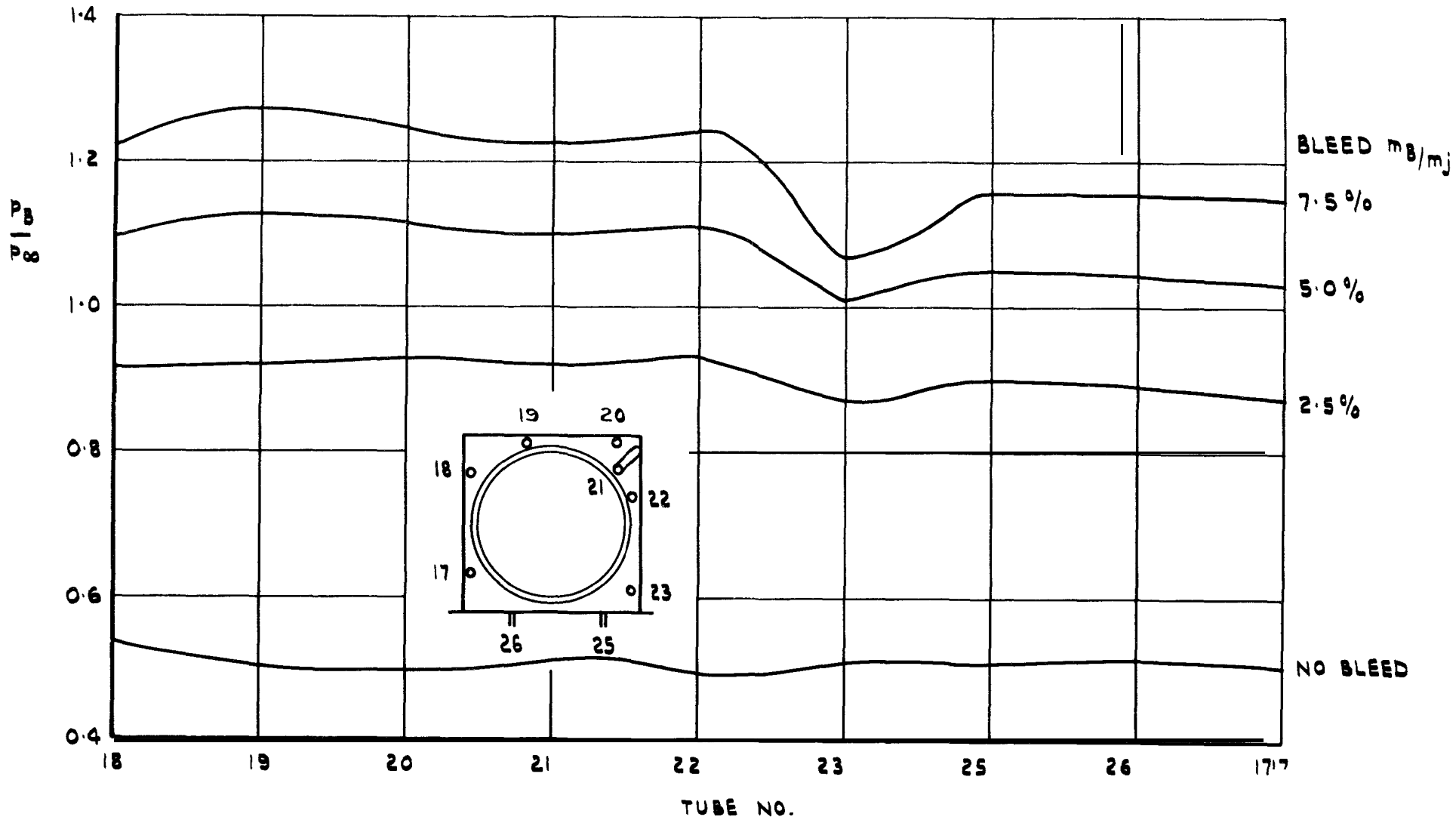

FIG. 18 DISTRIBUTION OF BASE PRESSURE ROUND THE EXIT (NOZZLE 1, SHROUDED

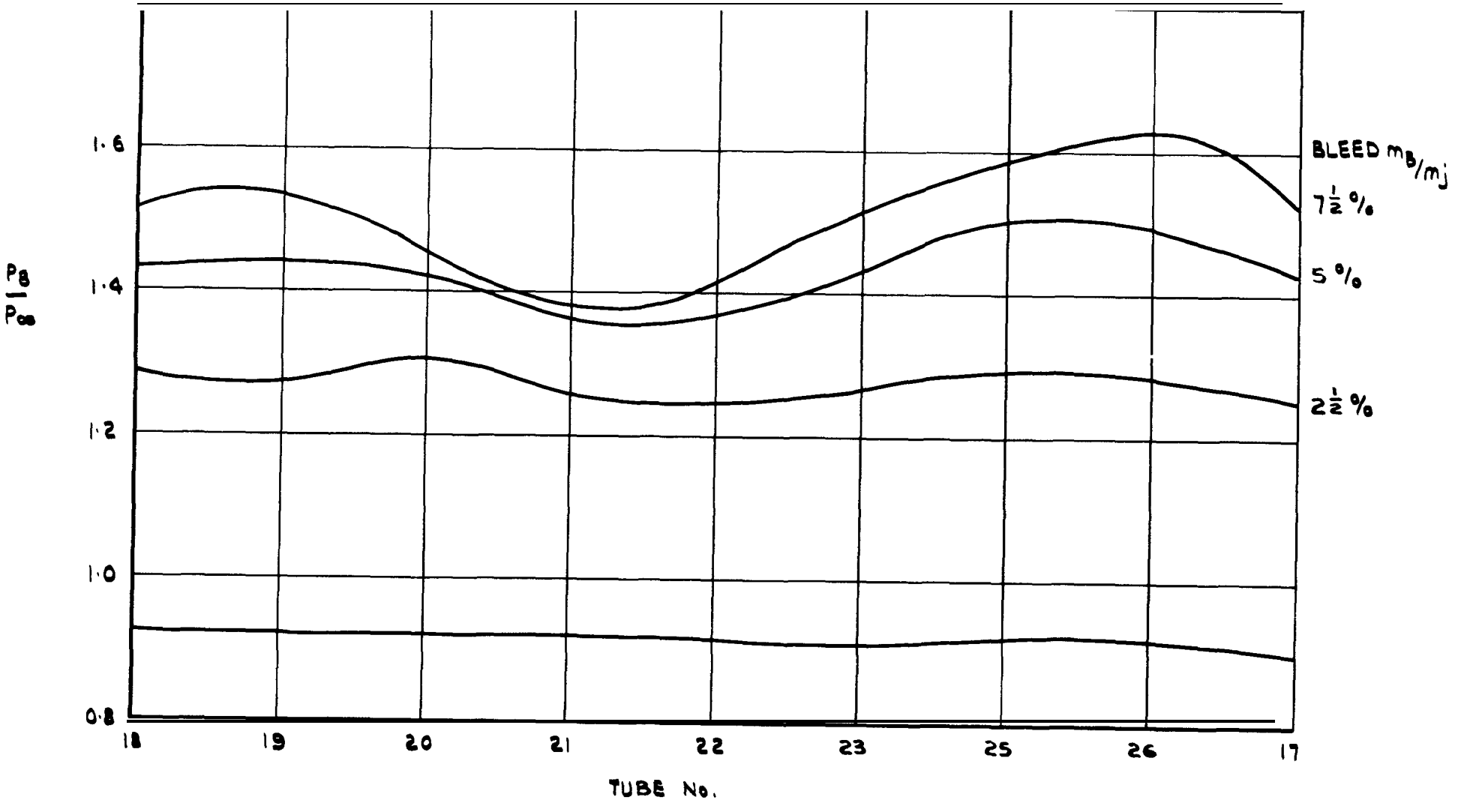

FIG. 19 DISTRIBUTION OF BASE PRESSURE ROUND THE EXIT NOZZLE H, SHROUDED

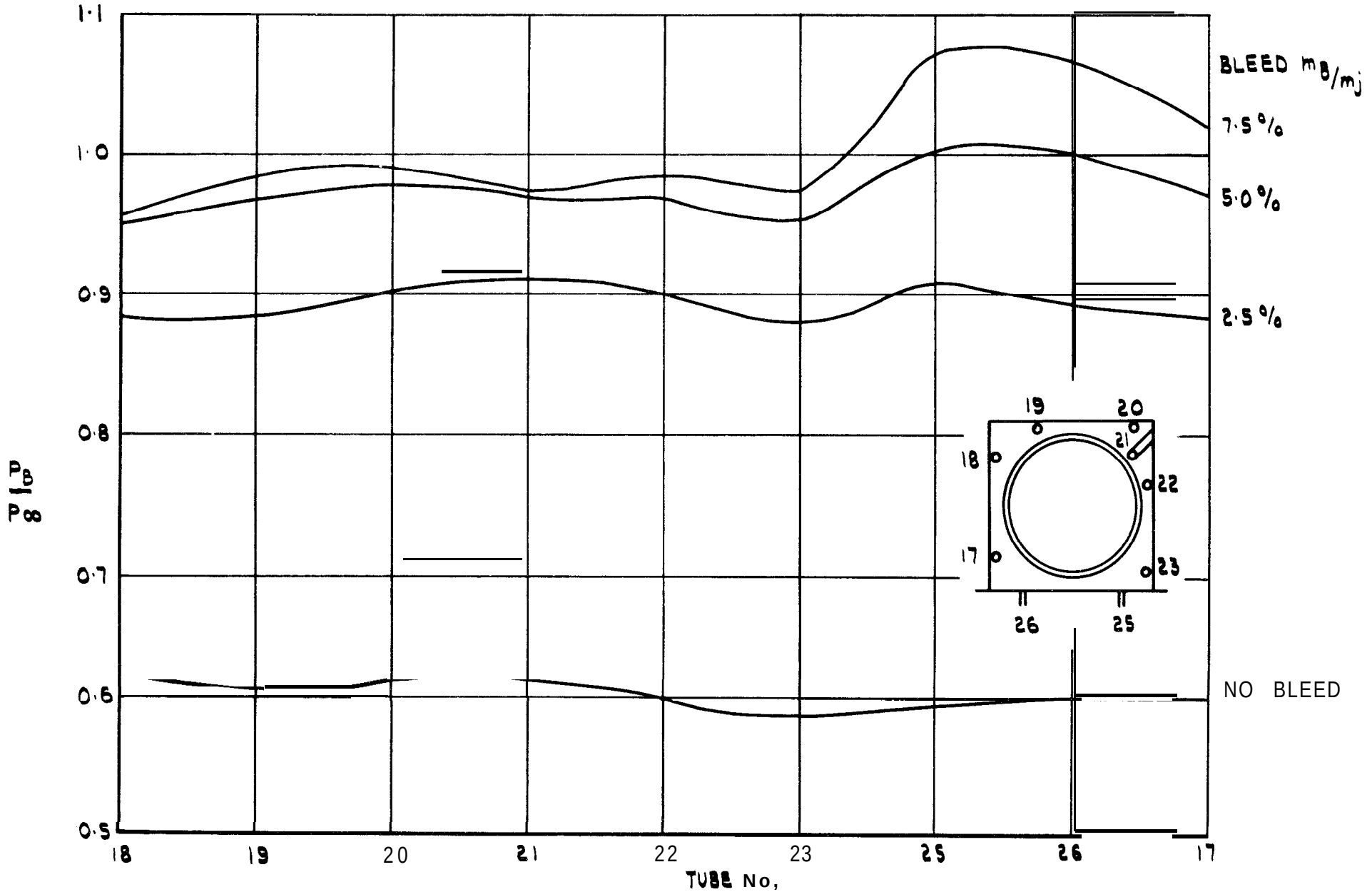

FIG.20 DISTRIBUTION OF BASE PRESSURE ROUND THE EXIT (NOZZLE 1, UNSHROUDED)

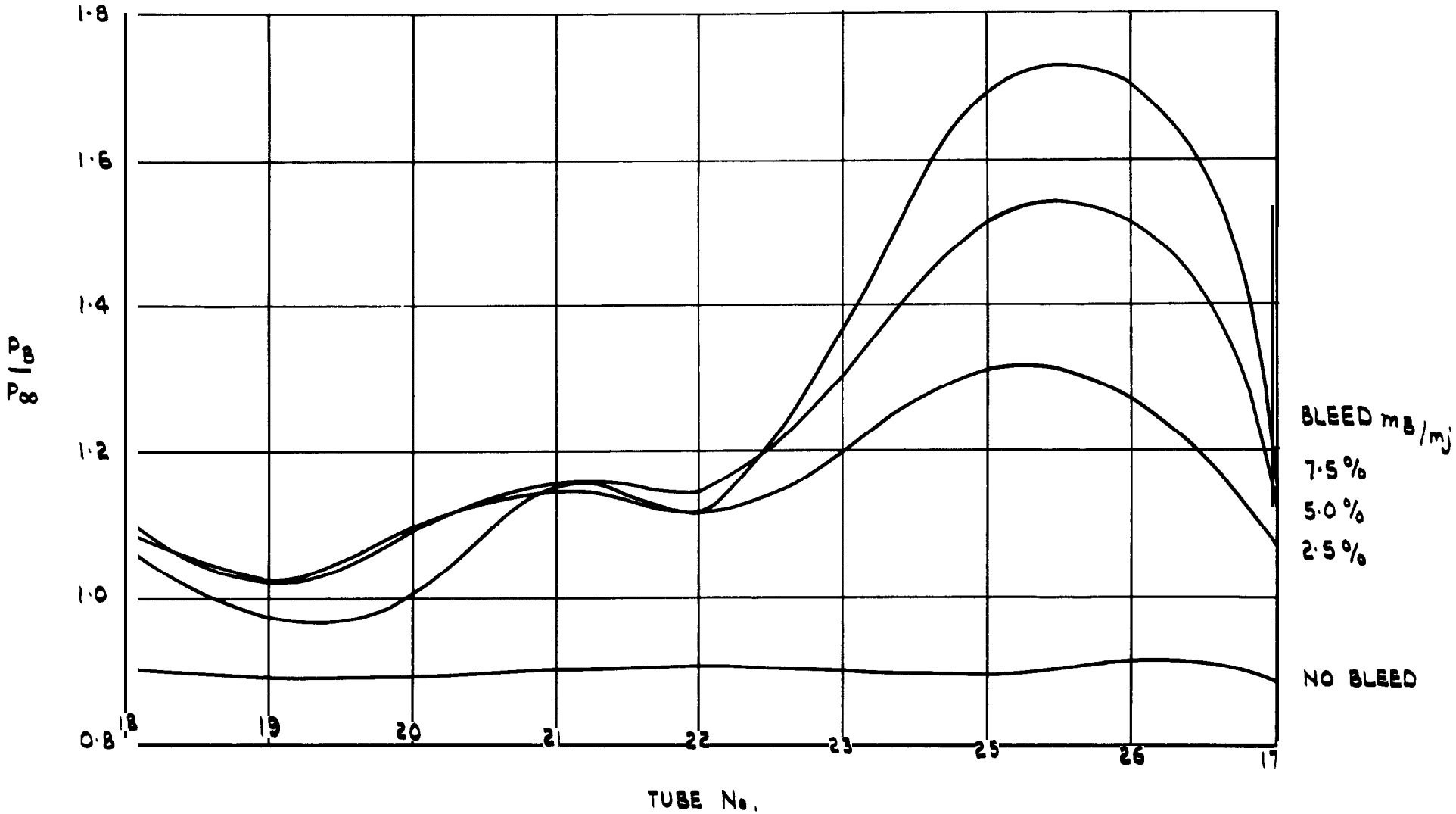

FIG 21 DISTRIBUTION OF BASE PRESSURE ROUND THE EXIT (NOZZLE A, UNSHROUDED)

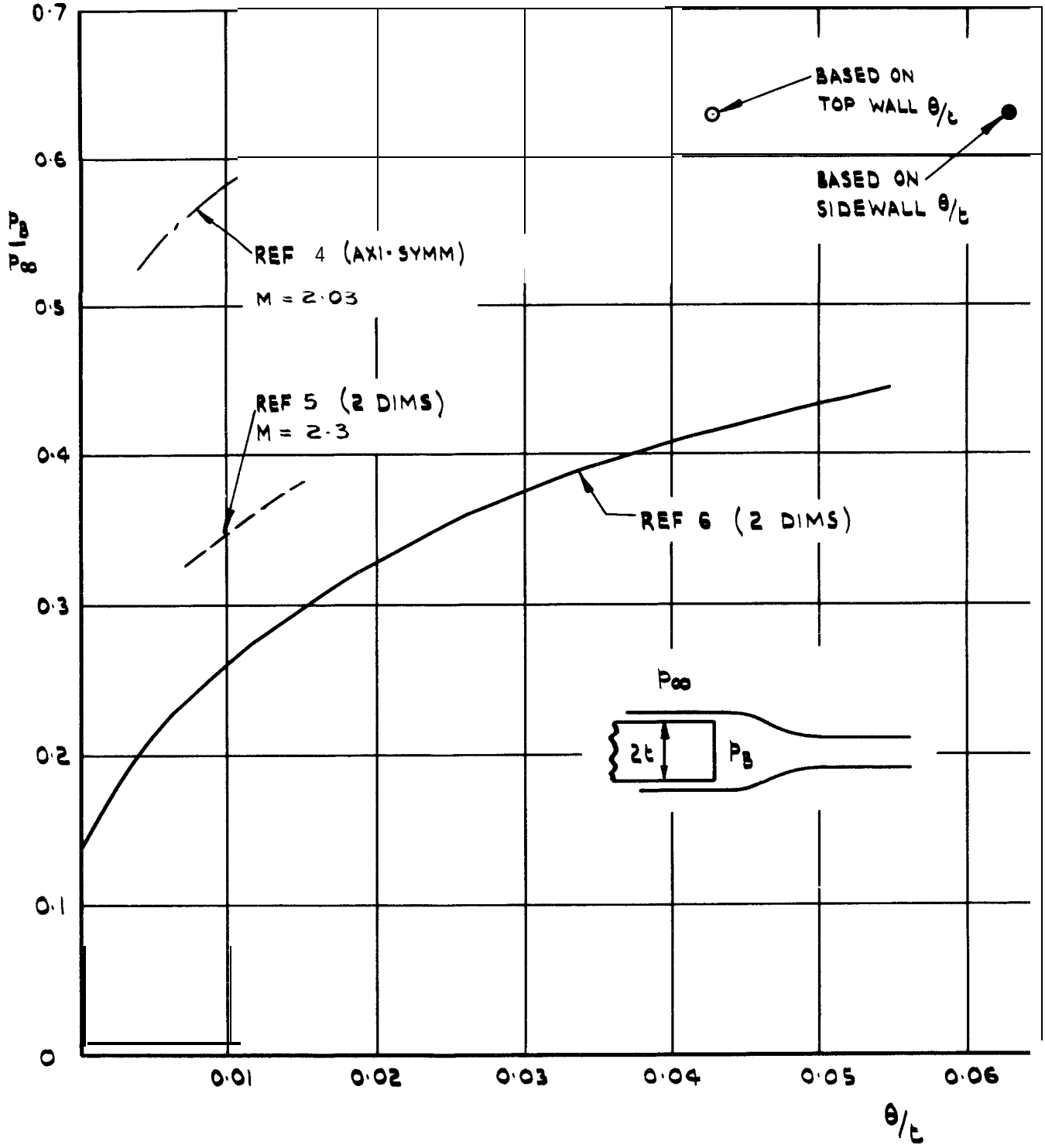

FIG. 22 EFFECT OF BOUNDARY LAYER THICKNESS ON BASE PRESSURE FOR NO JET & NO BLEED

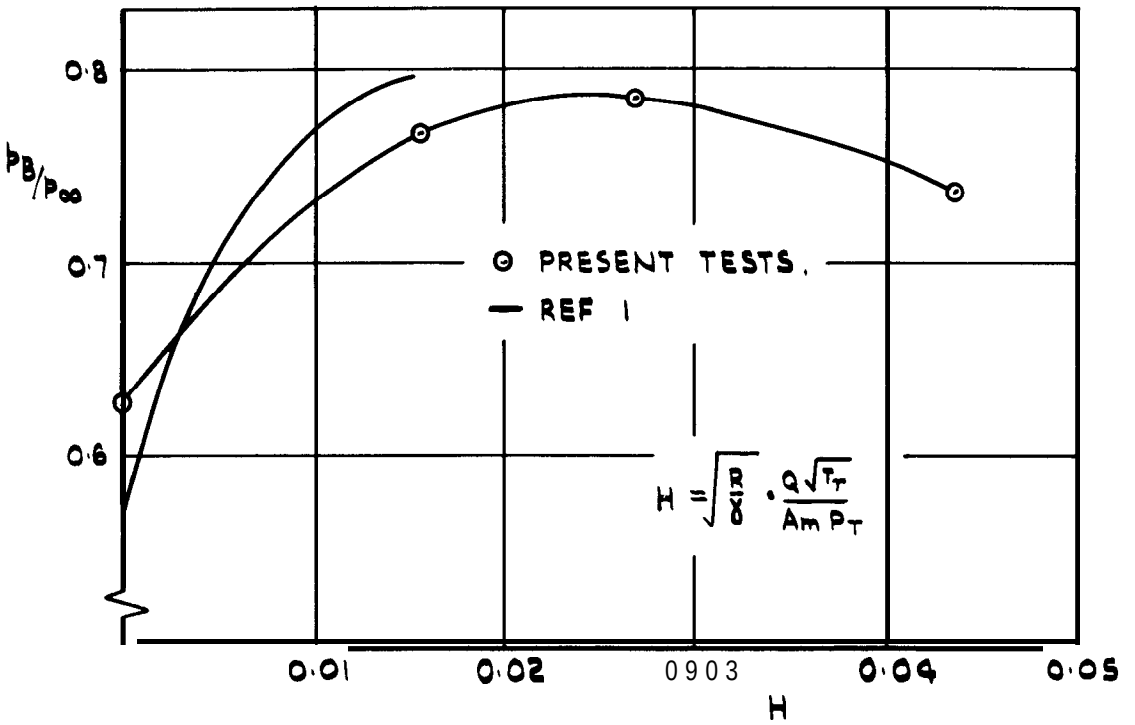

FIG. 23 (a) VARIATION OF BASE PRESSURE WITH BLEED QUANTITY (3 DIMENSIONAL)

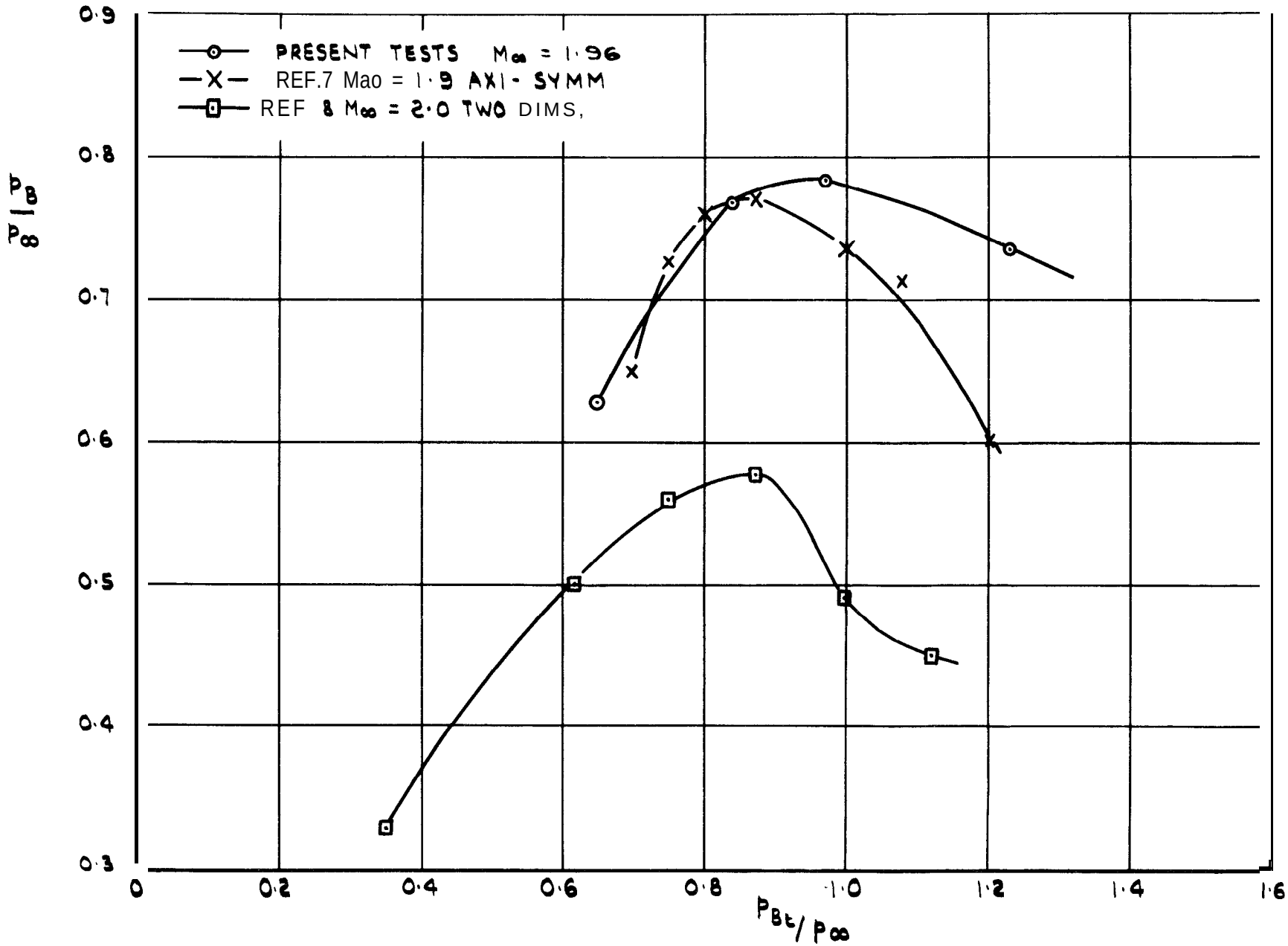

FIG 23 (b) BASE PRESSURE VARIATION **WITH BLEED** PRESSURE RATIO

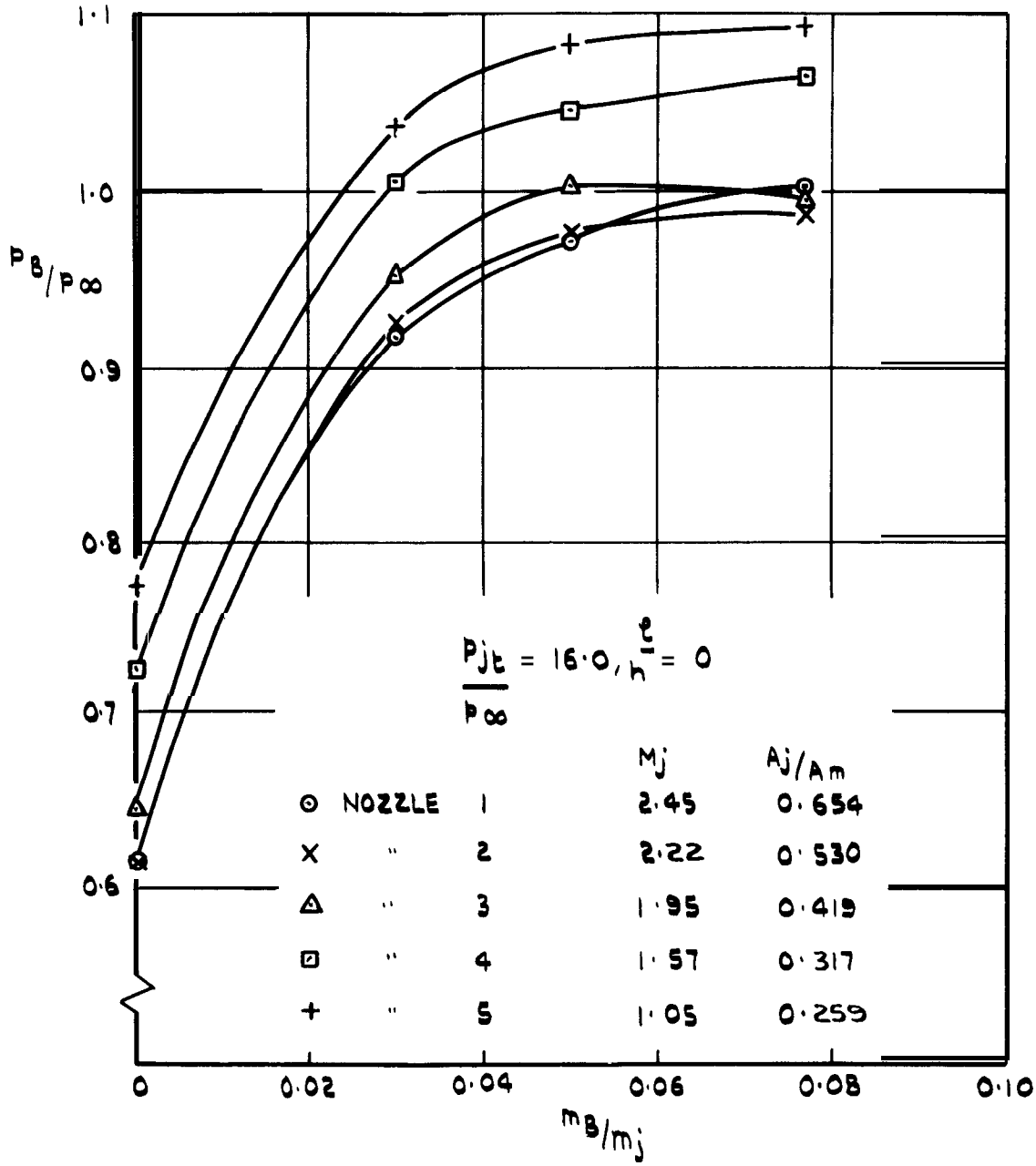

FIG. 24 VARIATION OF BASE PRESSURE WITH BLEED FLOW (UNSHROUDED NOZZLES)

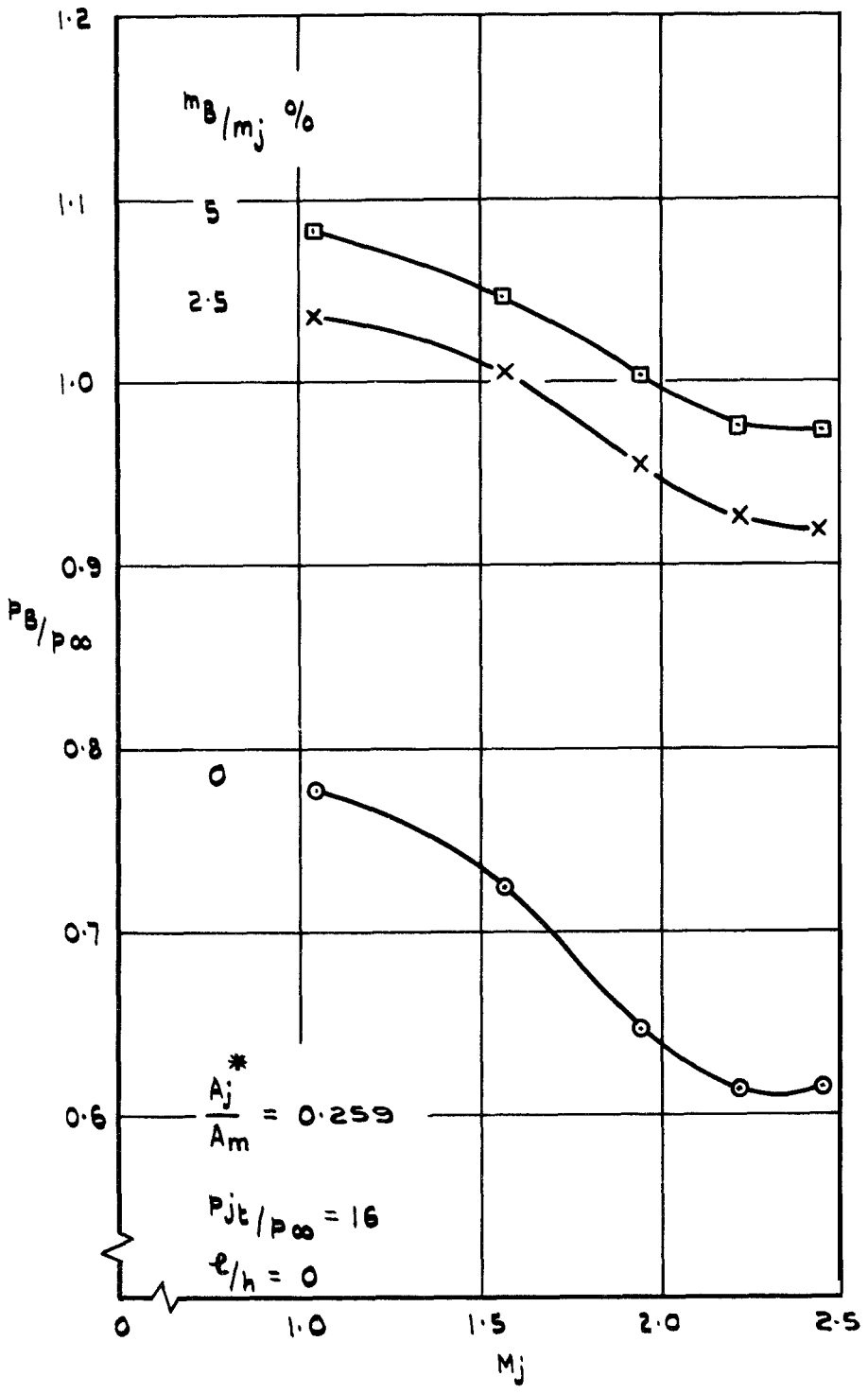

FIG. 25 VARIATION OF BASE PRESSURE WITH NOZZLE DESIGN MACH NUMBER (UNSHROUDED NOZZLES)

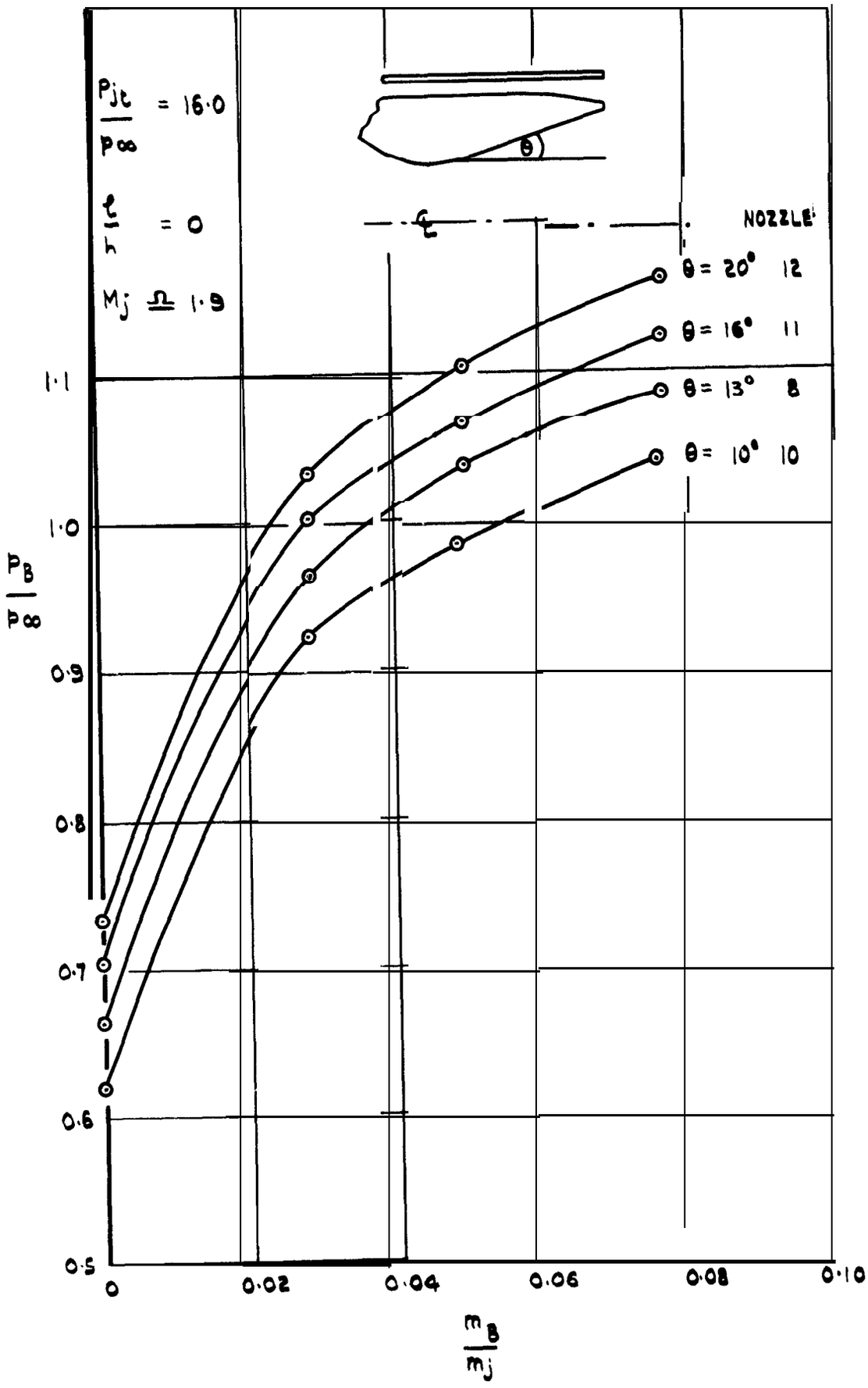

FIG.26 EFFECT OF NOZZLE DIVERGENCE ON BASE PRESSURE (UNSHROUDED)

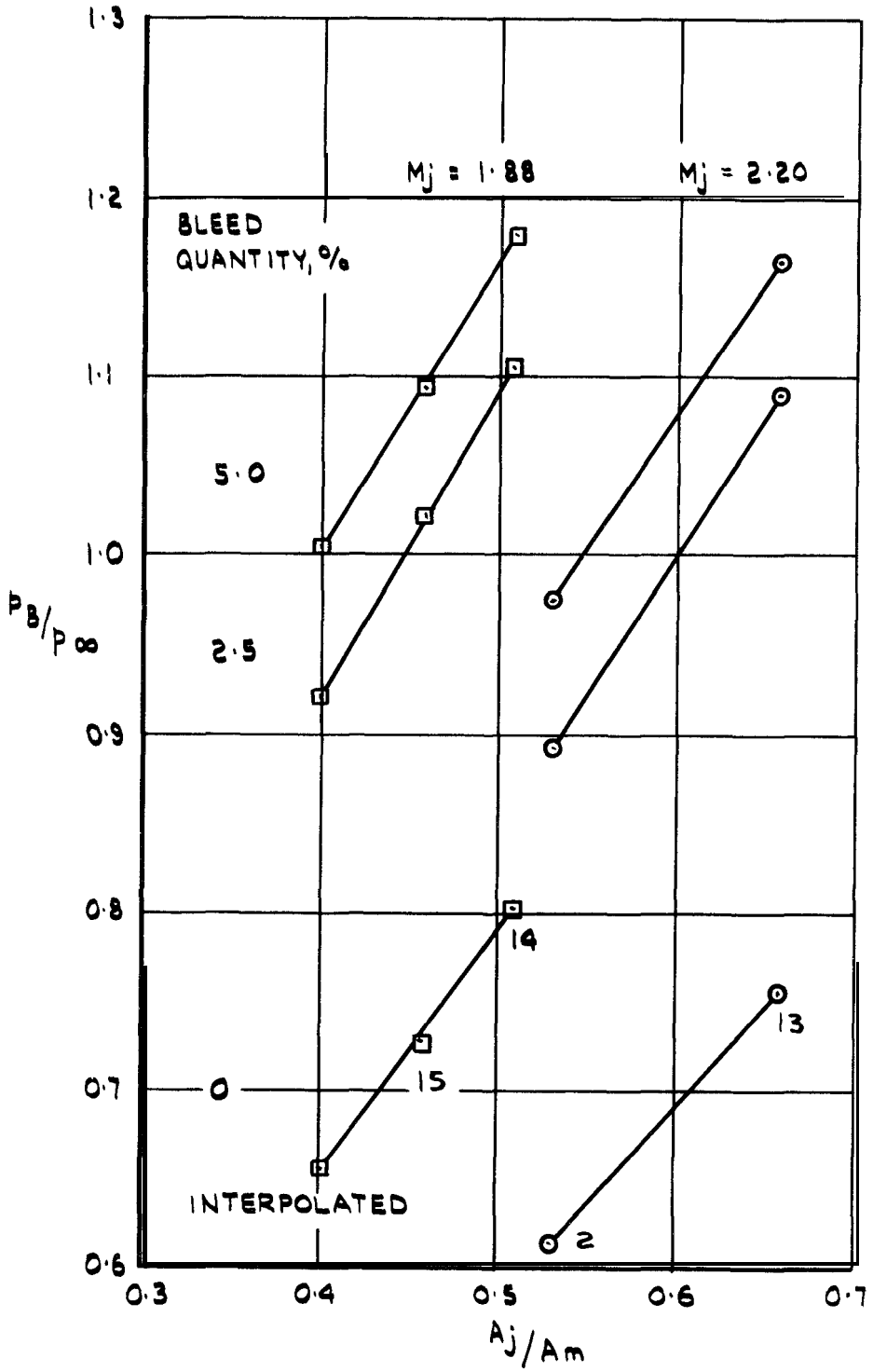

FIG.27 VARIATION OF BASE PRESSURE WITH JET EXIT AREA (UNSHROUDED)

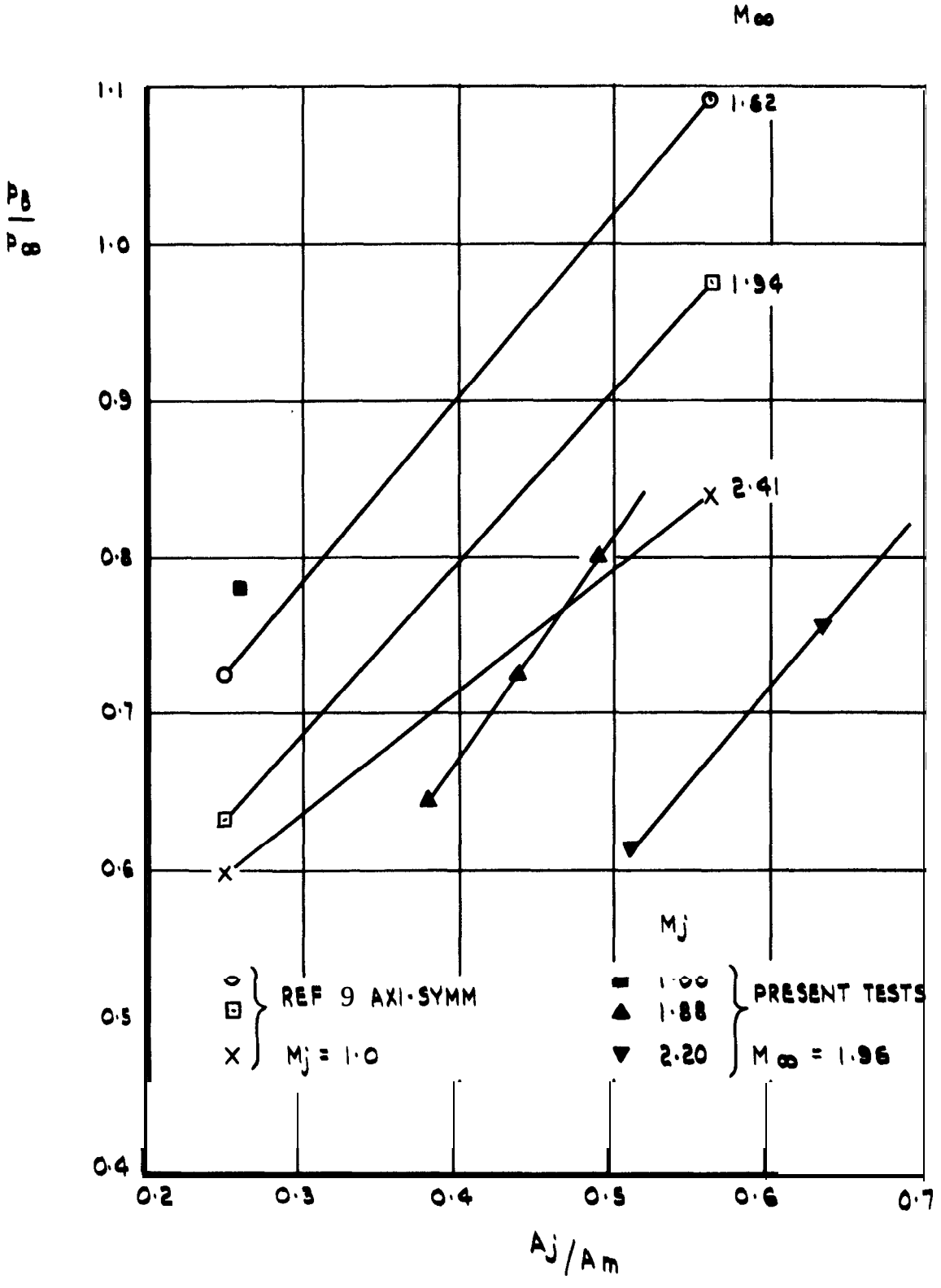

FIG. 28 VARIATION OF BASE PRESSURE WITH 'STEP HEIGHT' FOR ZERO BLEED - COMPARISON WITH RESULTS OF REF. 9

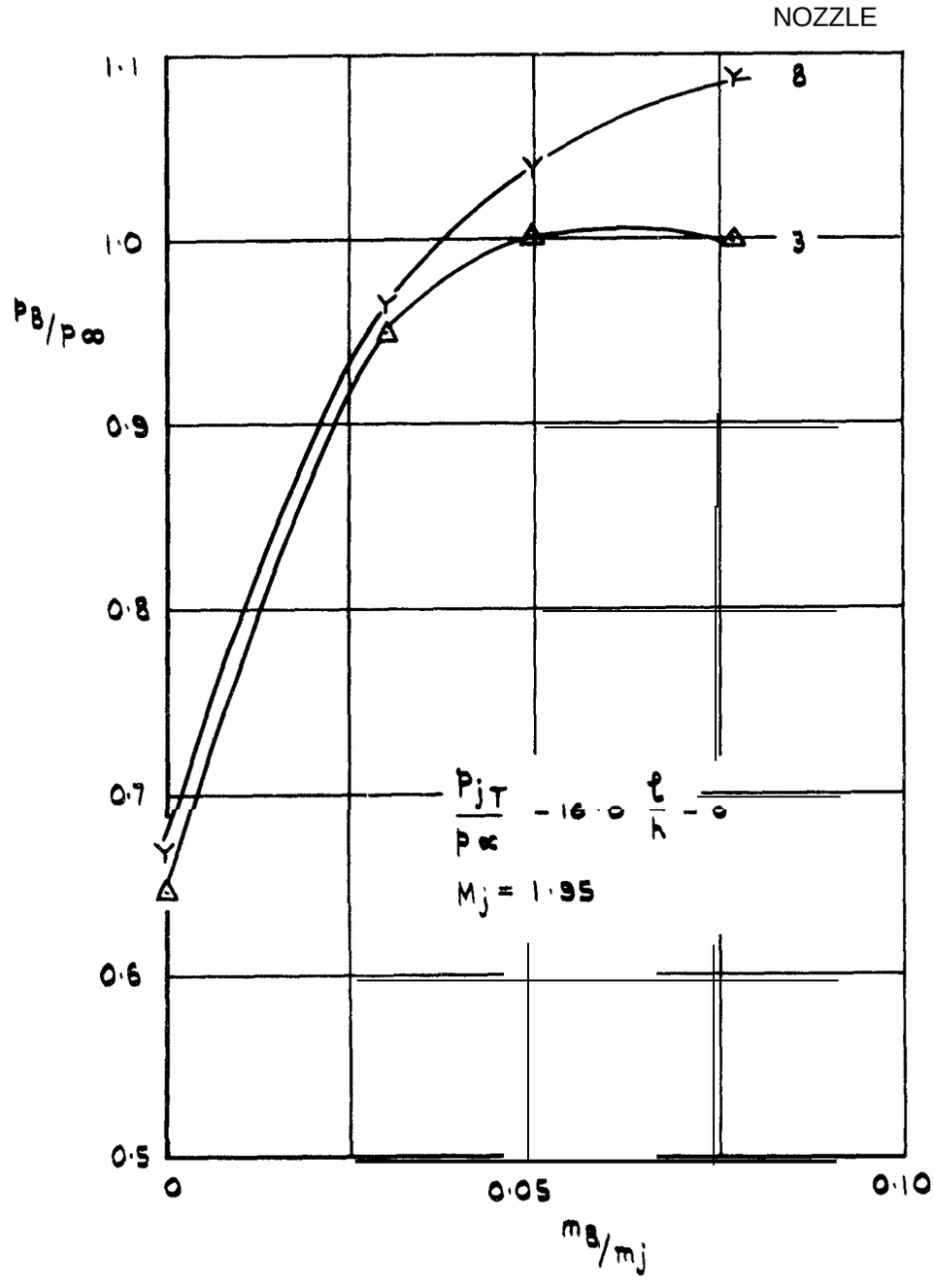

FIG. 29 EFFECT OF BLEED DUCT (UNSHROUDED) EXIT AREA

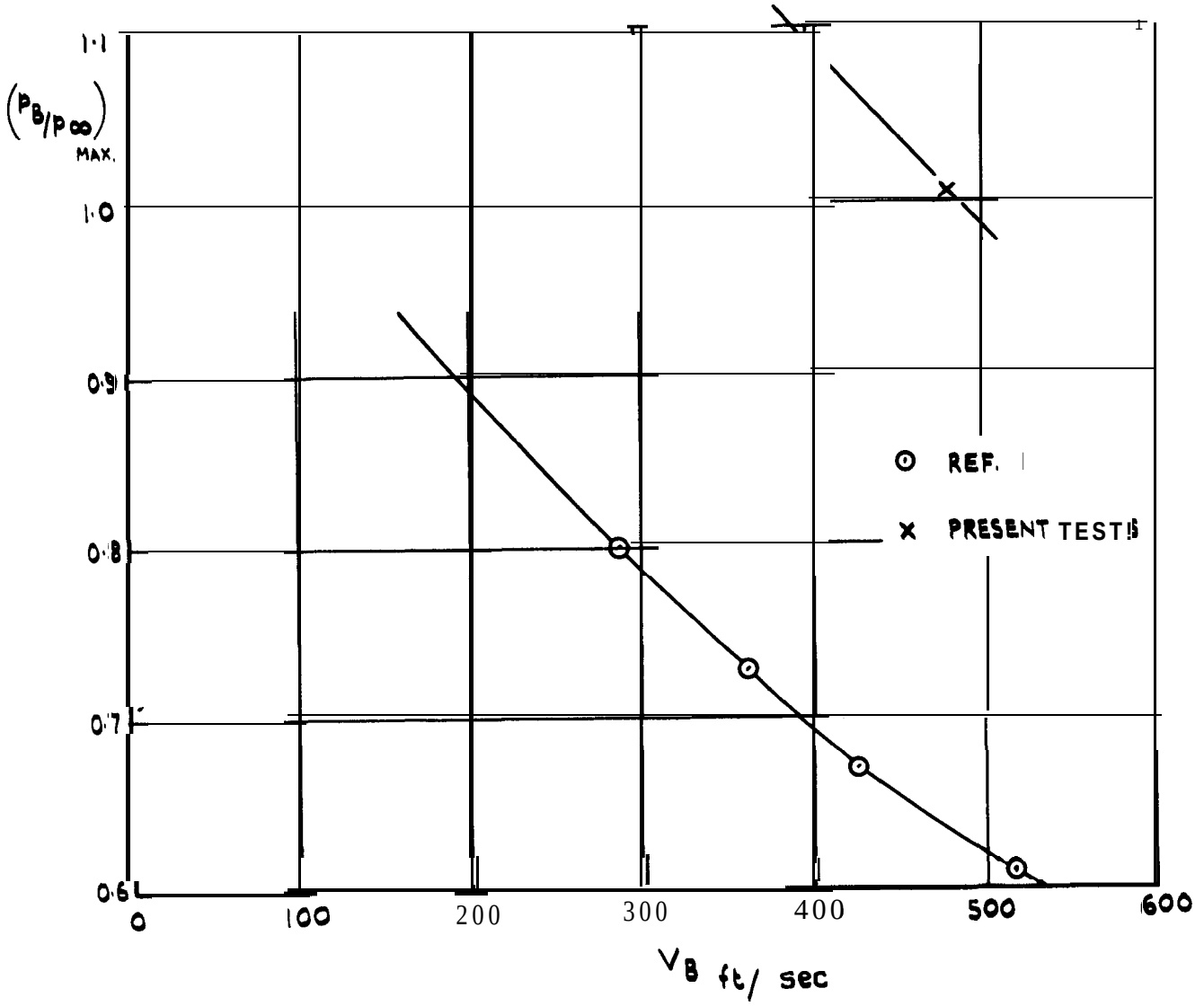

FIG. 30 VARIATION OF MAXIMUM BASE PRESSURE WITH BLEED VELOCITY

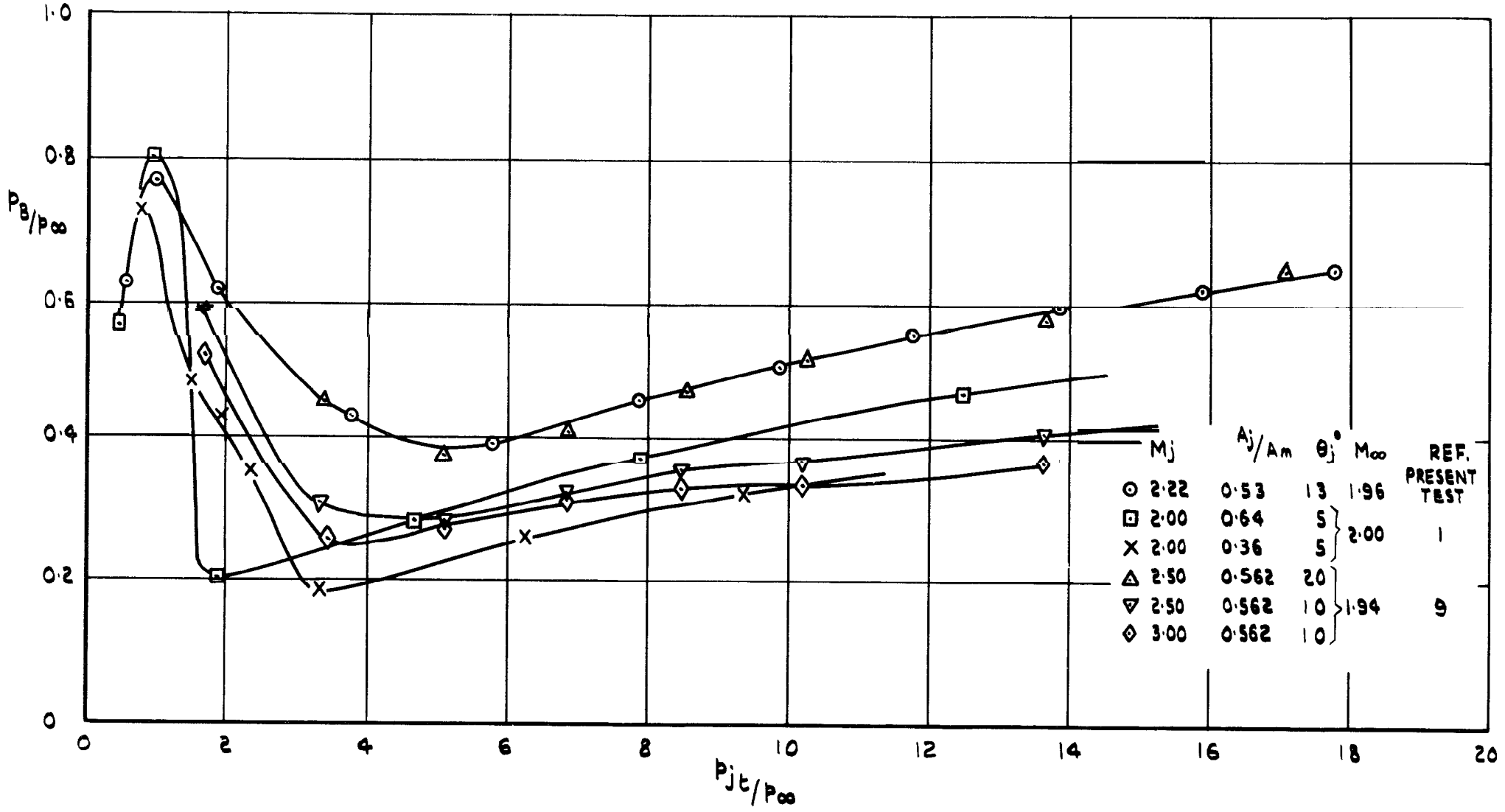

FIG.31 EFFECT OF JET PRESSURE RATIO (UNSHROUDED & WITH ZERO BLEED)

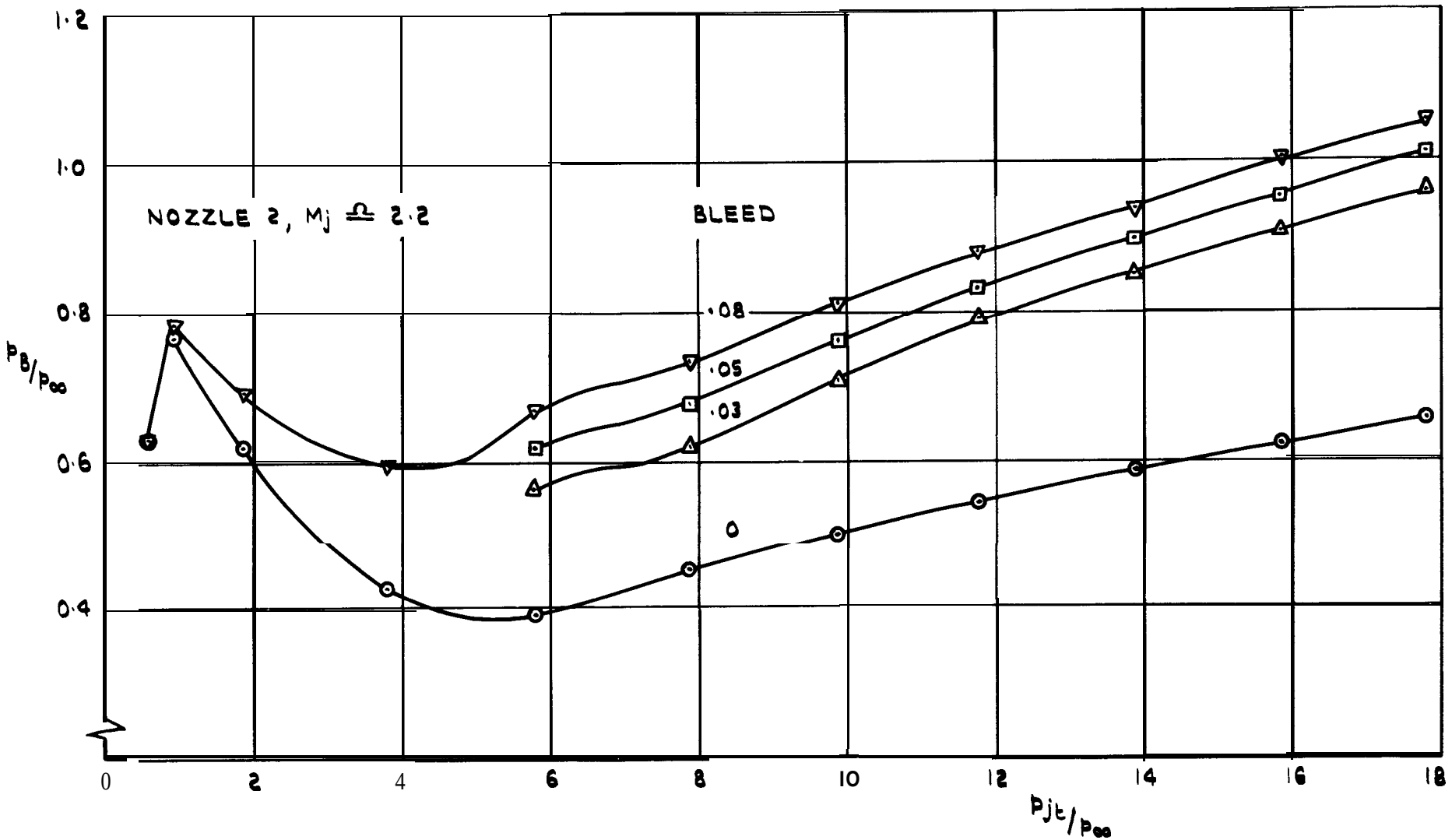

FIG. 32 TYPICAL VARIATION OF BASE PRESSURE WITH JET PRESSURE RATIO & BLEED FLOW (UNSHROUDED)

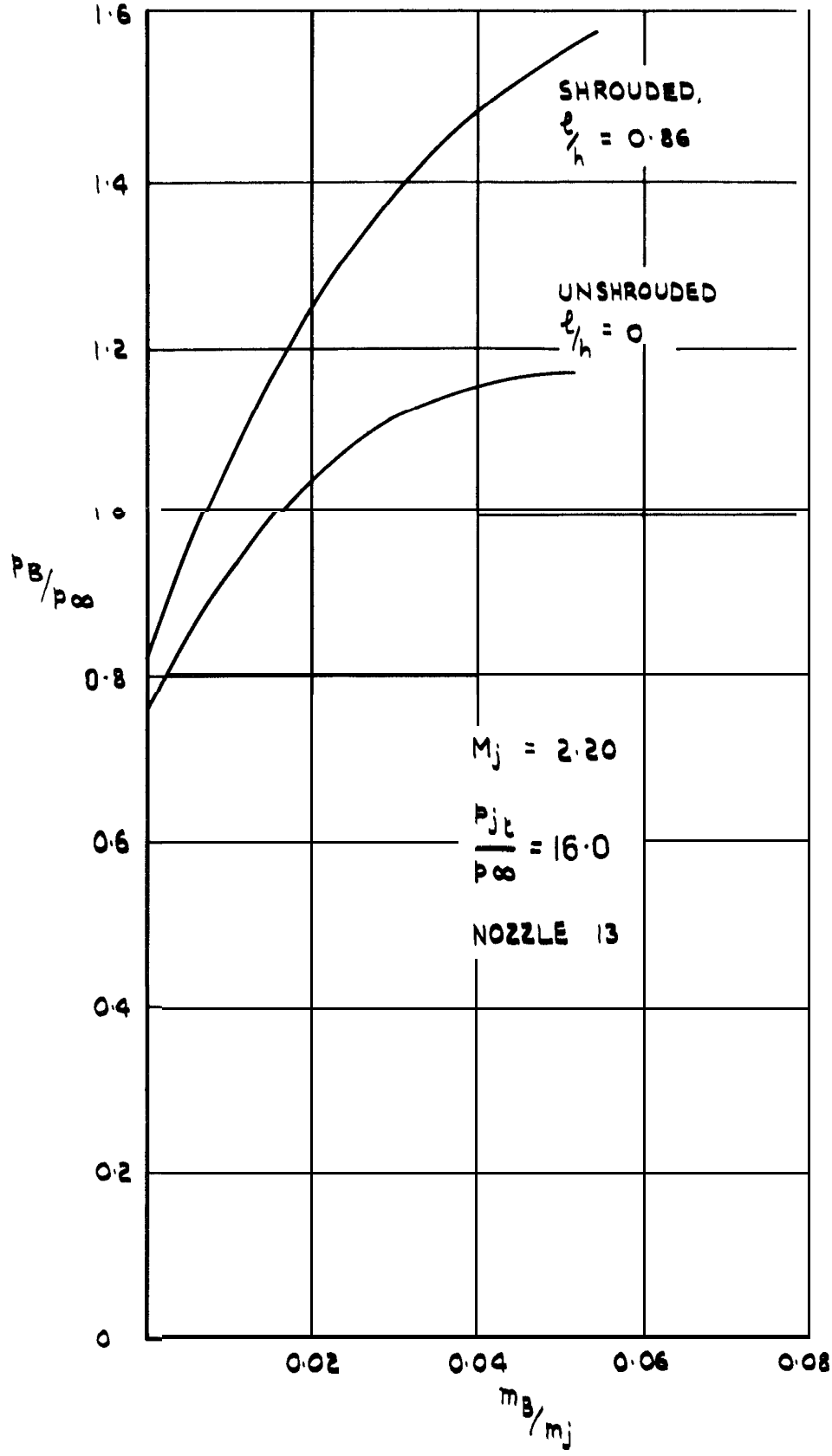

FIG.33 EFFECT OF SHROUD ON BASE PRESSURE

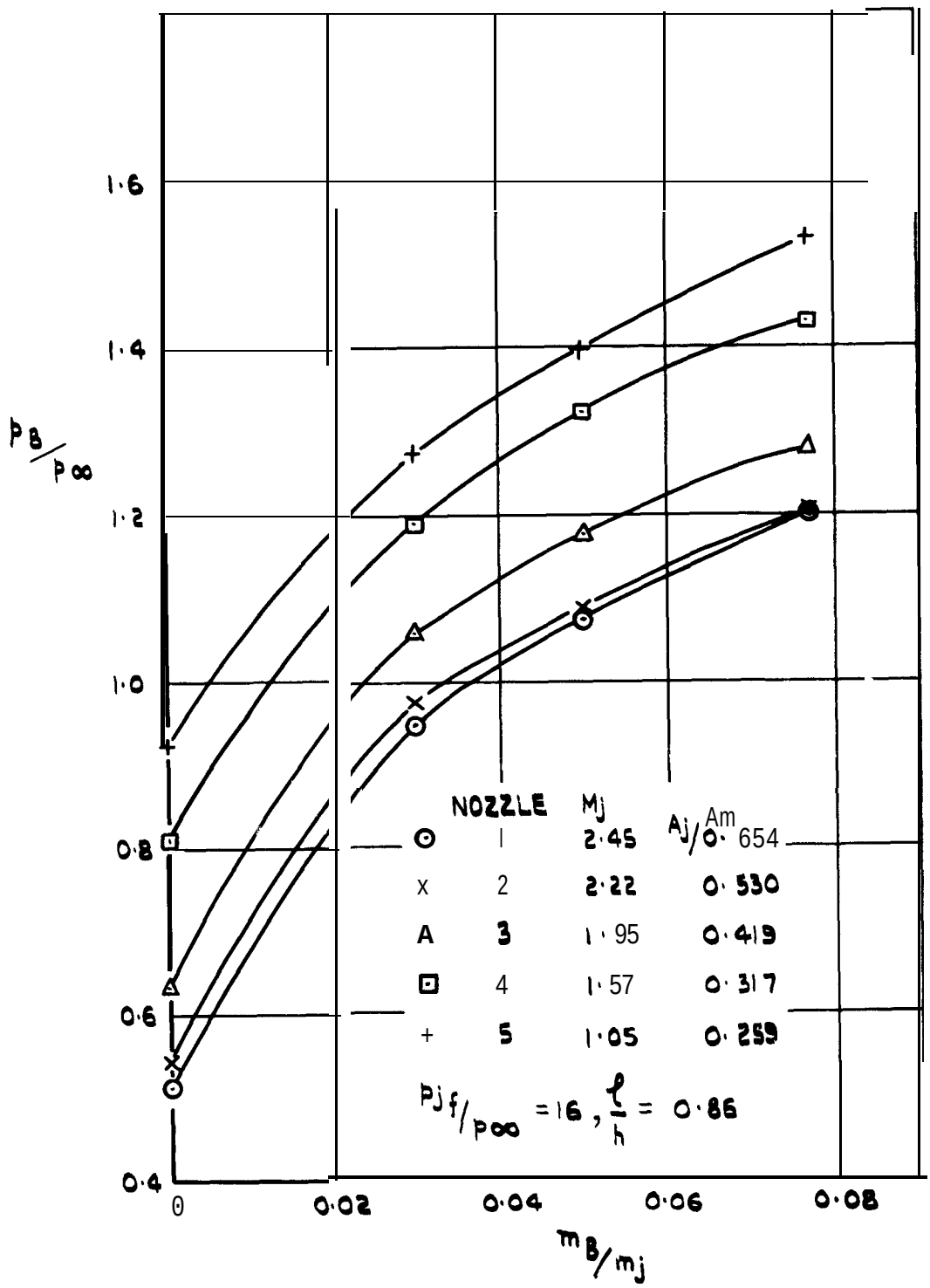

FIG. 34 VARIATION OF BASE PRESSURE WITH BLEED FLOW (SHROUDED NOZZLES)

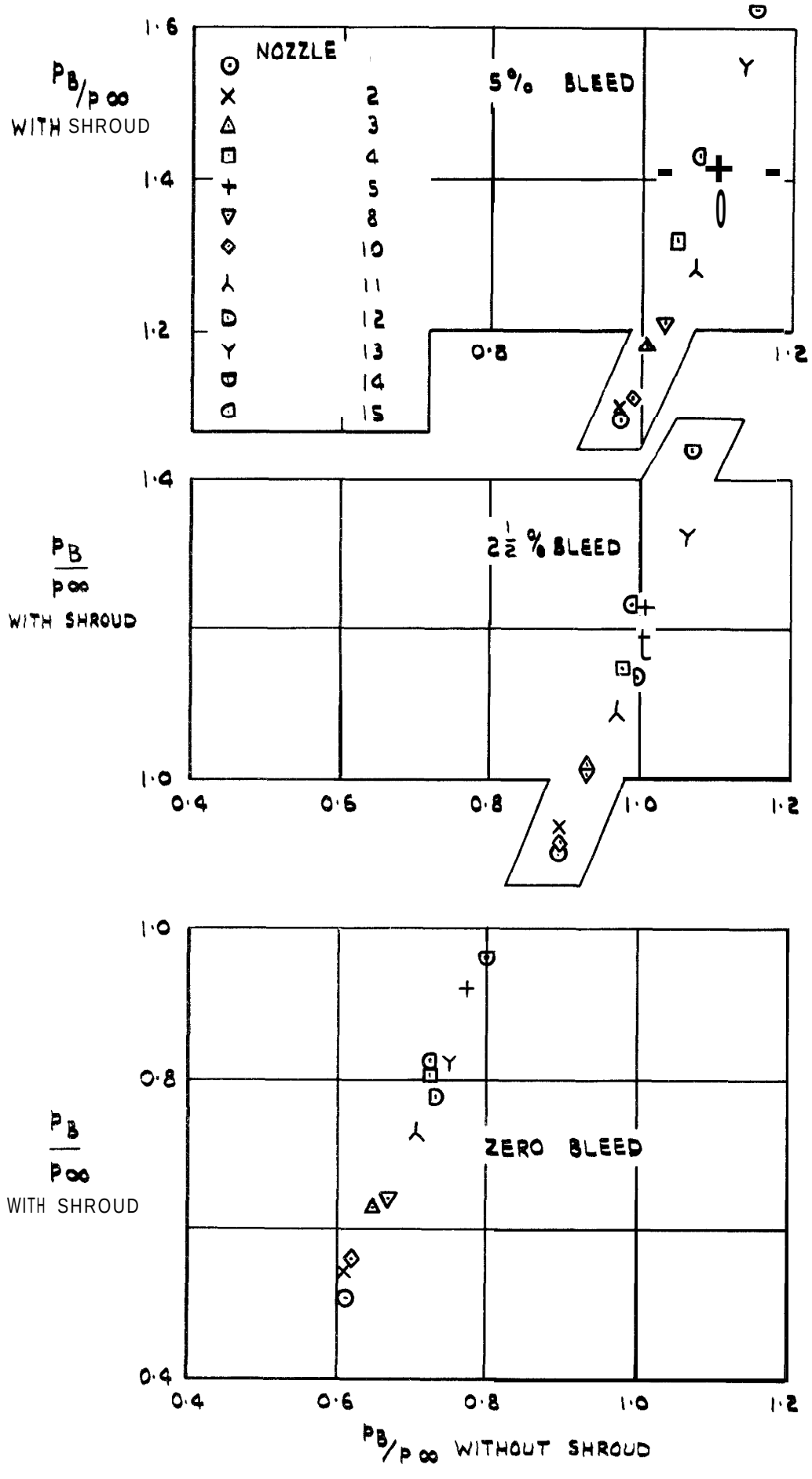

FIG.35 EFFECT OF SHROUD ON BASE PRESSURE

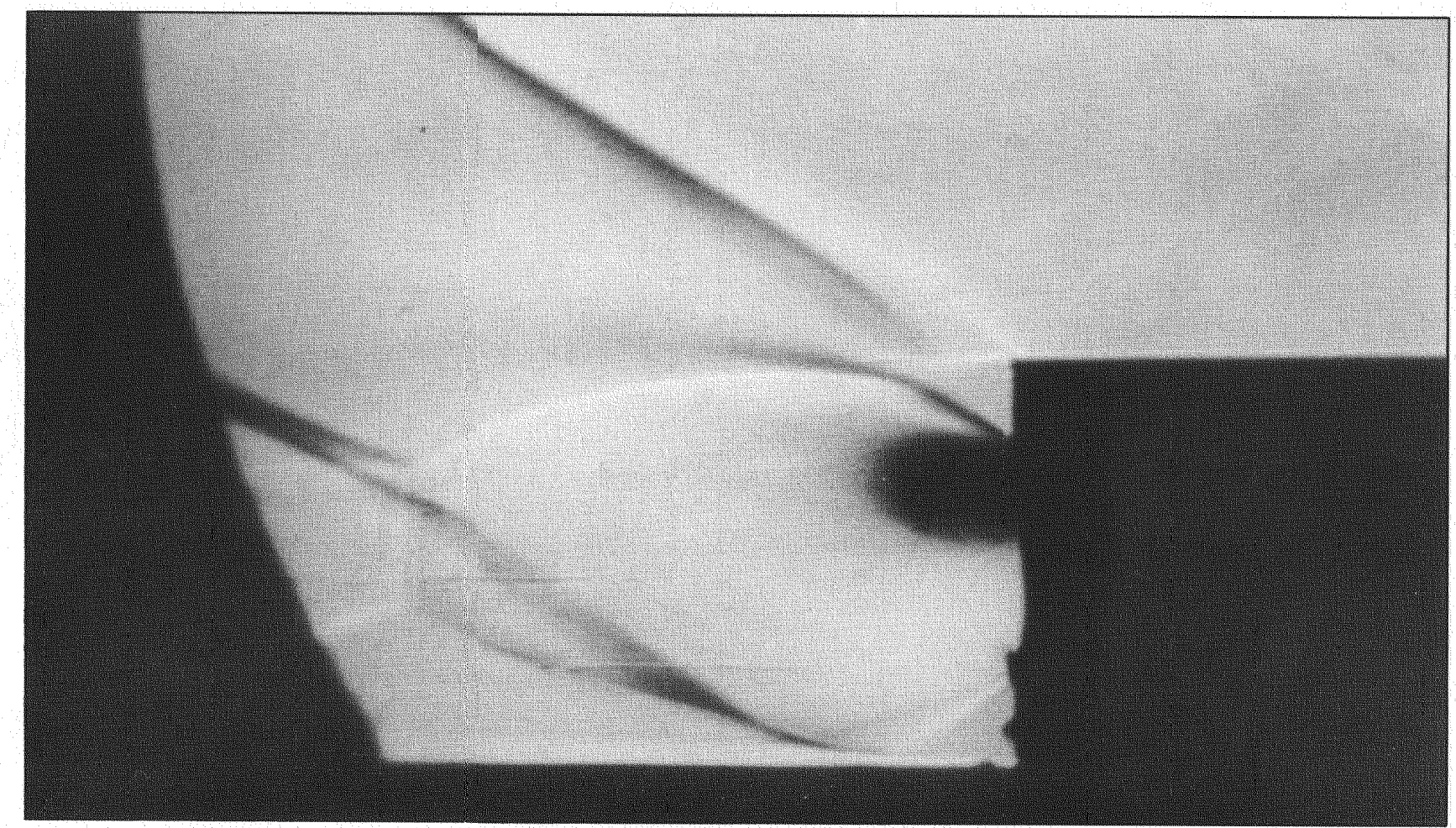

Fig.36.Schlieren photograph of nozzle 5 (no bleed)

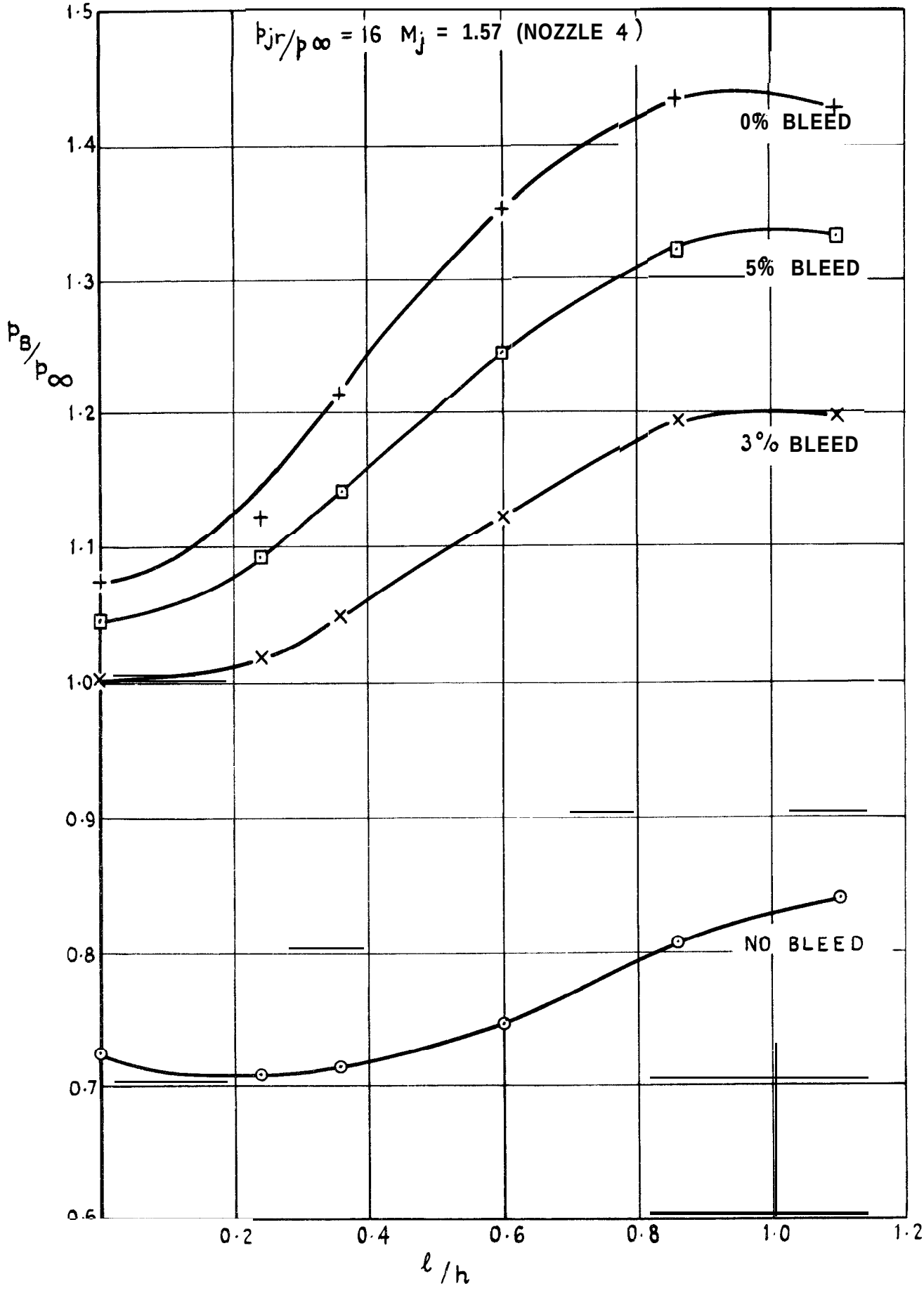

FIG. 37(a) **DEPENDENCE OF BASE PRESSURE ON SHROUD LENGTH,** $M_j = 1 \cdot 57$

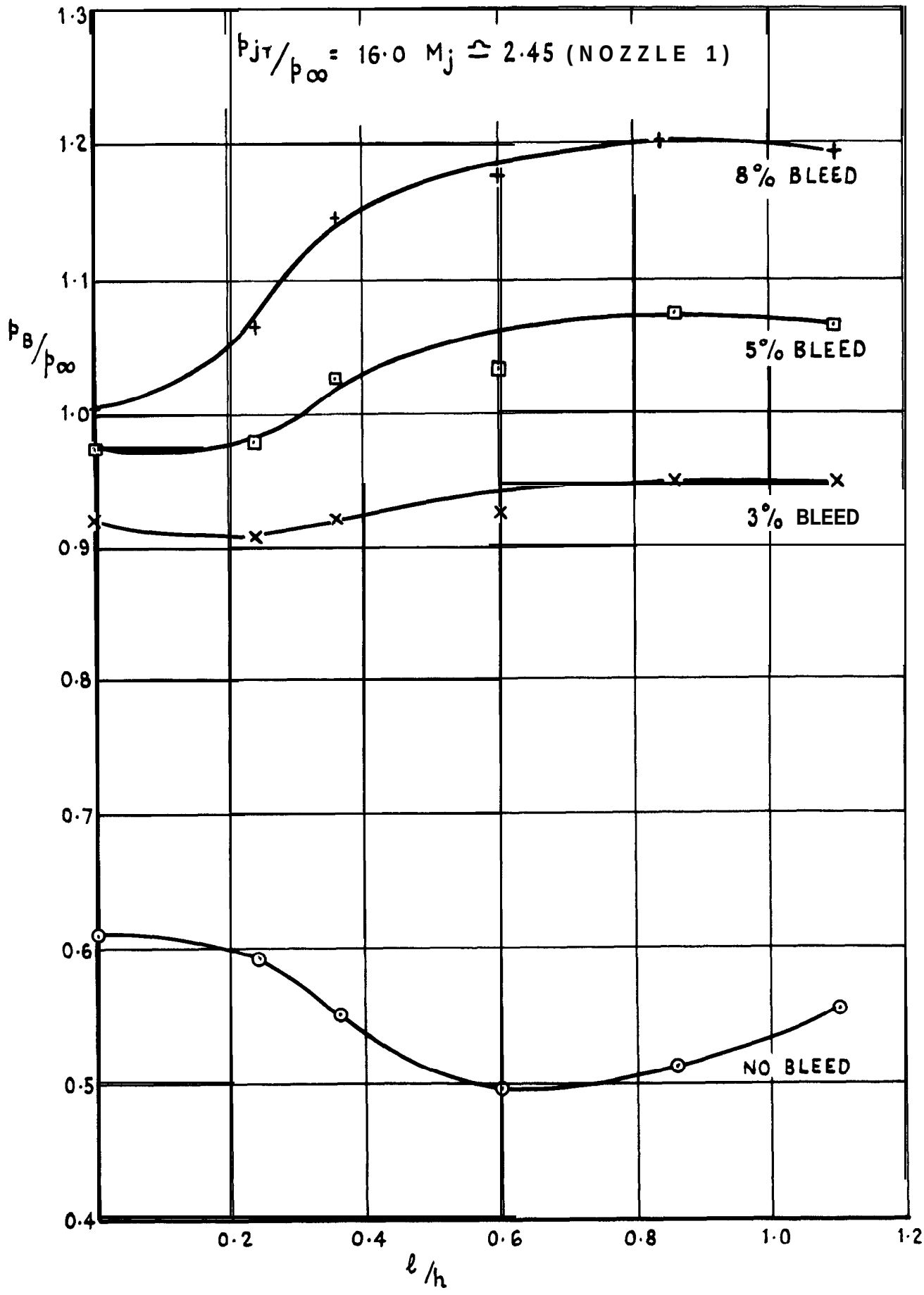

FIG. 37 (b) DEPENDENCE OF BASE PRESSURE ON SHROUD LENGTH, Mj = 2·45

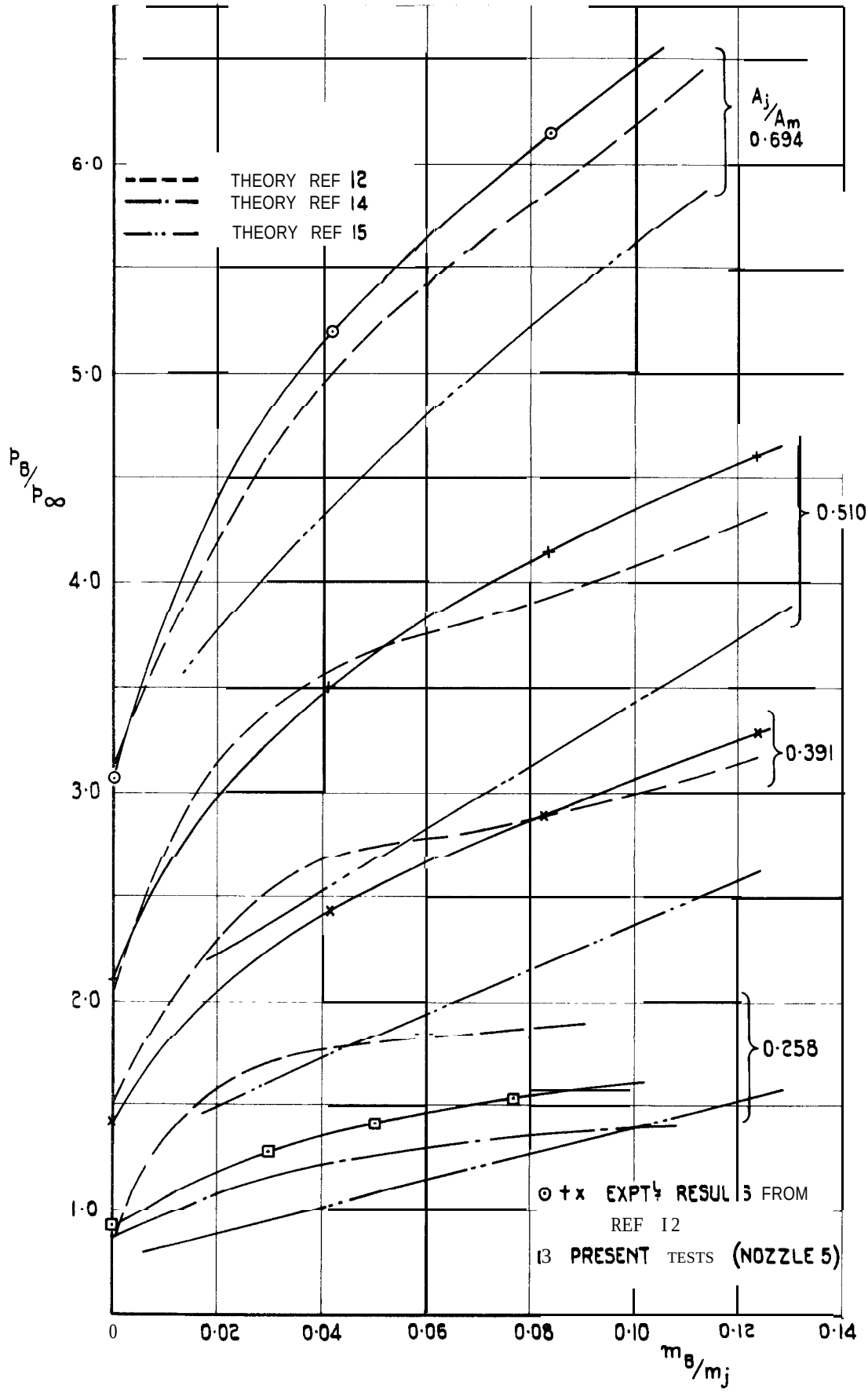

FIG. 38 (a) COMPARISON OF CALCULATED & MEASURED BASE PRESSURES FOR NOZZLE 5 (SHROUDED) & FOR THE RESULTS OF REF.12

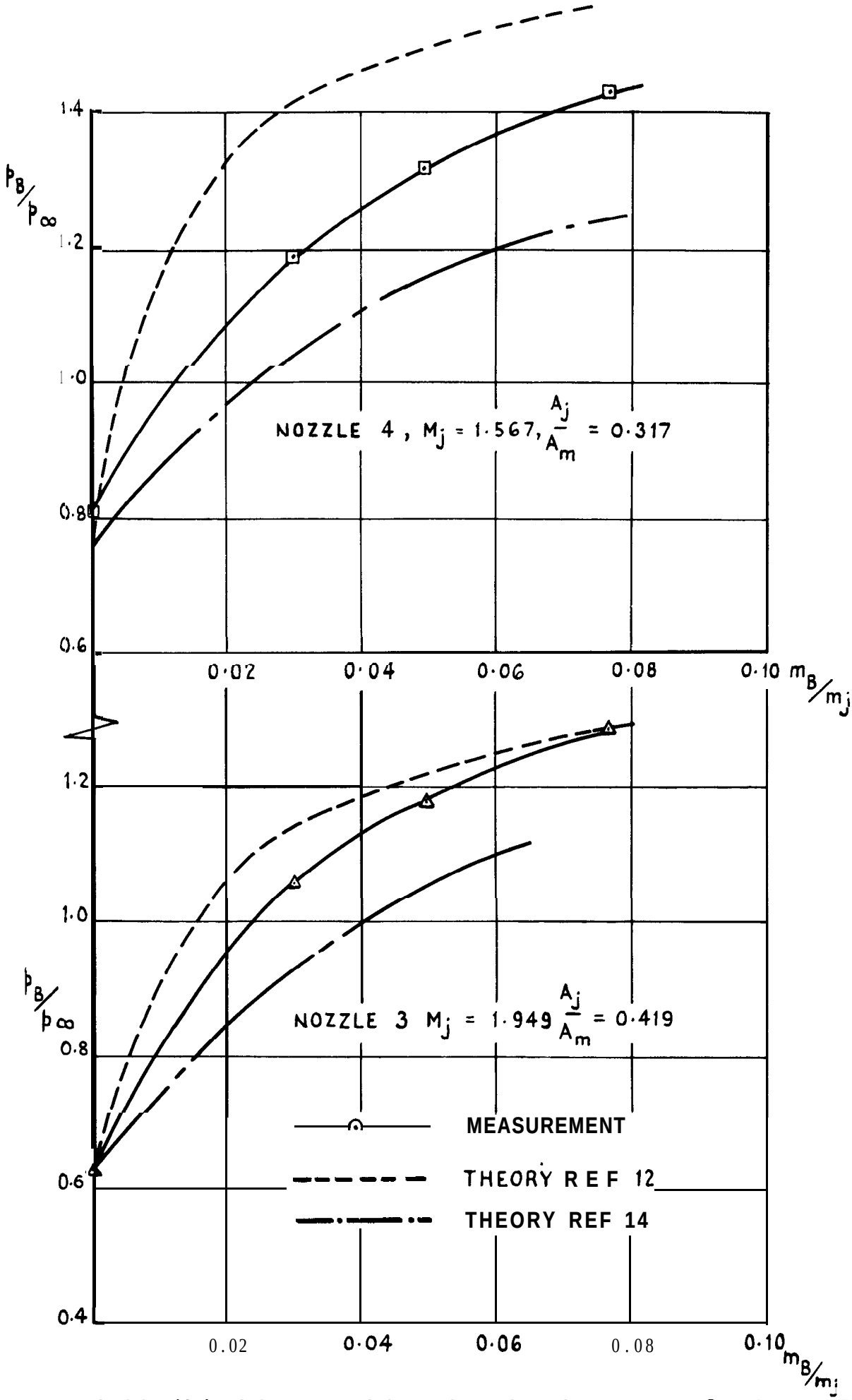

FIG.38 (b) COMPARISON OF CALCULATED & MEASURED BASE PRESSURES FOR NOZZLES 3 & 4 (SHROUDED)

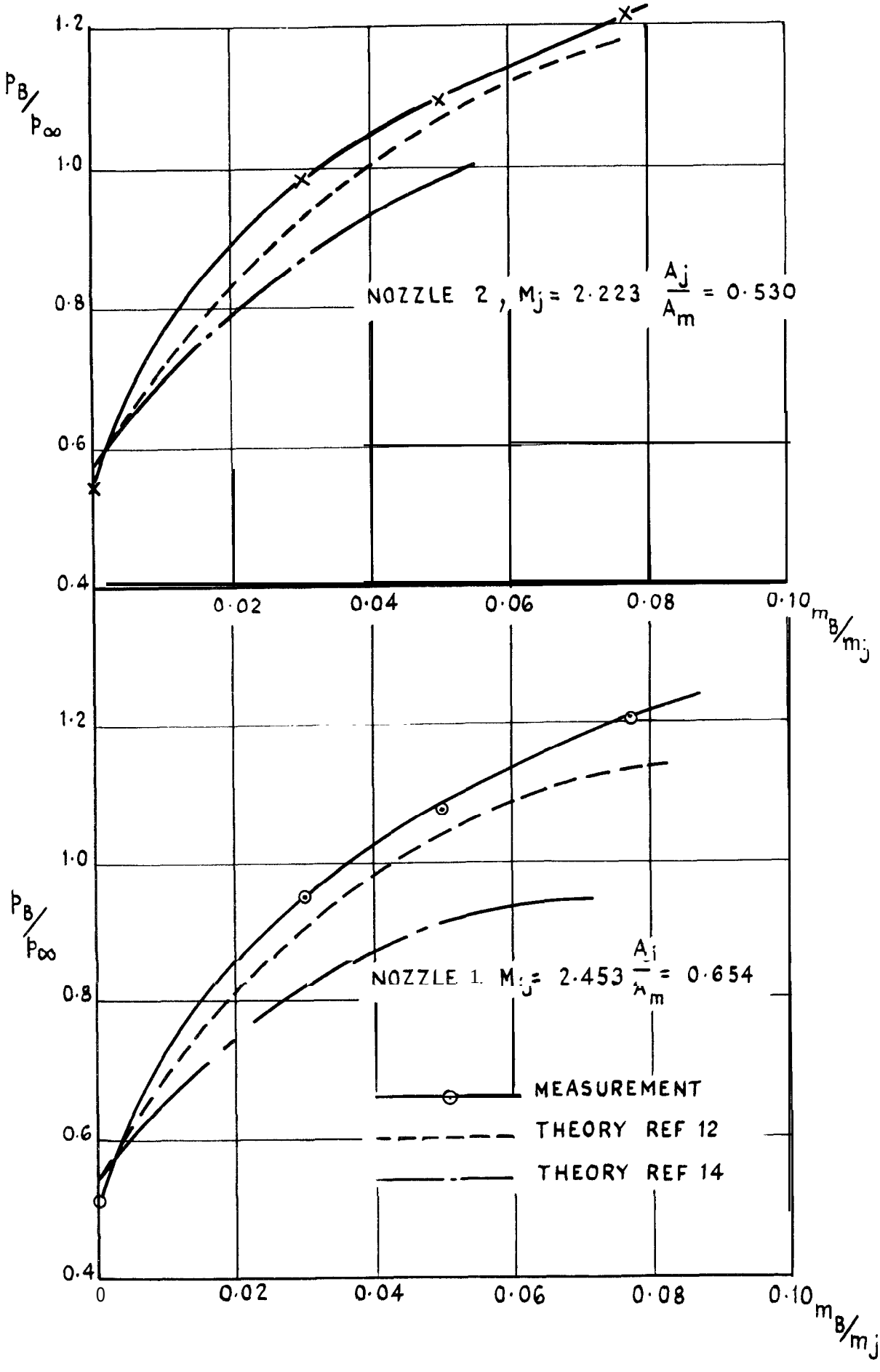

FIG.38(c) COMPARISON OF CACULATED & MEASURED BASE PRESSURES FOR NOZZLES1 & 2 (SHROUDED)

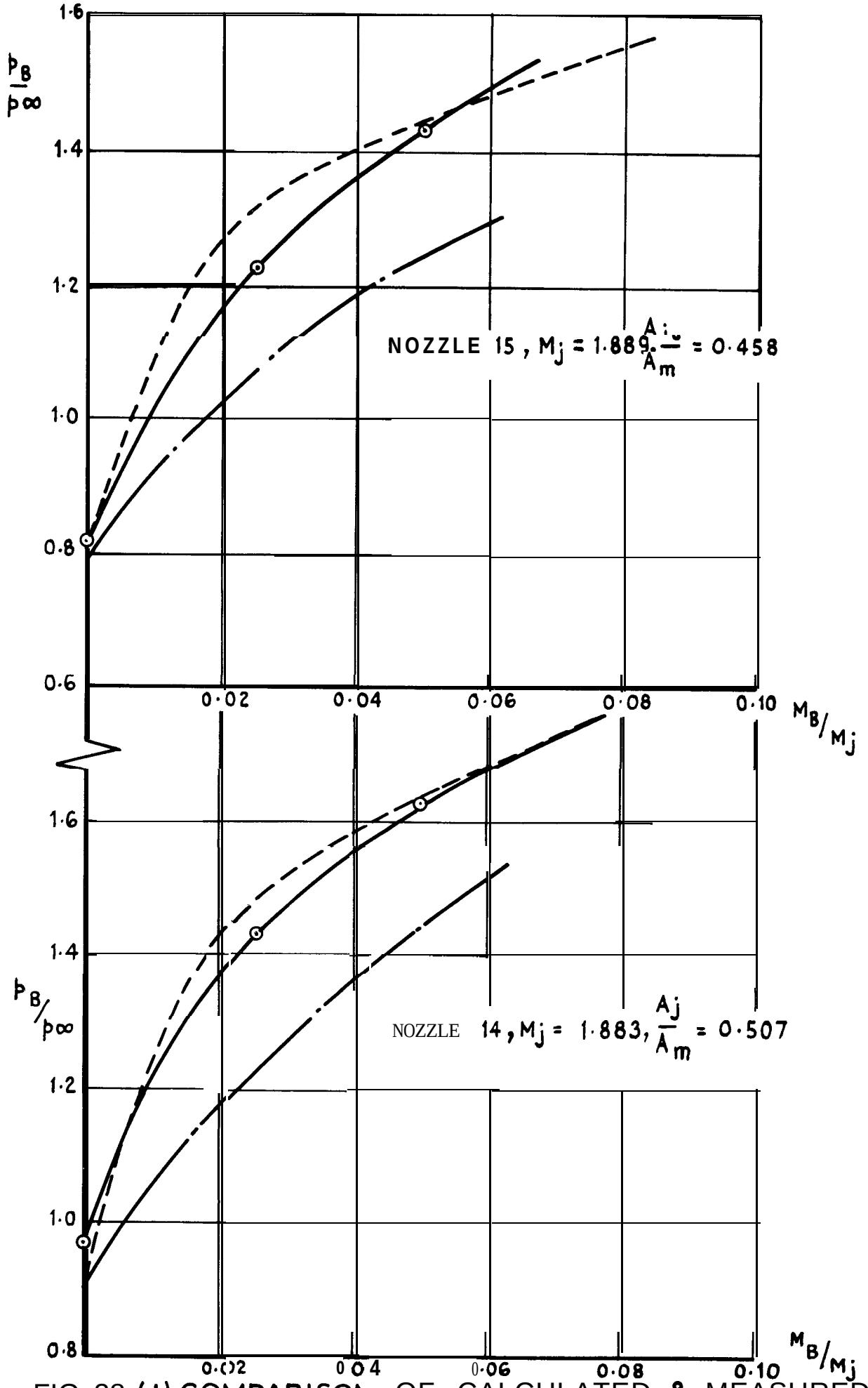

FIG 38 (d) COMPARISON OF CALCULATED & MEASURED BASE PRESSURES FOR NOZZLES 14 & 15 (SHROUDED)

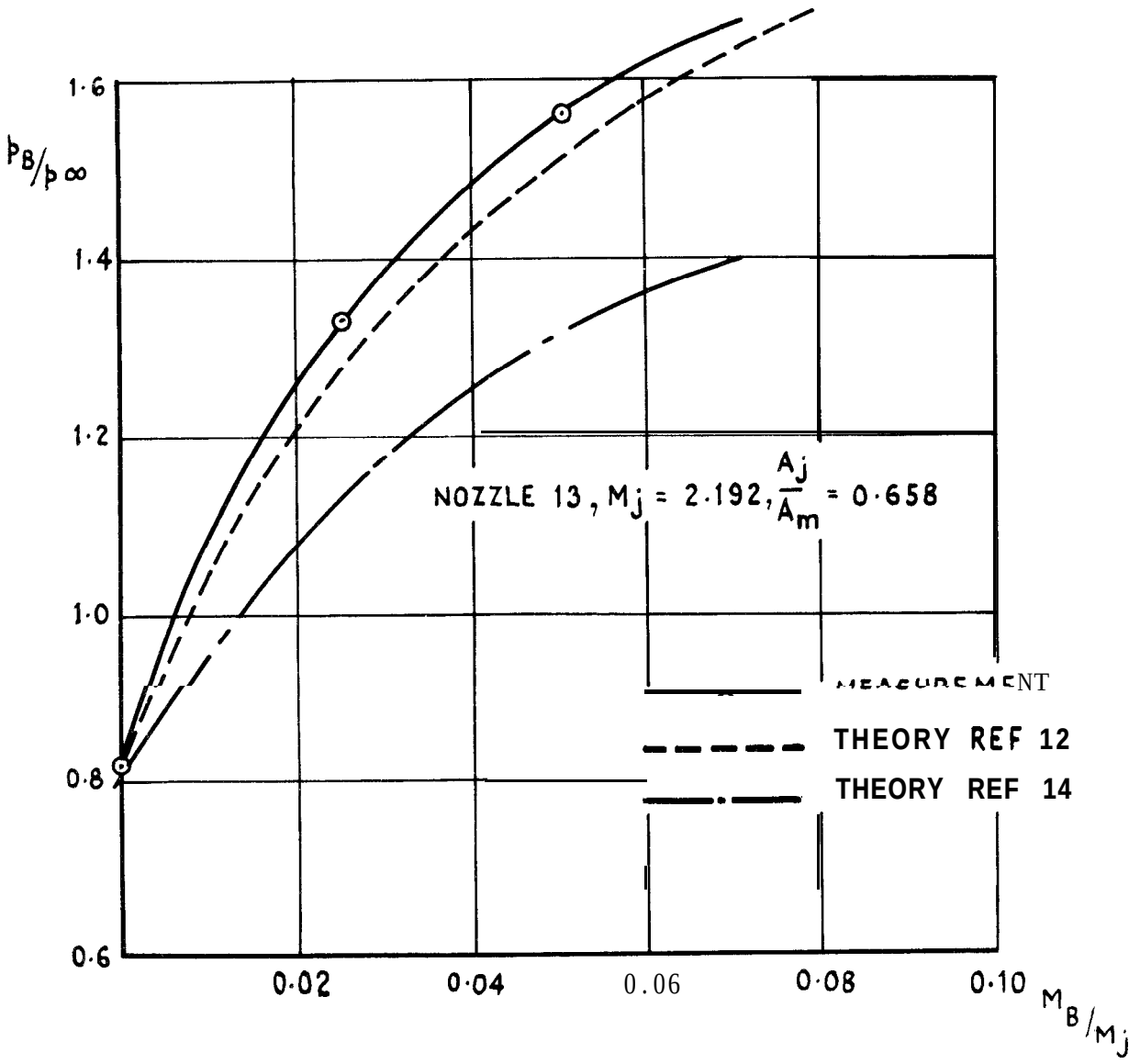

FIG 38 (e) COMPARISON OF CALCULATED & MEASURED BASE PRESSURES FOR NOZZLE 13 (SHROUDED)

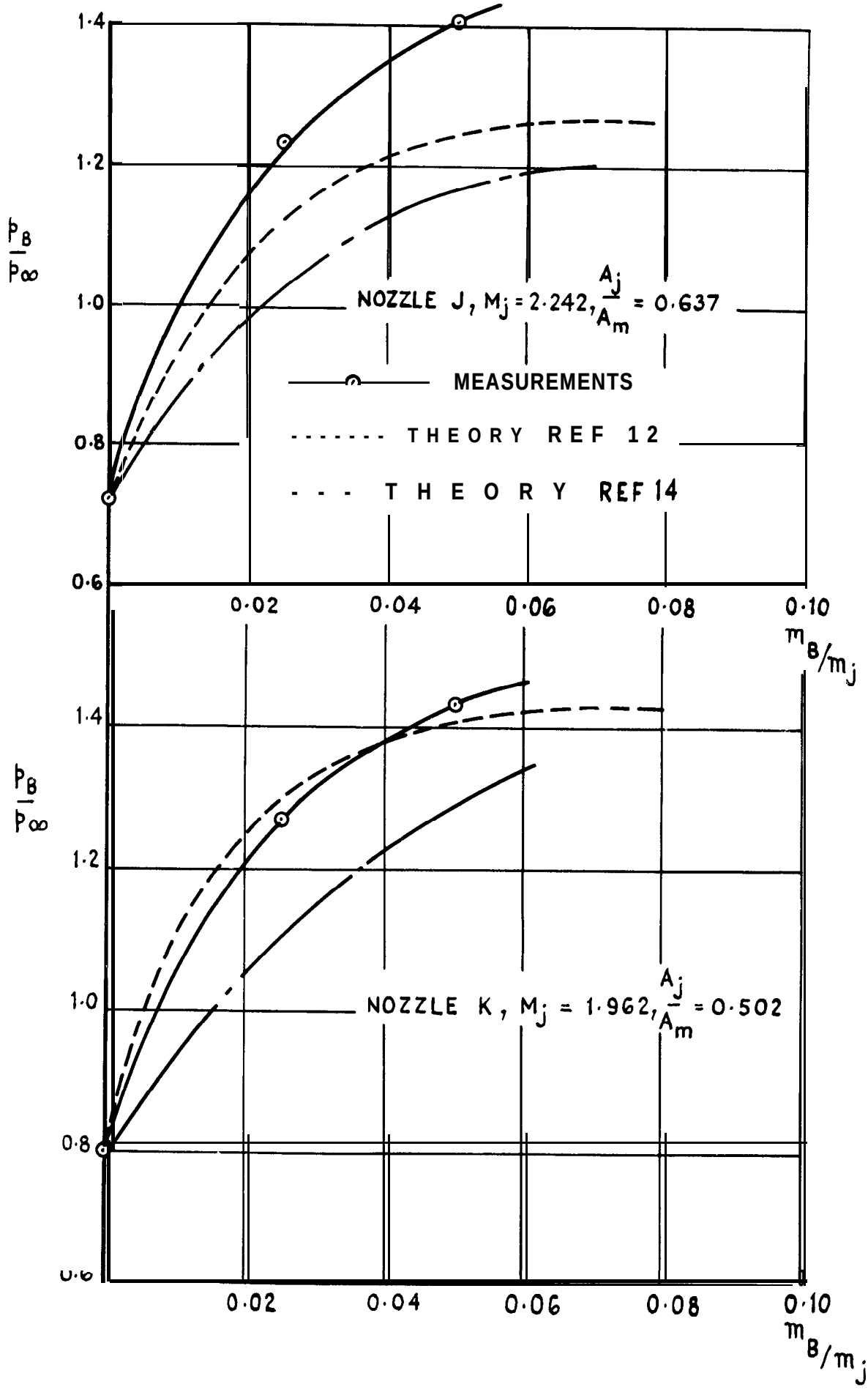

FIG. 38(f) COMPARISON OF CALCULATED & MEASURED BASE PRESSURES FOR NOZZLES J & K (SHROUDED)

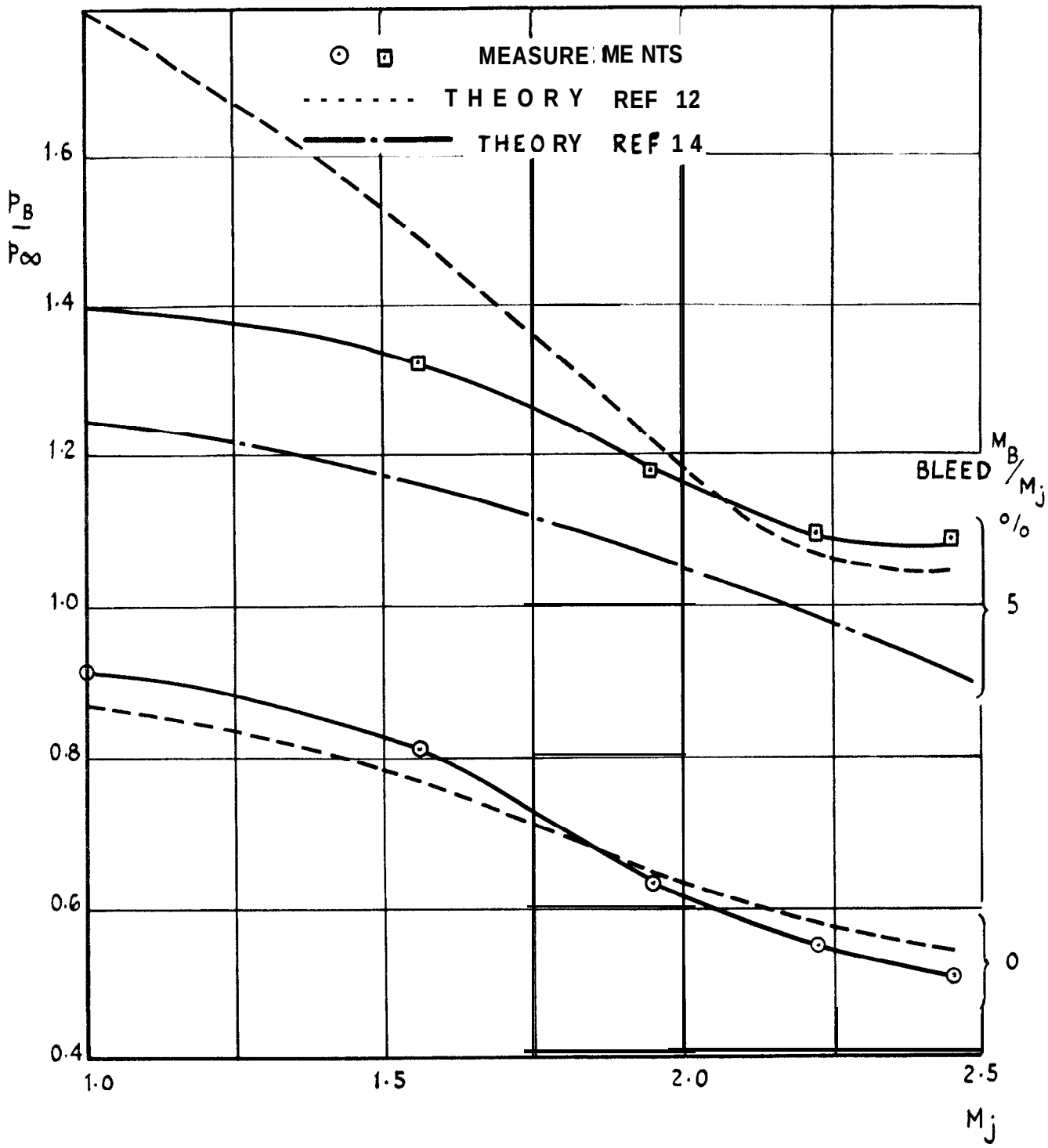

FIG.39 EFFECT OF NOZZLE DESIGN MACH NUMBER-COMPARISON OF THEORY & EXPERIMENT FOR ROUND NOZZLES WITH SHROUD

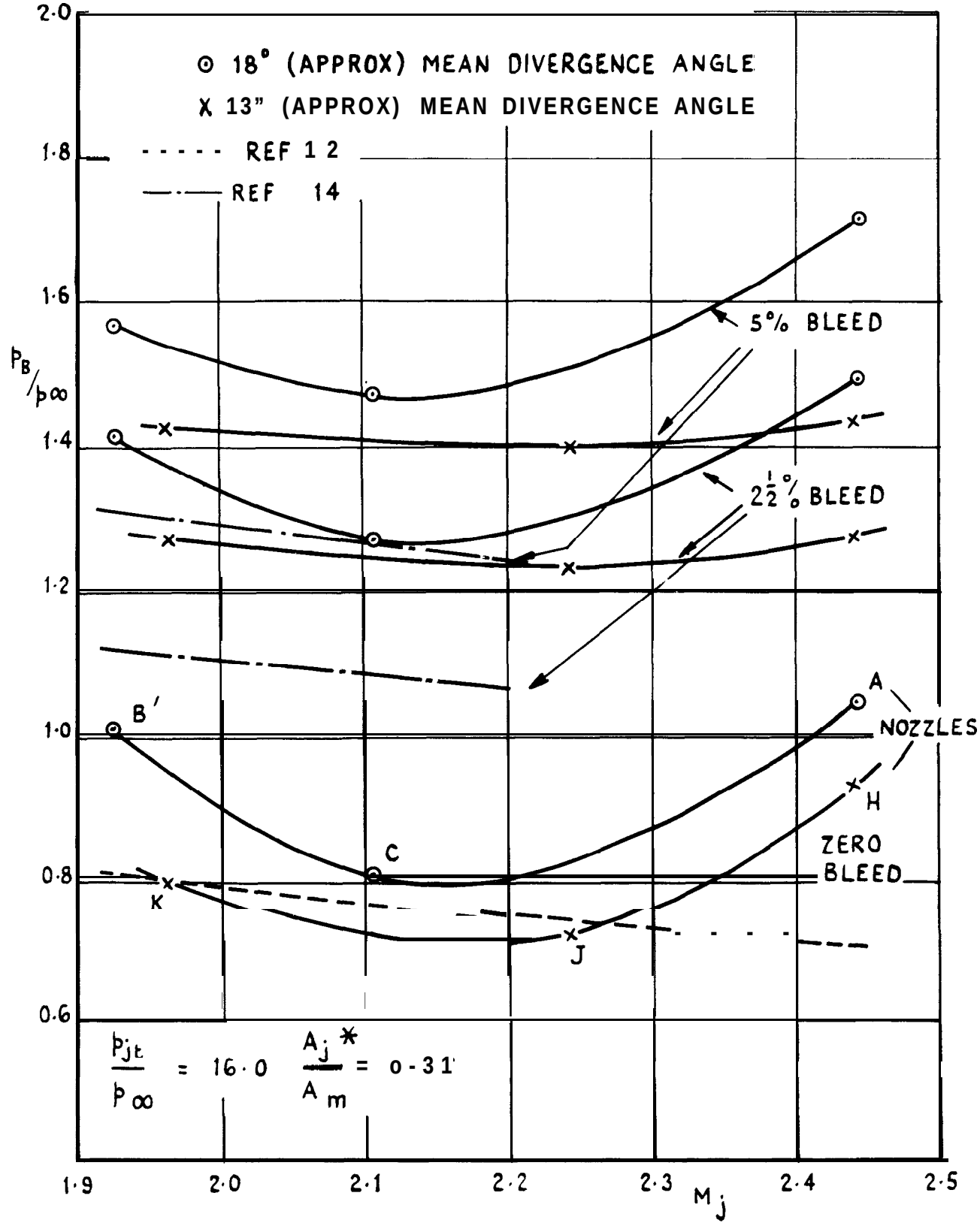

FIG.40 EFFECT OF JET DESIGN MACH NUMBER & NOZZLE DIVERGENCE ANGLE FOR SQUARE NOZZLES WITH SHROUD

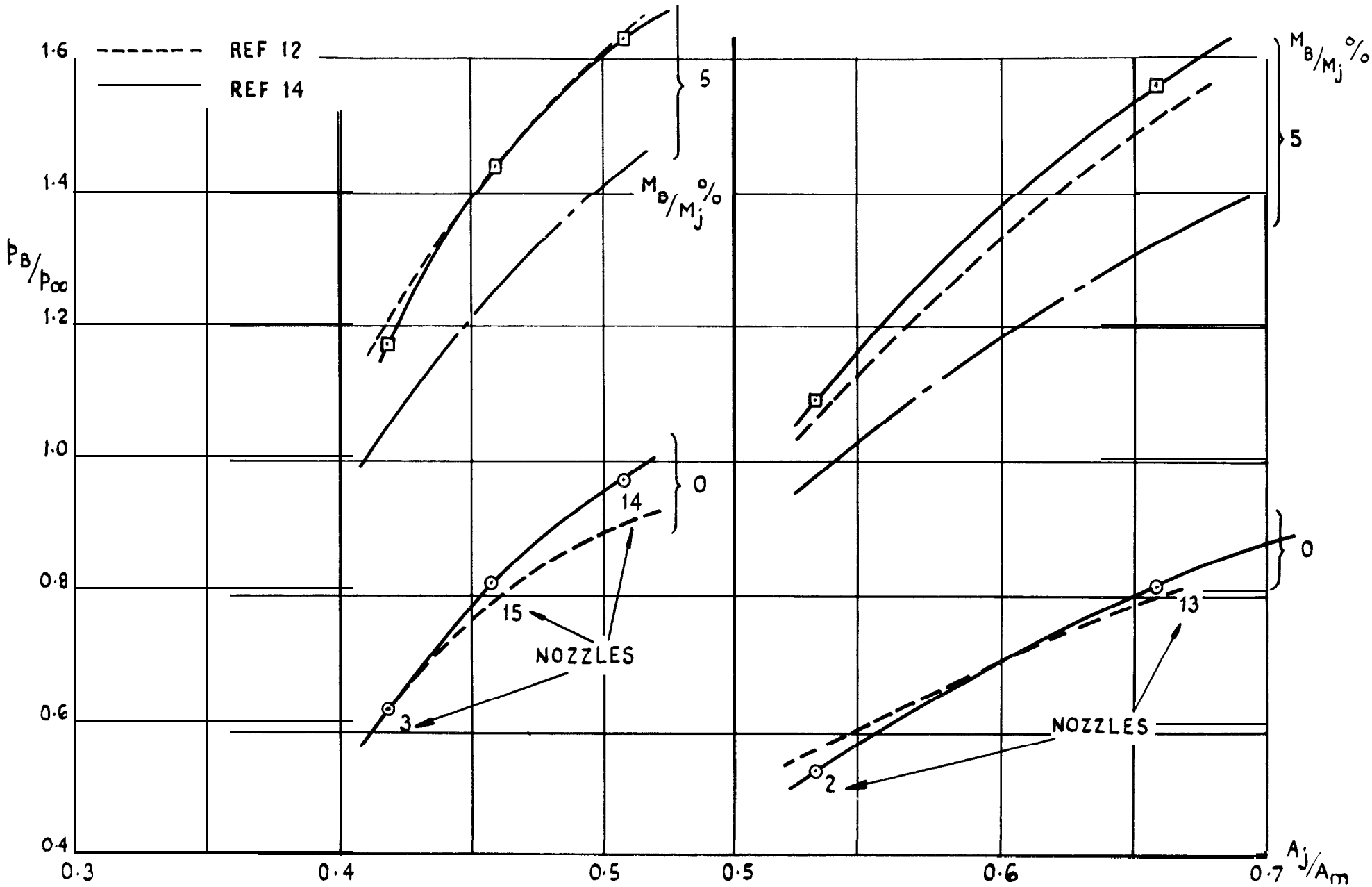

FIG, 41 VARIATION OF BASE PRESSURE WITH JET EXIT/SHROUD AREA FOR ROUND NOZZLES ($\theta j = 13°$) WITH SHROUD

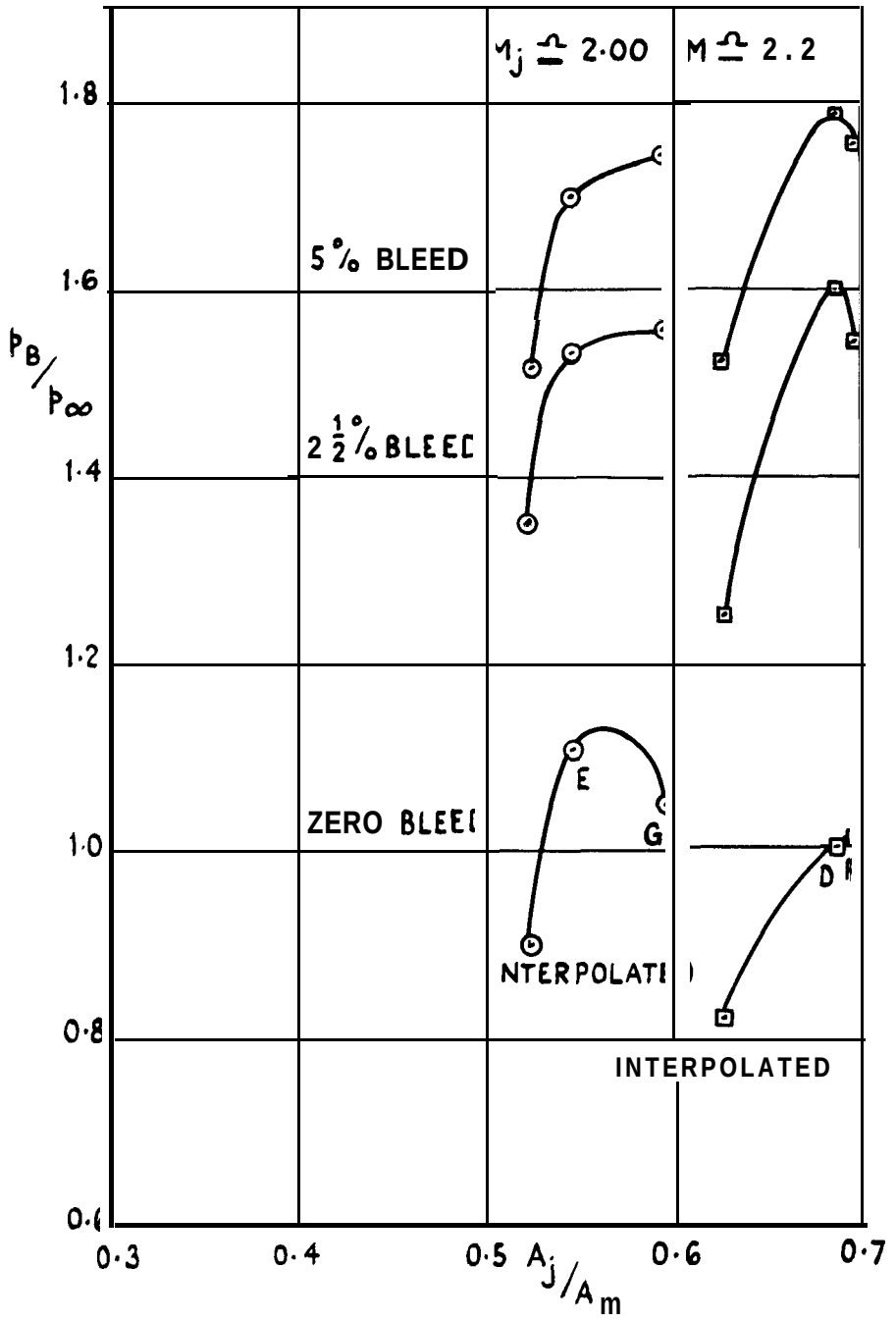

FIG.42 VARIATION OF BASE PRESSURE WITH JET EXIT AREA FOR SQUARE NOZZLES WITH SHROUD ($\theta_i \triangleq 18°$)

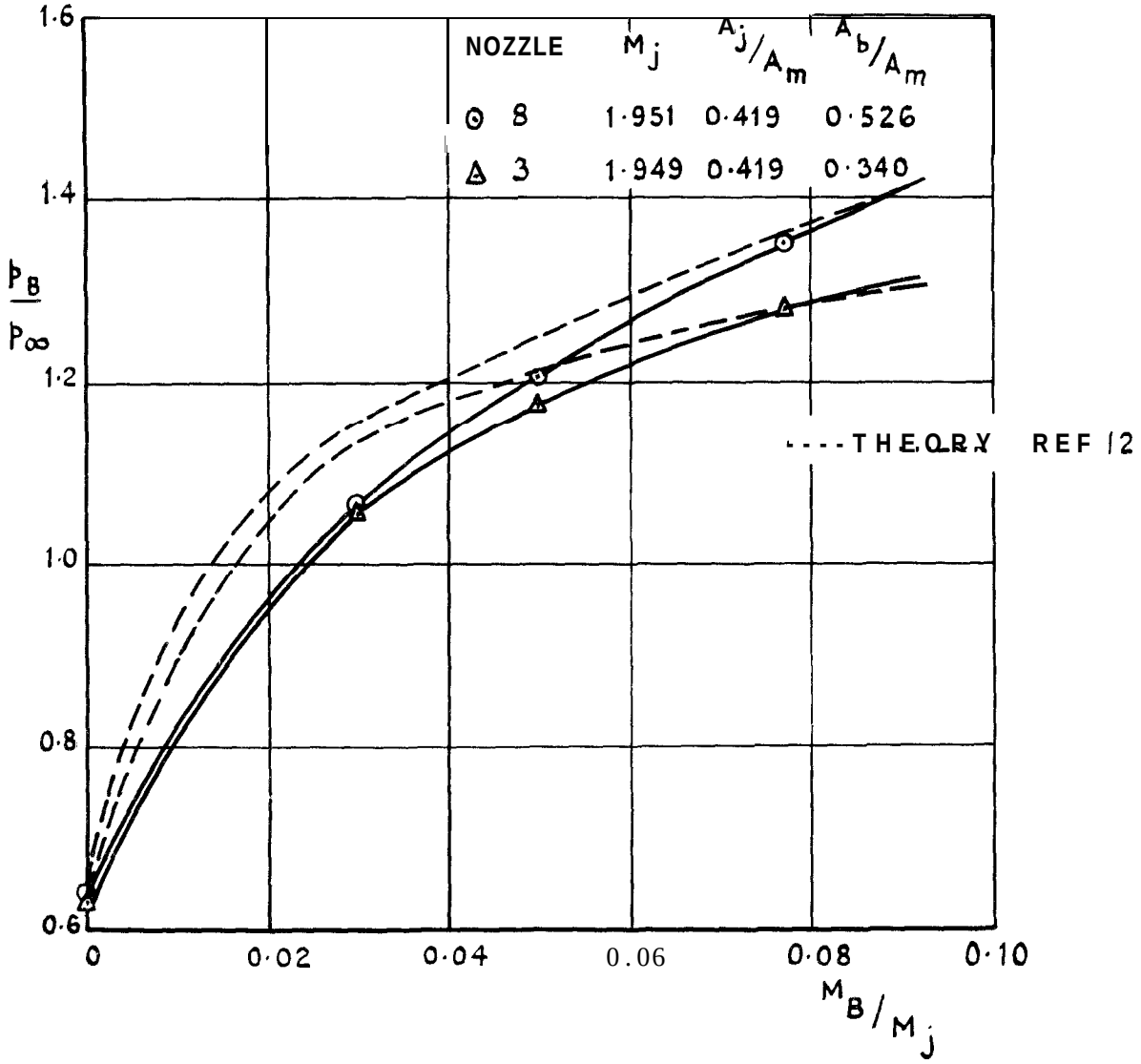

FIG.43 EFFECT OF BLEED DUCT EXIT AREA (SHROUDED)

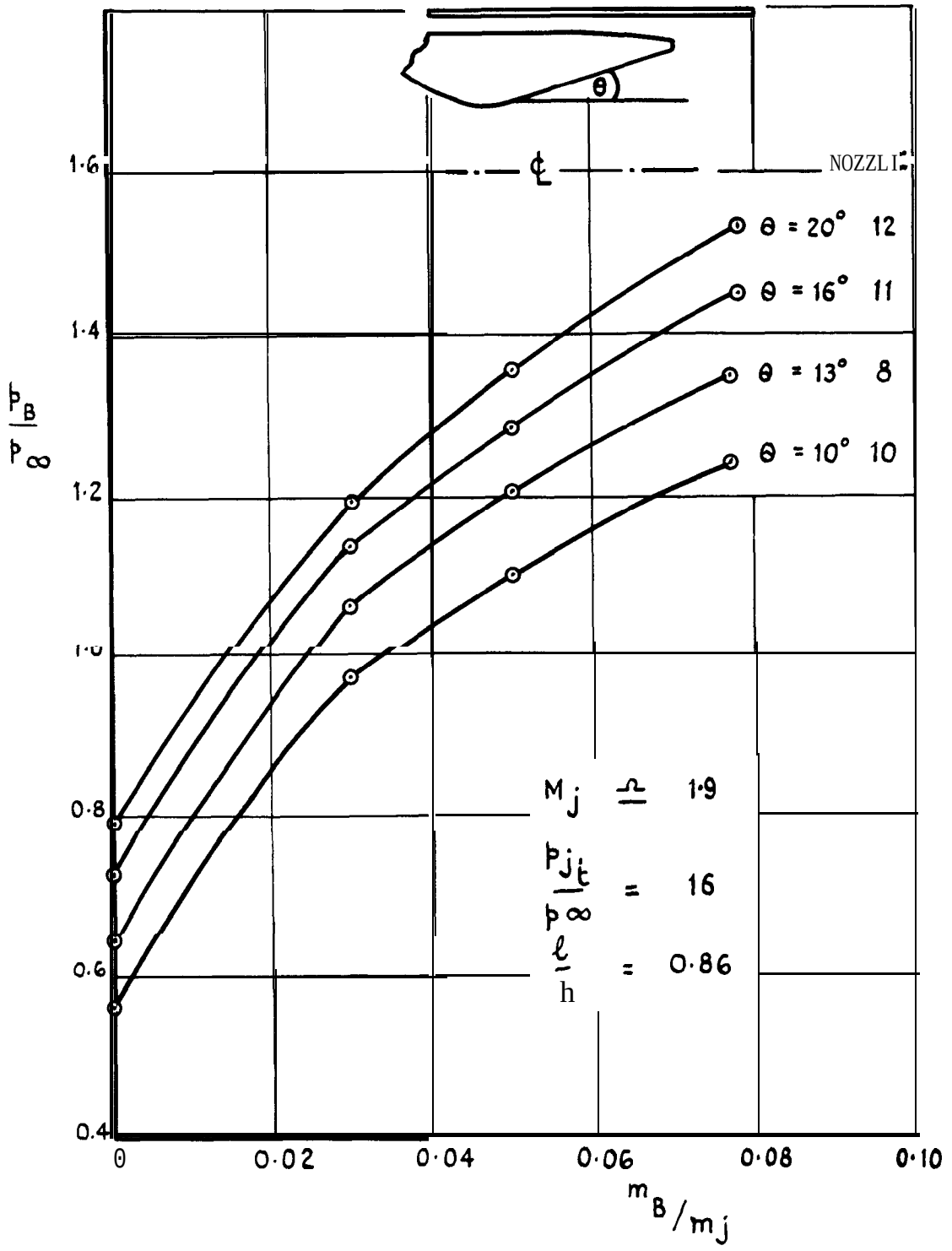

FIG. 44 (a) EFFECT OF NOZZLE DIVERGENCE **ANGLE** ON BASE PRESSURE (SHROUDED)

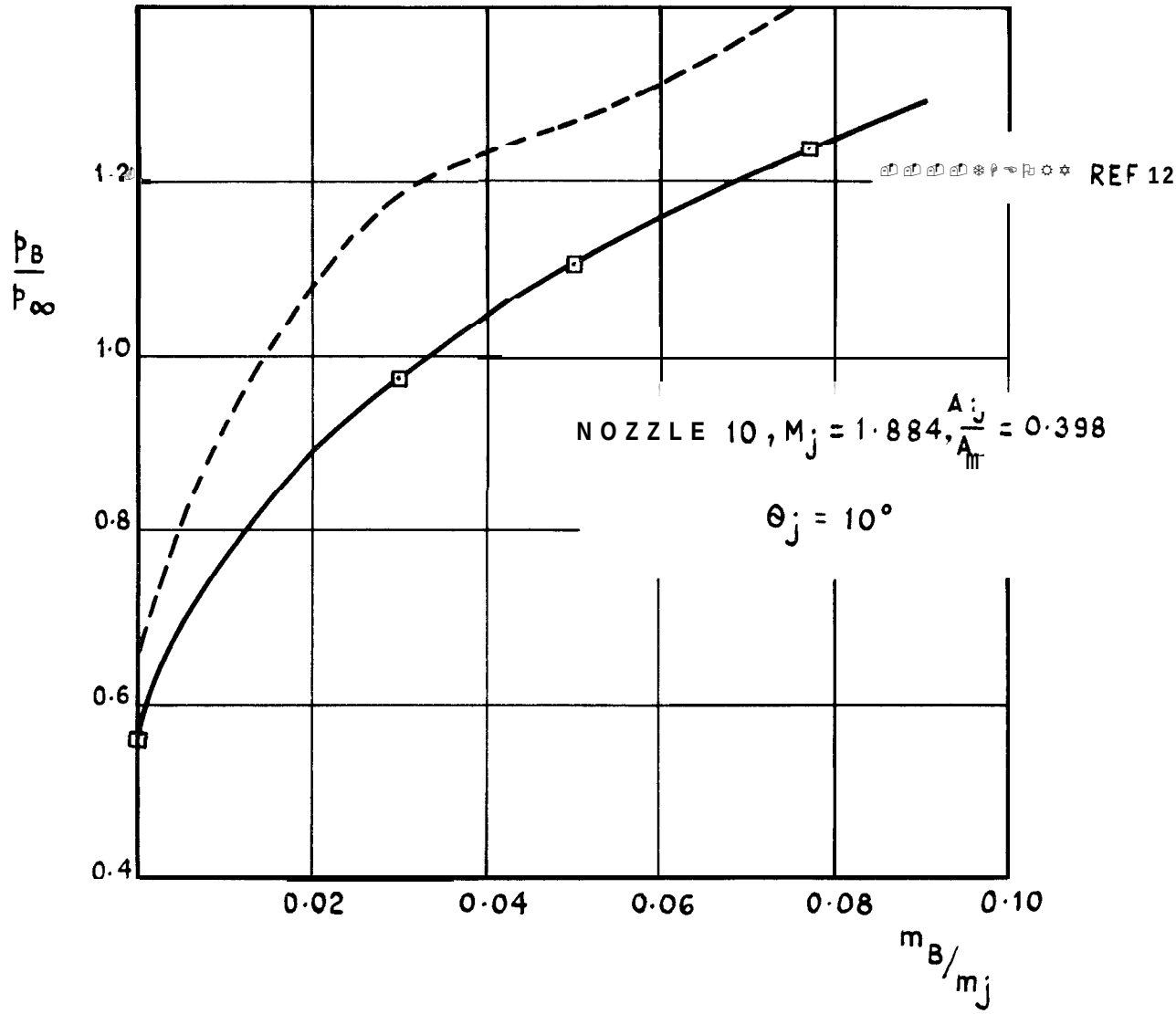

FIG.44 (b) COMPARISON OF CALCULATED & MEASURED BASE PRESSURES FOR NOZZLE 10 (θ_j = 10°, SHROUDED)

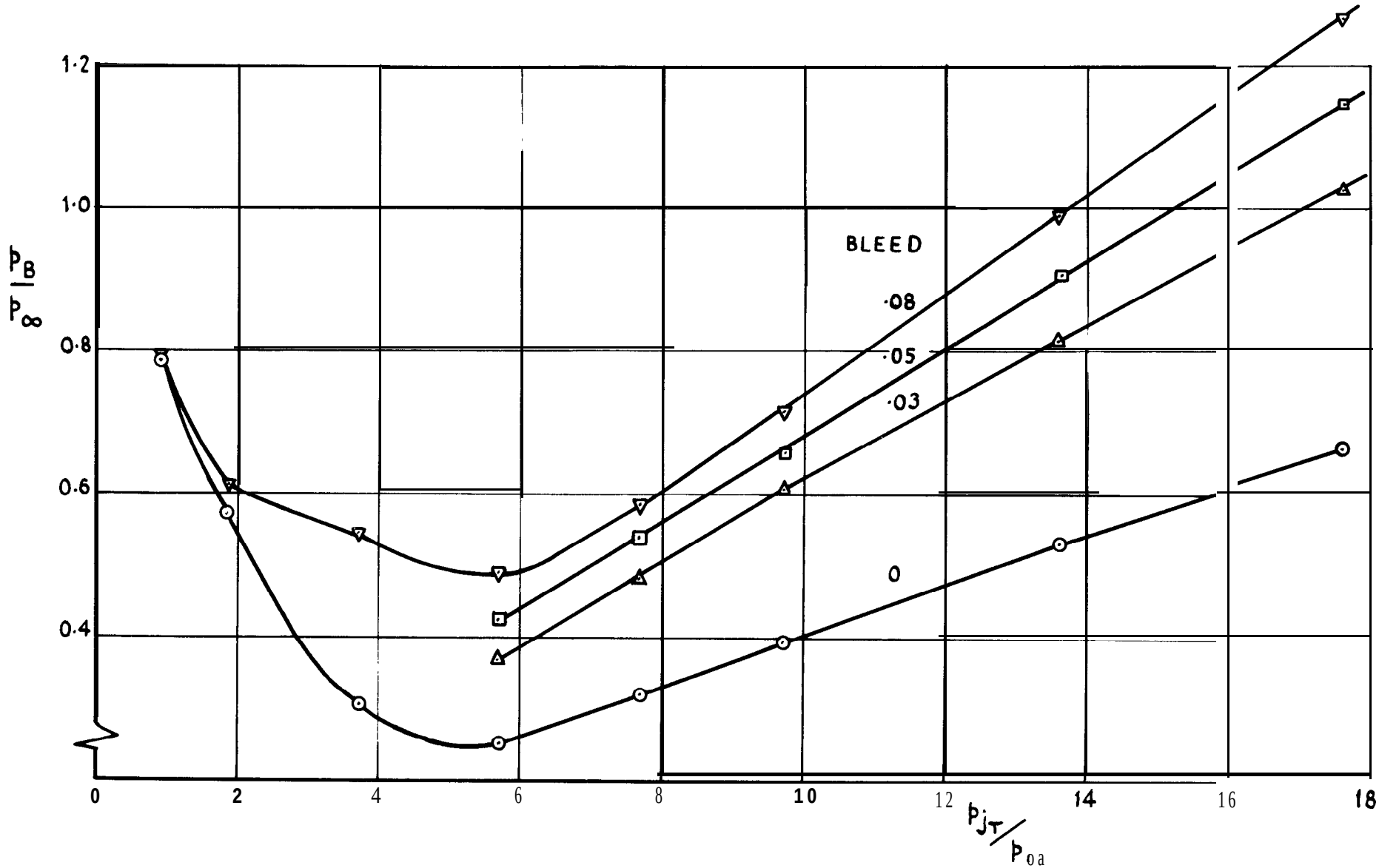

FIG.45 BASE PRESSURE vs JET PRESSURE RATIO (NOZZLE 2, SHROUDED)

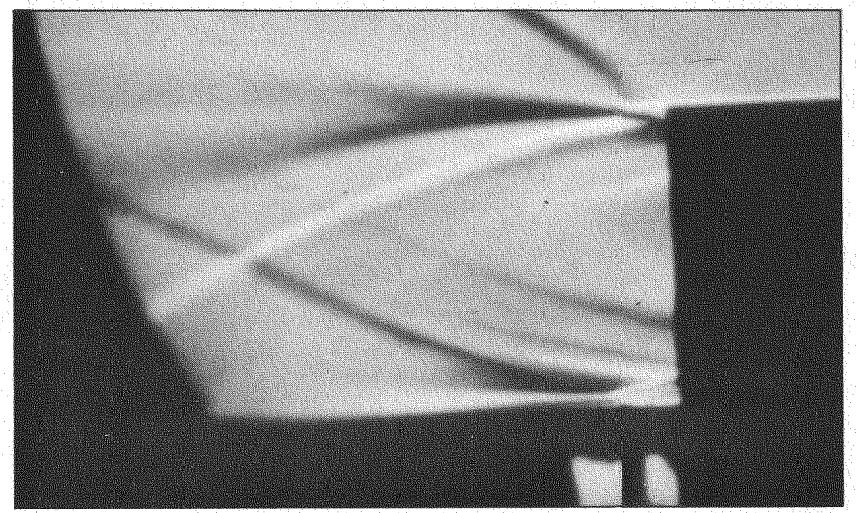

Zero bleed

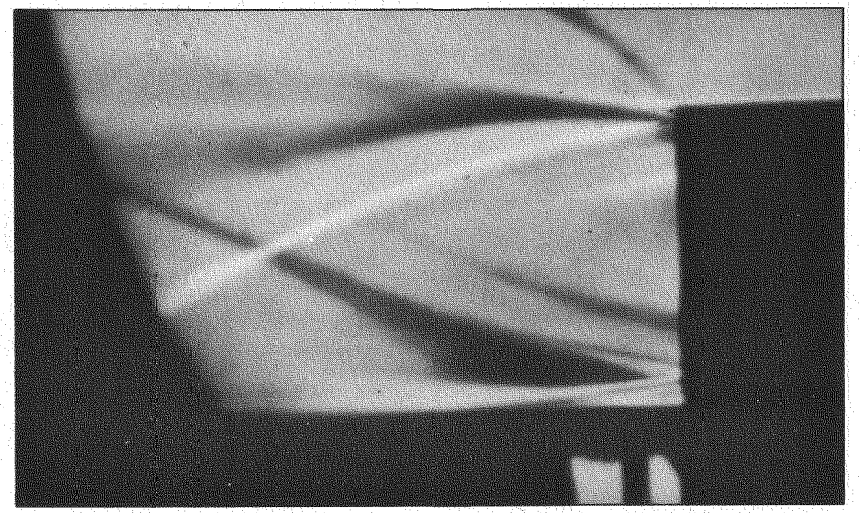

2.5% bleed

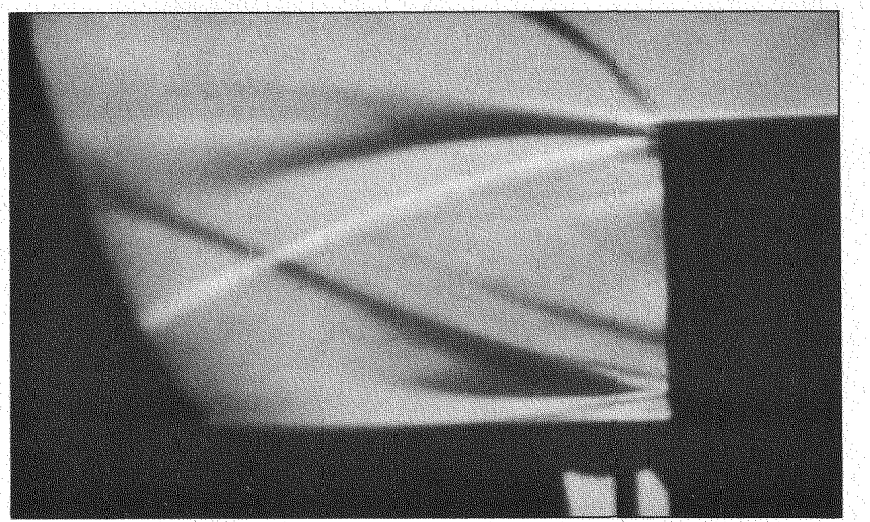

4% bleed

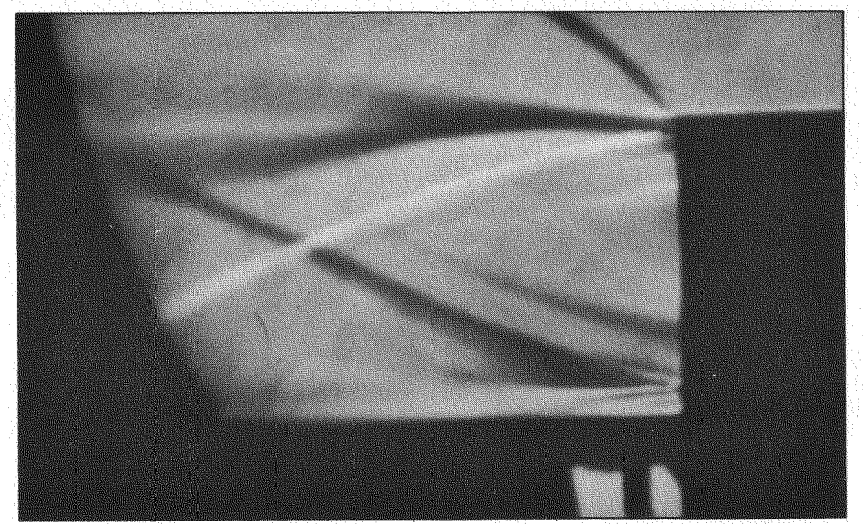

7% bleed

Fig.46. Schlieren photographs, showing effect of bleed

(NOZZLE A, p_{jt}/p_{∞} = 16.0, UNSHROUDED)

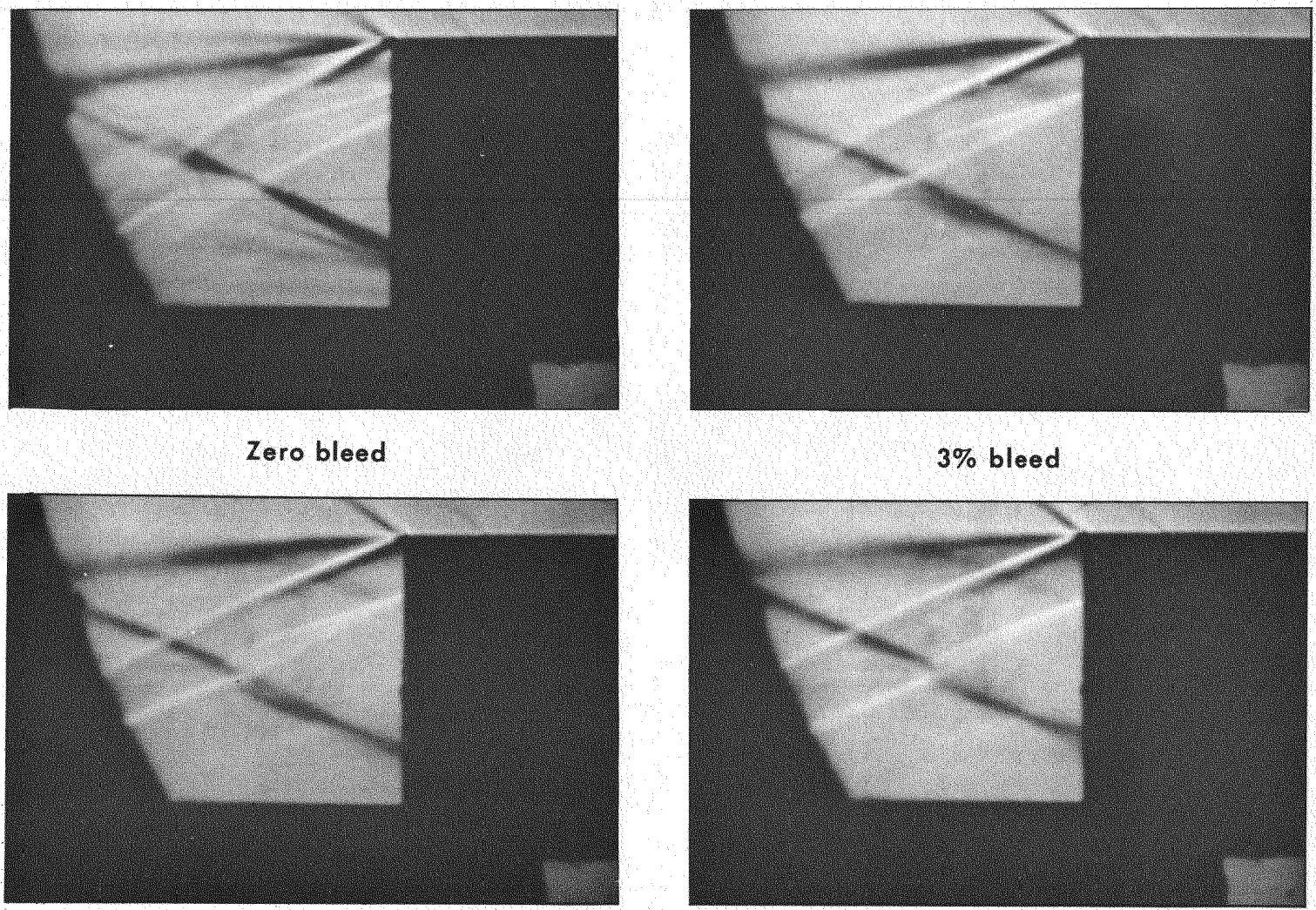

Fig.47. Schlieren photographs, showing effect of bleed

(NOZZLE 3, $p_{jt}/p_{\infty} = 16.0$, SHROUDED)

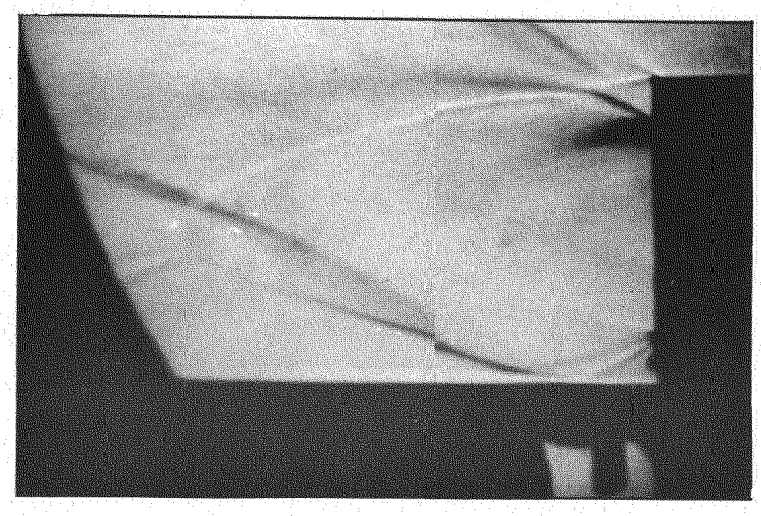

Zero bld

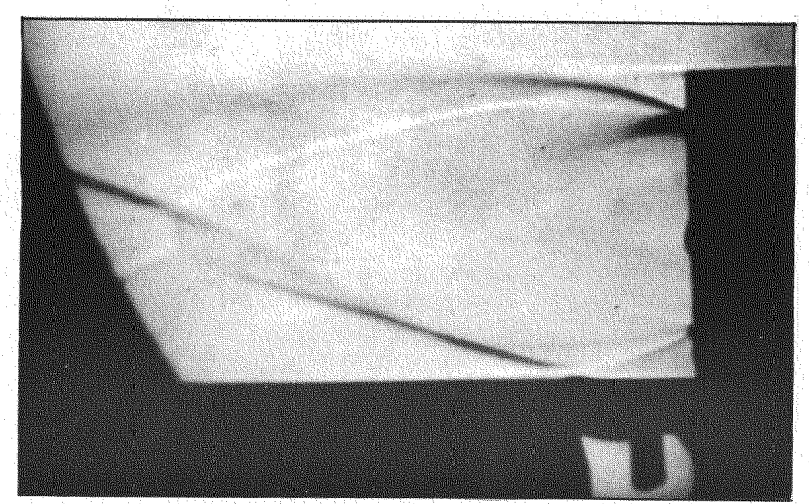

3% bleed

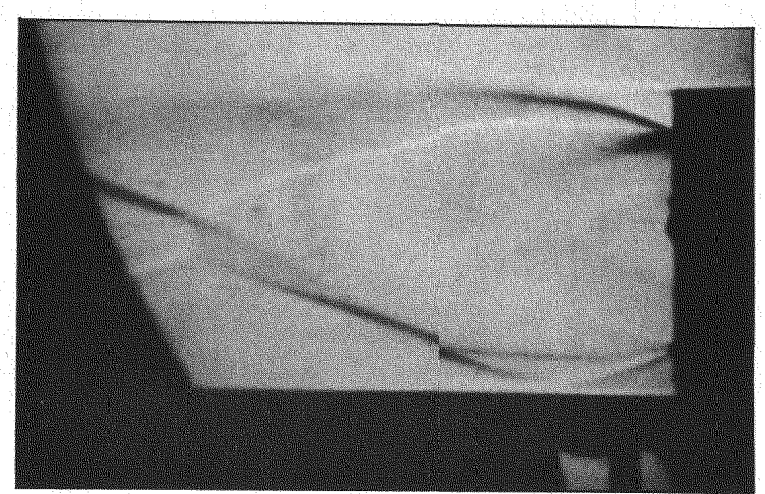

5% ble

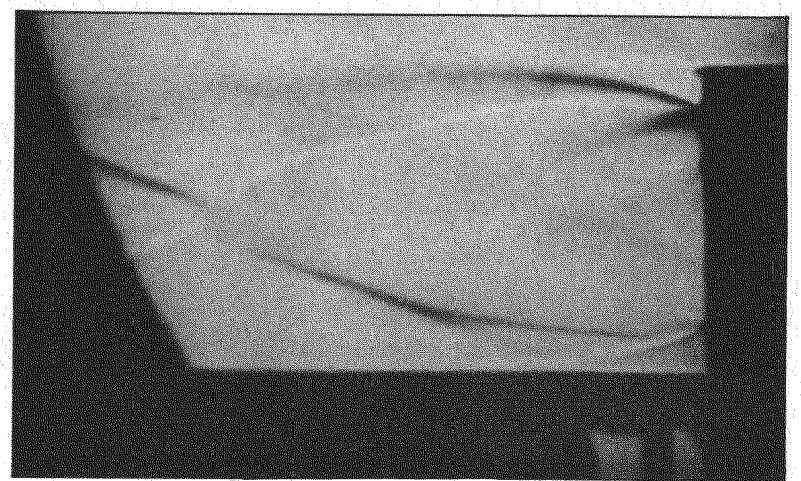

8% bleed

Fig.4ESchlieren photographs, showing effect of bleed

(NOZZLE 3, p_{jt}/p_{∞} = 16.0, UNSHROUDED)

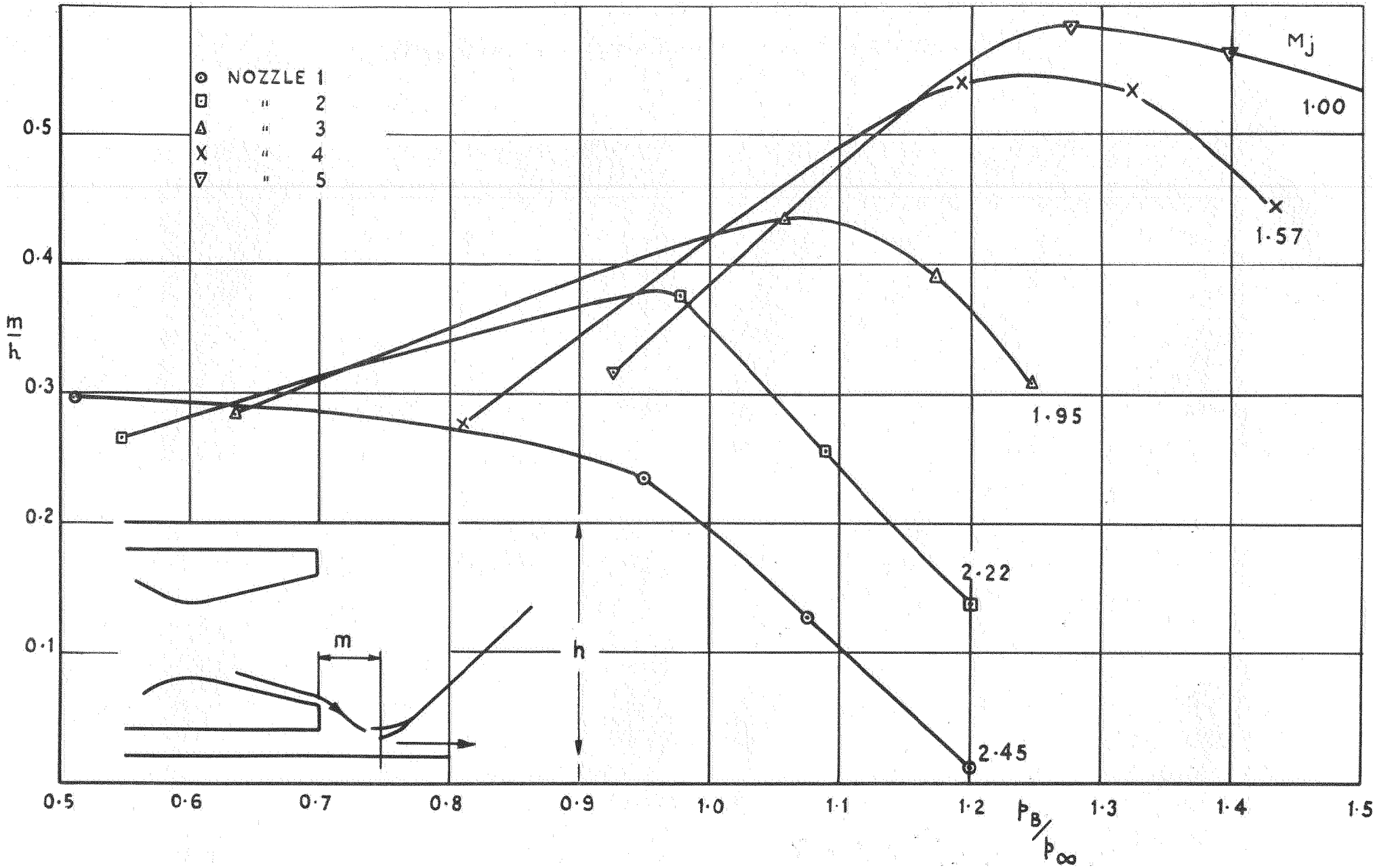

FIG.49 DISTANCE OF SHOCK BEYOND NOZZLE VS BASE PRESSURE (SHROUDED

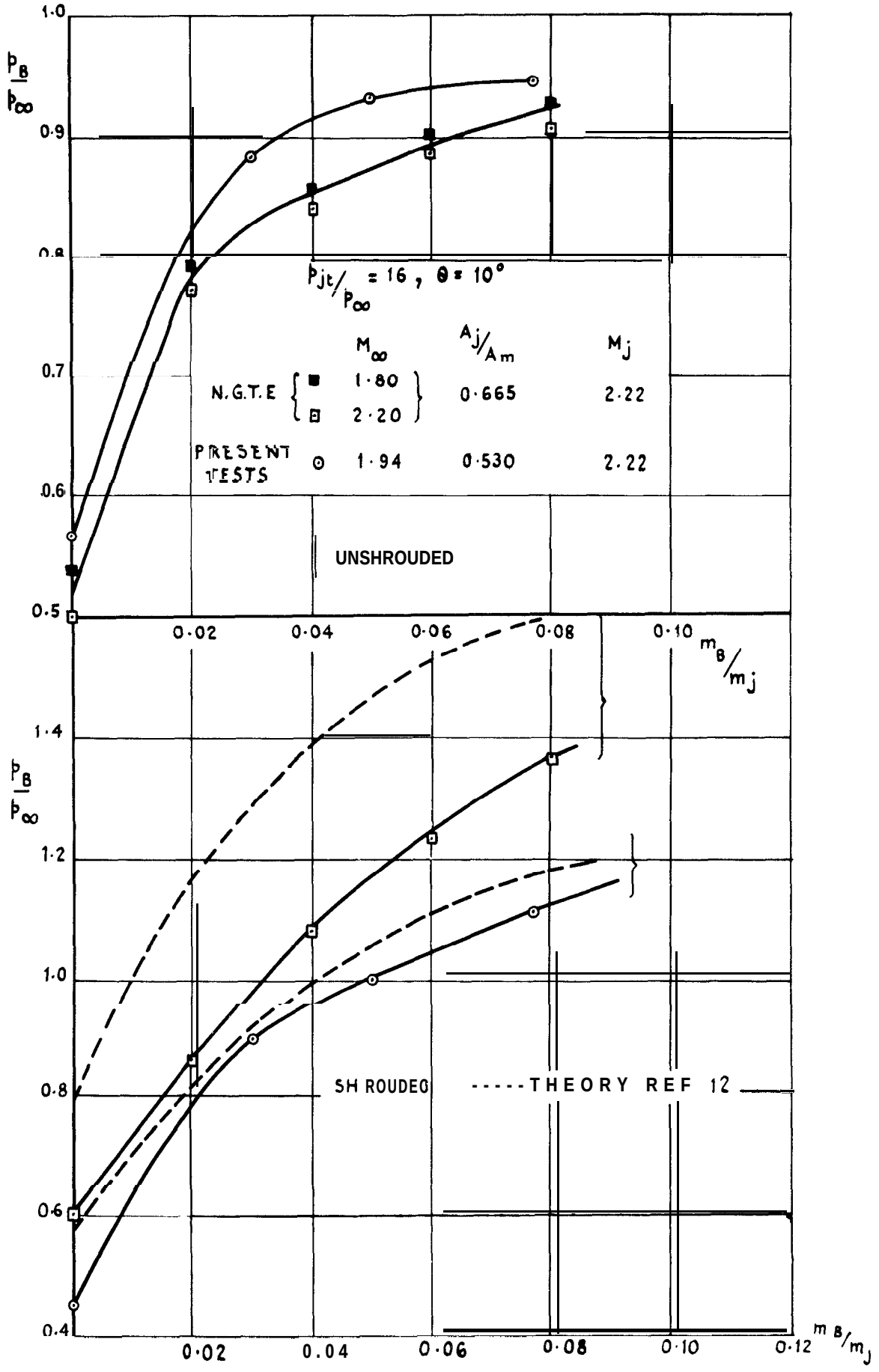

FIG.50 COMPARISON OF RAE & N GTE EXPERIMENTAL RESULTS

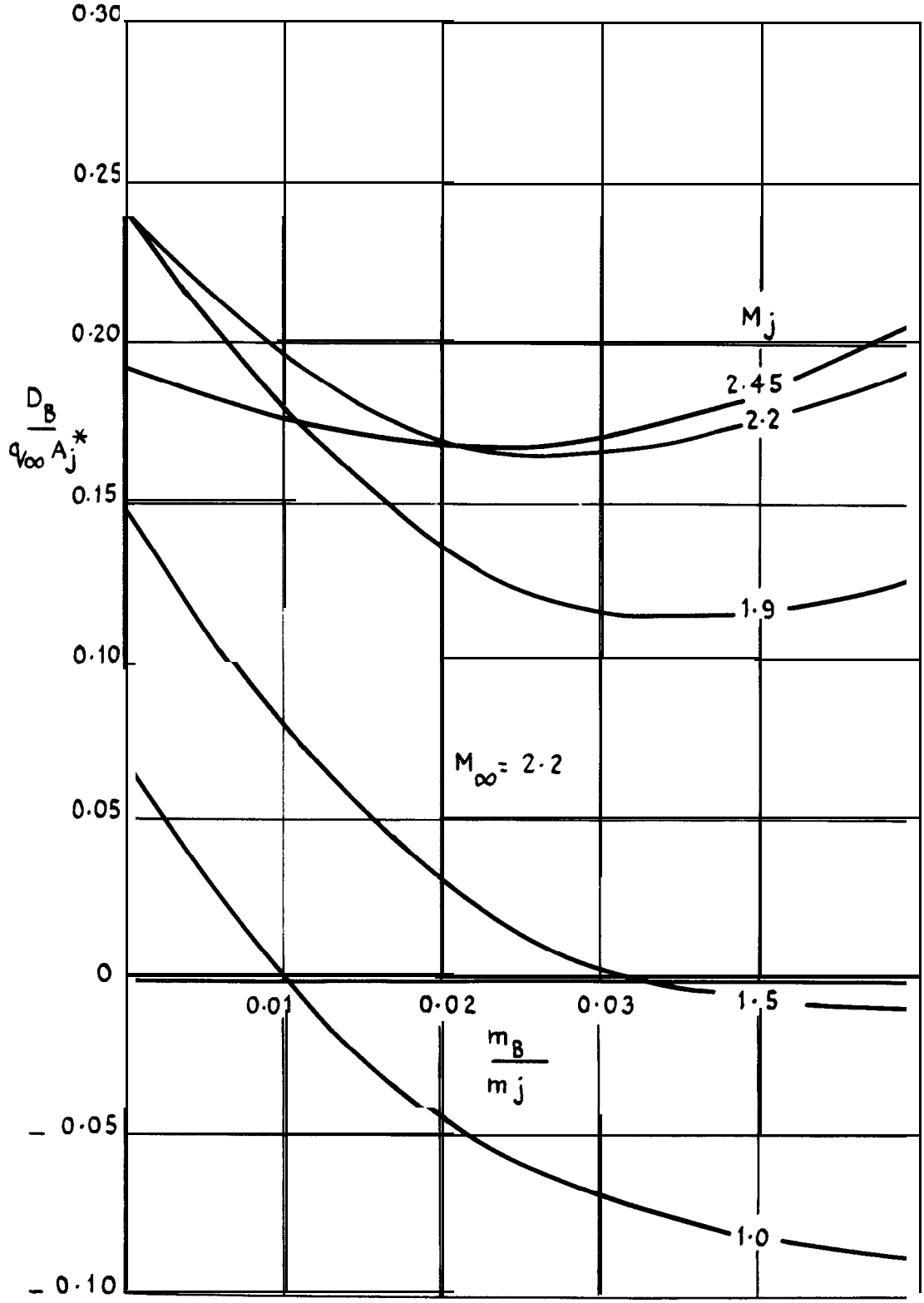

FIG.51 VARIATION OF BLEED DRAG WITH BLEED FLOW & JET MACH NUMBER (SHROUDED NOZZLES)

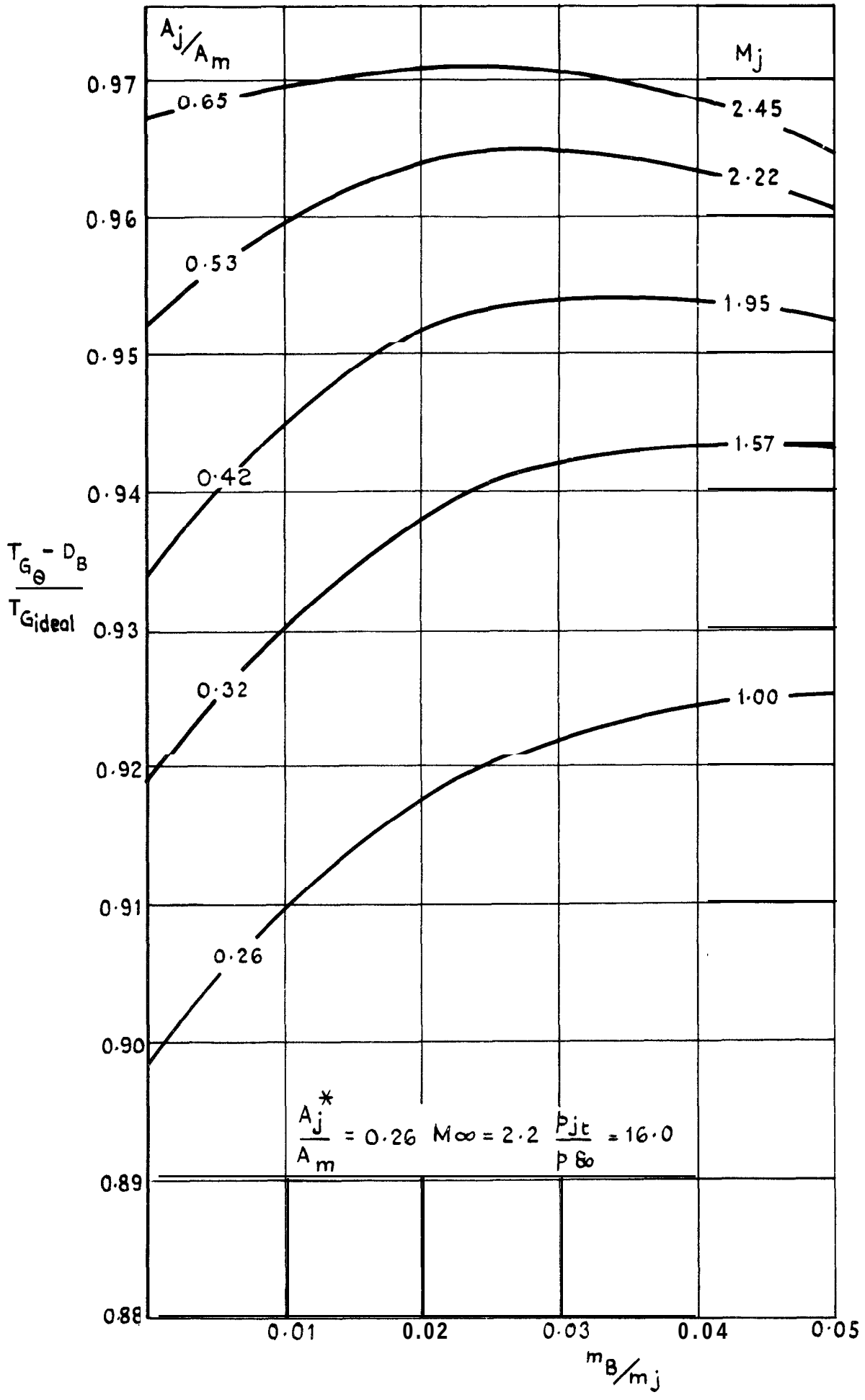

FIG.52 VARIATION OF THRUST EFFICIENCY WITH BLEED FLOW (SHROUDED NOZZLES)

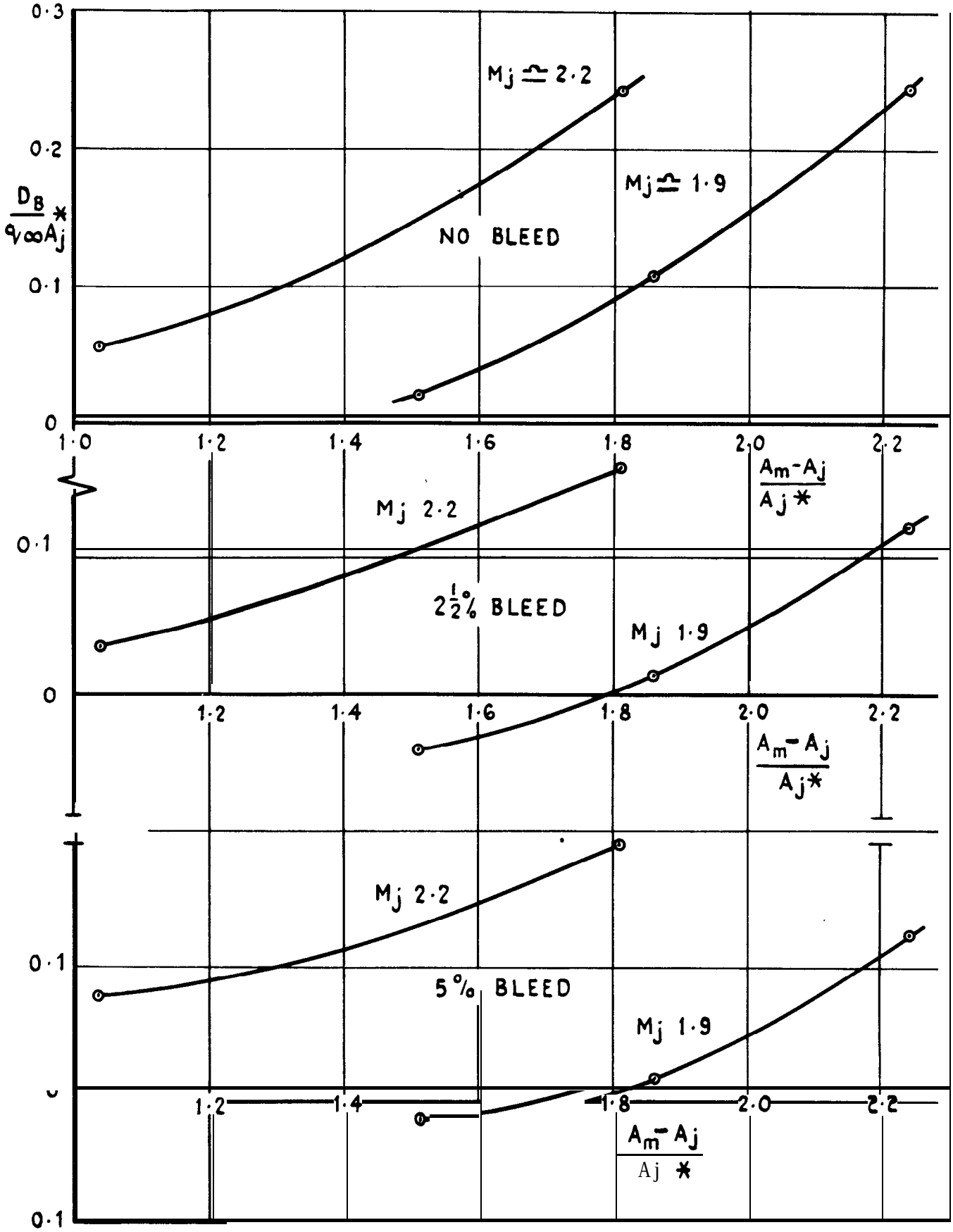

FIG.53 VARIATION OF BLEED DRAG WITH BLEED MASS FLOW, JET MACH NUMBER AND BLEED EXIT AREA AT $M_\infty = 2 \cdot 2$

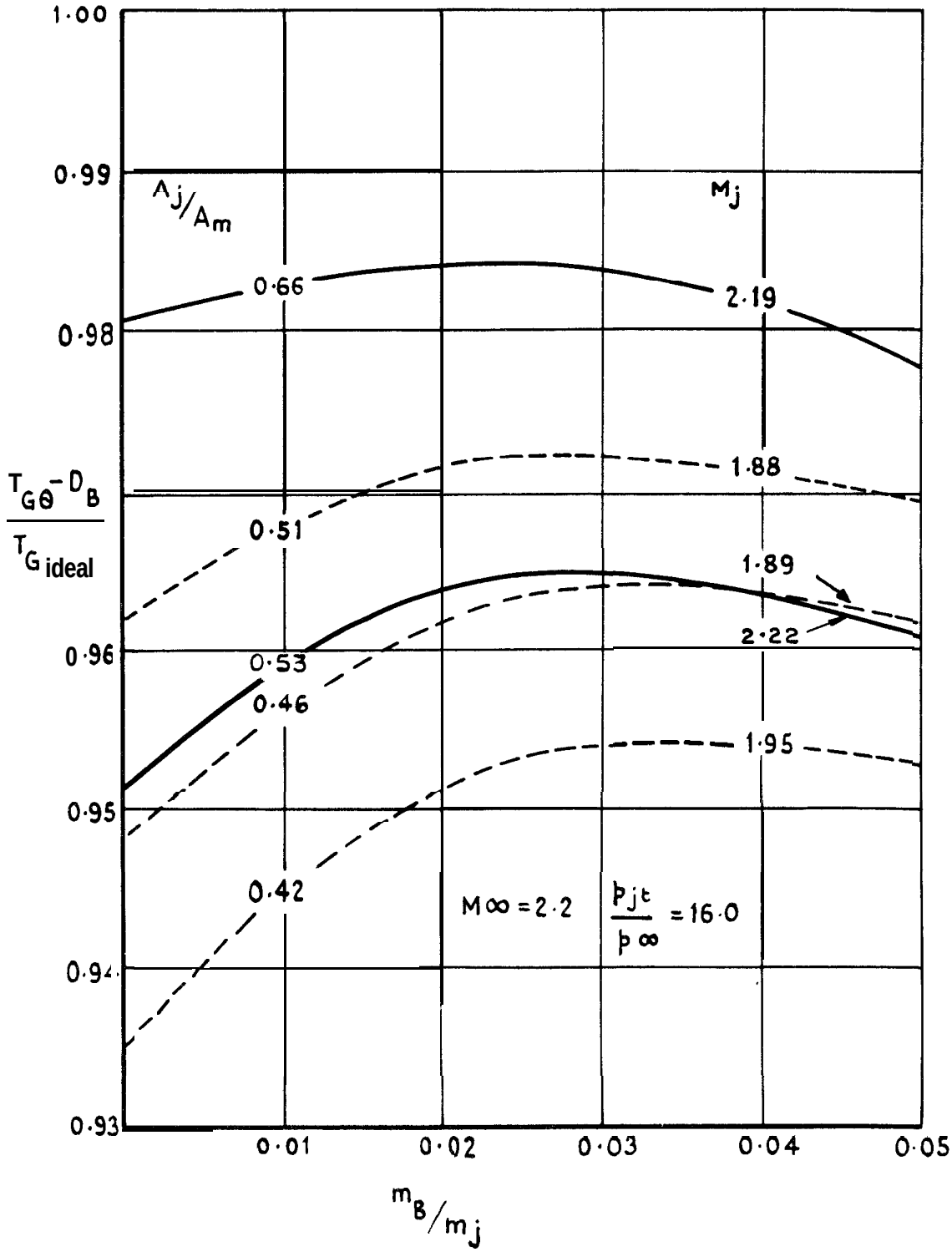

FIG. 54 VARIATION OF THRUST **EFFICIENCY WITH BLEED FLOW (SHROUDED NOZZLES)**

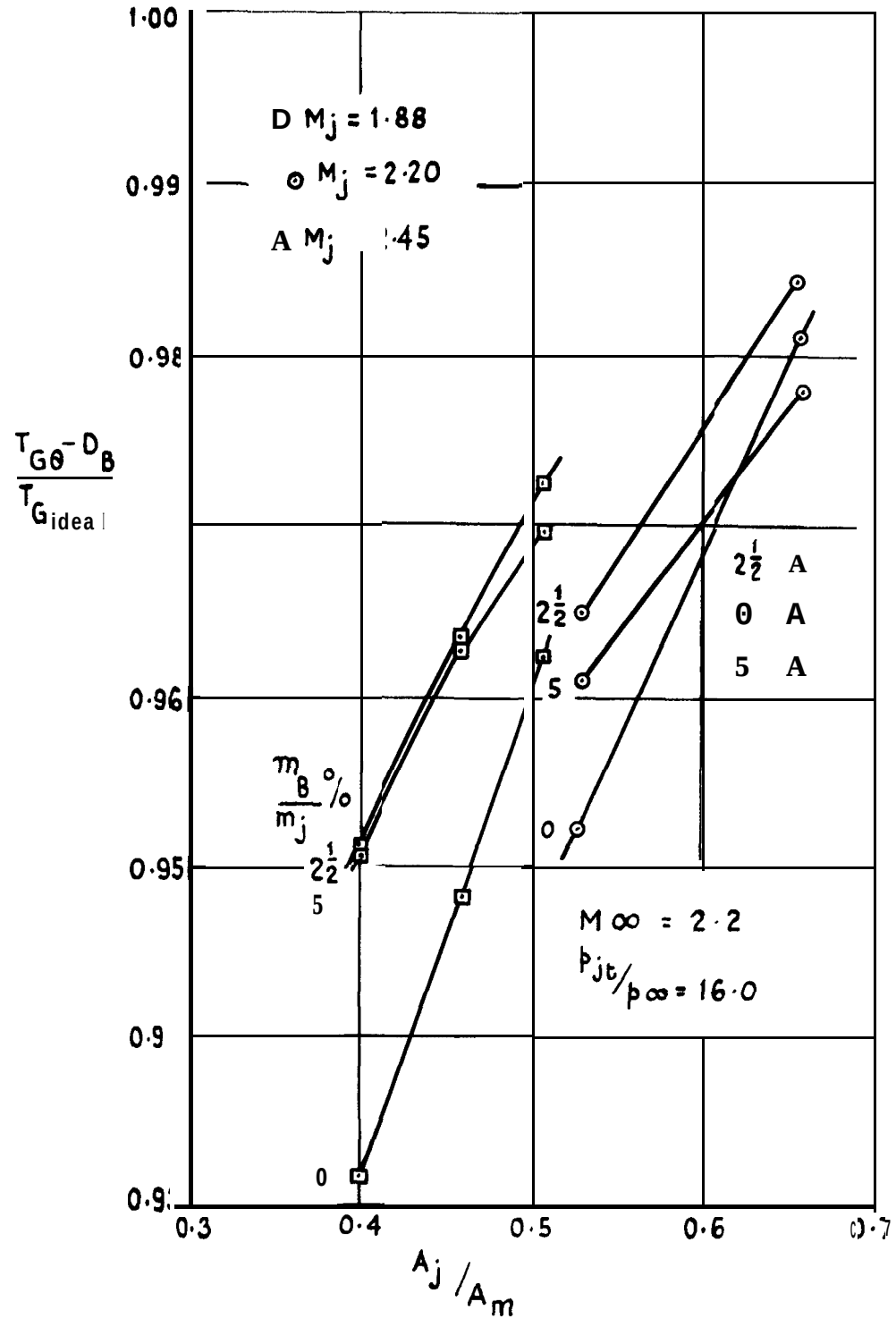

FIG.55 VARIATION OF THRUST EFFICIENCY WITH JET EXIT AREA

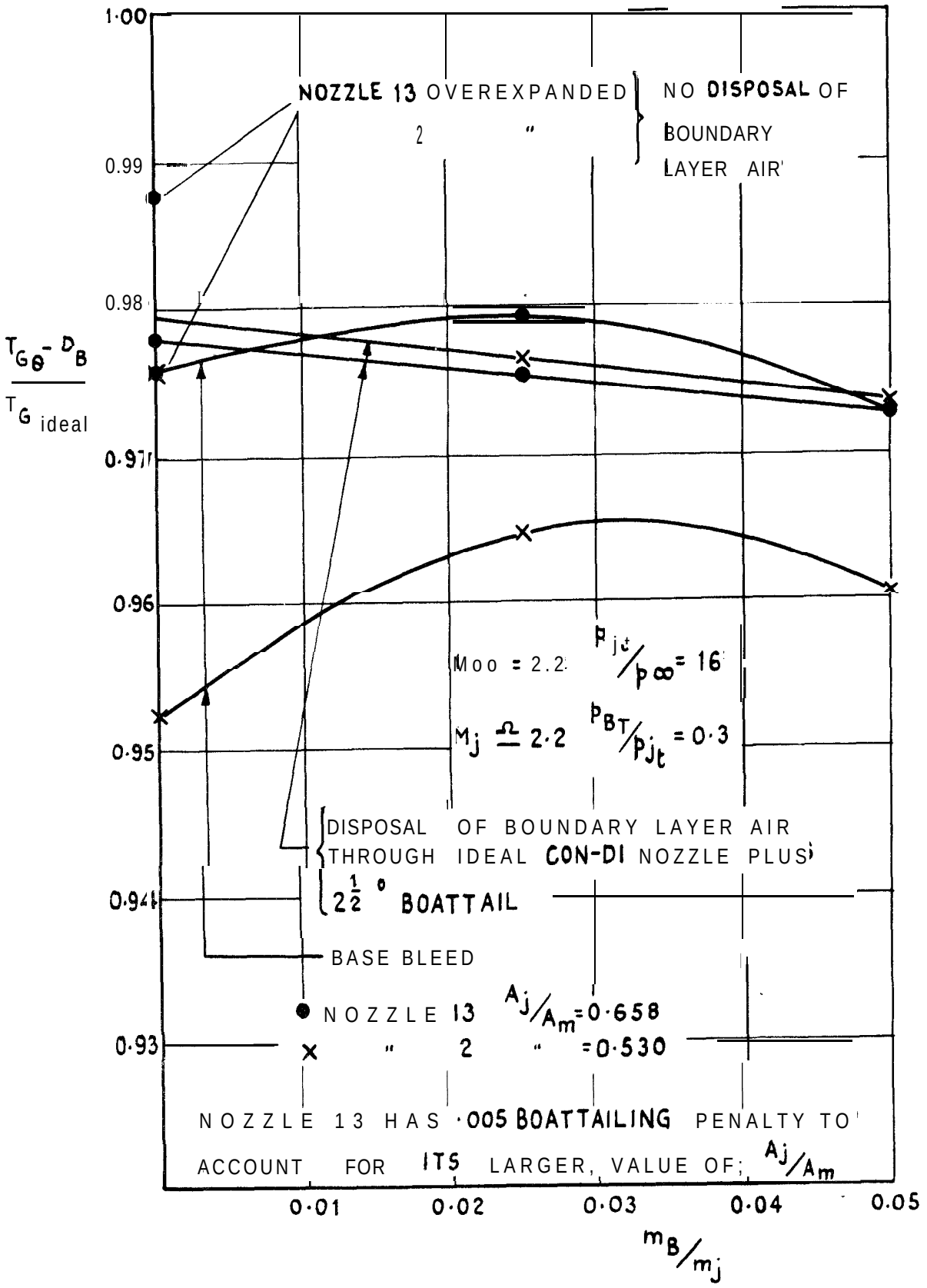

FIG. 56 COMPARISON OF THRUST EFFICIENCIES OBTAINED BY NOZZLE OVEREXPANSION, BASE BLEED, AND SEPARATE DISPOSAL OF BOUNDARY LAYER AIR

Printed in England for Her Majesty's Stationery *Office by the Royal Aircraft Establishment, Farnborough. Dd.129528. K.4.*

A.R.C.C.P. No.962
June 1966

Shaw, M.M.

533.6.048.2 :
533.697.5 :
533.6g7.4 :
533.6.011.5

THE EFFECT OF BASE BLEED ON THE BASE PRESSURE OF SEVERAL SHROUDED AND UNSHROUDED PROPELLING NOZZLES AT M = 1.96

Base pressure measurements have been made on a bluff area surrounding a propulsive jet with and without base bleed. The effects of altering the jet Mach number and the ratio of jet exit area to total base area have been indicated. The tests were extended to measuring base pressure inside a shroud, and a correlation between the unshrouded and shrouded results is obtained. The results from the shrouded tests are compared with those from simple one-dimensional theories, with sane success.

Calculations of thrust efficiency show that high values can be obtained with the right combination of nozzle design Mach number, bleed flow and jet to maximum area ratio. If air of low total head, e.g. Iran an intake bleed, has to be disposed of, then feeding It into a duct surrounding a shrouded jet nozzle can be an efficient means of disposal.

A.R.C.C.P. No.962
June 1966

Shaw, M.M.

533.6.048.2 :
533.697.5 :
533.697.4 :
533.6.011.5

THE EFFECT OF BASE BLEED ON THE BASE PRESSURE OF SEVERAL SHROUDED AND UNSHROUDED PROPELLING NOZZLES AT M_∞ = 1.96

Base pressure measurements have been made on a bluff area surrounding a propulsive jet with and without base bleed. The effects of altering the jet Mach number and the ratio of jet exit area to total base area have been indicated. The tests were extended to measuring base pressure inside a shroud, and a correlation between the unshrouded and shrouded results is obtained. The results from the shrouded tests are compared with those from simple one-dimensional theories, with sane success.

Calculations of thrust efficiency show that high values can be obtained with the right combination of nozzle design Mach number, bleed flow and jet to maximum area ratio. If air of low total head, e.g. from an intake bleed, has to be disposed of, then feeding It into a duct surrounding a shrouded jet nozzle can be an efficient means of disposal.

A.R.C.C.P. No.962
June 1966

Shaw, M.M.

533.6.048.2 :
533.697.5 :
533.697.4 :
533.6.011.5

THE EFFECT OF BASE BLEED ON THE BASE PRESSURE OF SEVERAL SHROUDED AND UNSHROUDED PROPELLING NOZZLES AT M = 1.96

Base pressure measurements have been made on a bluff area surrounding a propulsive jet with and without base bleed. The effects of altering the jet Mach number and the ratio of jet exit area to total base area have been Indicated. The tests were extended to measuring base pressure Inside a shroud, and a correlation between the unshrouded and shrouded results Is obtained. The results fran the shrouded tests are compared with those from simple one-dimensional theories, with sane success.

Calculations of thrust efficiency show that high values can be obtained with the right combination of nozzle design Mach number, bleed flow and jet to maximum area ratio. If air of low total head e.g. from an intake bleed, has to be disposed of, then feeding it Into a duct surrounding a shrouded jet nozzle can be an efficient means of disposal.

DETACHABLE ABSTRACT CARDS

Published by
HER MAJESTY'S STATIONERY OFFICE.

To be purchased from
49 High Holborn, London W.C.1
423 Oxford Street. London W.1
13A Castle Street, Edinburgh 2
109 St. Mary Street, Cardiff
Brazennose Street, Manchester 2
50 Fairfax Street, Bristol 1
35 Smallbrook, Ringway, Birmingham 5
7-11 Linenhall Street, Belfast 2
or through any bookseller

C.P. No. 962

S.O. CODE No. 23-9017-62